



Faculty of Health, Engineering & Sciences

# **Vibroacoustic Transformer Condition Monitoring**

A dissertation submitted by

**Dean Mark Starkey**

**Student ID: 0061038897**

in fulfilment of the requirement of

**ENG4112 Research Project Part 2**

towards the degree of

**Bachelor of Engineering (Honours)**

**Major Power Engineering**

**October 2016**

# ABSTRACT

Throughout the life of a transformer the effects of mechanical shocks, insulation aging, thermal processes and short circuit forces will cause deformations in the winding. This deformation can lead to vibration in the transformer and mechanical fatigue of the solid insulation. Defects which form in a transformers structure can cause faults such as partial discharge, hot spots and arcing. These faults generate combustible gases which can be analysed for condition assessment of the transformer.

The development of a suitable and cost effective vibration measurement system forms a key part of this research project. A monitoring system is developed for real-time vibration analysis. An embedded capacitive accelerometer is used in conjunction with an Arduino microcontroller to record vibrations. The sensor platform is designed to communicate wirelessly via XBee radios to a terminal computer. A software program and user interface is designed as a tool for analysis.

The outcomes and benefits of these works are primarily based on determining the condition of transformer insulation through measurements of vibration. Following a working measurement system, suitable transformer sites are monitored. Spectral analysis is performed in the frequency domain to determine a correlation with gas analysis results. The validity of vibroacoustic measurement as a predictive maintenance tool is subsequently evaluated.

Six transformers are chosen for vibration monitoring with analysis of the vibration signatures correlated to the dissolved gas analysis reports at each site. The vibration signatures at each location are analysed using the Short Time Fourier Transform and frequency peaks compared for the different sites. It was noted that sensor location does not have a large impact on vibration magnitudes and identifying the frequency components present in the signal. However, from the signatures obtained there is not enough variation in magnitude or frequency components to suggest that this method can identify the type of fault present.

# **LIMITATIONS OF USE**

The Council of the University of Southern Queensland, its Faculty of Health, Engineering & Sciences, and the staff of the University of Southern Queensland, do not accept any responsibility for the truth, accuracy or completeness of material contained within or associated with this dissertation.

Persons using all or any part of this material do so at their own risk, and not at the risk of the Council of the University of Southern Queensland, its Faculty of Health, Engineering & Sciences or the staff of the University of Southern Queensland.

This dissertation reports an educational exercise and has no purpose or validity beyond this exercise. The sole purpose of the course pair entitled “Research Project” is to contribute to the overall education within the student’s chosen degree program. This document, the associated hardware, software, drawings, and other material set out in the associated appendices should not be used for any other purpose: if they are so used, it is entirely at the risk of the user.

# CERTIFICATION

I certify that the ideas, designs and experimental work, results, analyses and conclusions set out in this dissertation are entirely my own effort, except where otherwise indicated and acknowledged.

I further certify that the work is original and has not been previously submitted for assessment in any other course or institution, except where specifically stated.

**Dean Starkey**

**Student Number 0061038897**

---

Signature

---

Date

# **ACKNOWLEDGEMENTS**

I would like to thank my supervisors Mr Andreas Helwig and Dr Narottam Das for their guidance, feedback and support during this project.

I would also like to thank my work colleague Matthew Gibson for providing the DGA information and reports needed. I would like to thank my parents for their continued support and encouragement throughout this journey. Above all I would like to thank my wife Yasmin Starkey for patiently supporting me in my studies over the past five years.

<b>ABSTRACT .....</b>	<b>i</b>
<b>LIMITATIONS OF USE .....</b>	<b>ii</b>
<b>CERTIFICATION .....</b>	<b>iii</b>
<b>ACKNOWLEDGEMENTS.....</b>	<b>iv</b>
<b>LIST OF FIGURES .....</b>	<b>ix</b>
<b>LIST OF TABLES .....</b>	<b>xiii</b>
<b>CHAPTER 1 .....</b>	<b>15</b>
<b>INTRODUCTION.....</b>	<b>15</b>
1.1    Project Aim .....	16
1.2    Project Objectives .....	17
1.3    Ethical Considerations .....	18
<b>CHAPTER 2 .....</b>	<b>20</b>
<b>BACKGROUND AND LITERATURE .....</b>	<b>20</b>
2.1    Magnetostriction .....	20
2.2    Acoustic Signals.....	22
2.3    Traditional Condition Monitoring.....	23
2.3.1    Chemical Detection.....	24
2.3.2    Acoustic Detection.....	26
2.3.3    Source location of partial discharge.....	26
2.4    Vibroacoustic Condition Monitoring .....	28
2.5    Signal Processing .....	29

2.5.1	Shannon Nyquist Sampling Theorem .....	29
2.5.2	Fast Fourier Transform (FFT).....	30
2.5.3	Window Function.....	30
2.5.4	Power Spectral Density (PSD) .....	31
2.6	Review of Information .....	32
<b>CHAPTER 3 .....</b>		<b>33</b>
<b>METHODOLOGY.....</b>		<b>33</b>
3.1	Measurement System Hardware .....	33
3.1.1	Sensor Selection .....	34
3.1.2	Microcontroller .....	38
3.1.3	Resource Analysis.....	40
3.2	Measurement System Software.....	42
3.3	Controlled Experiment.....	44
3.4	Field Testing .....	46
3.4.1	Condition Analysis.....	46
3.4.2	Site Selection.....	47
3.5	Risk Assessment .....	50
<b>CHAPTER 4 .....</b>		<b>51</b>
<b>VIBRATION MONITORING SYSTEM.....</b>		<b>51</b>

4.1	Hardware Development .....	51
4.1.1	Wireless communication .....	51
4.1.2	Sensor Encapsulation .....	55
4.2	Software Development.....	58
4.2.1	Programming Software .....	59
4.2.2	GUI Layout and Structure.....	61
4.2.3	Program Initialisation.....	62
4.2.4	Process Measurement.....	64
4.2.5	Feature Extraction .....	66
4.2.6	Exporting and Loading Data .....	68
4.2.7	Filtering Data .....	70
<b>CHAPTER 6.....</b>		<b>72</b>
<b>TESTING AND RESULTS.....</b>		<b>72</b>
6.1	Initial System Testing .....	72
6.2	Wireless testing .....	73
6.2.1	Transmission data accuracy .....	74
6.2.2	Transmission Range Testing.....	75
6.3	Controlled Experiment .....	76
6.4	Field Testing .....	78



6.4.1	Location of accelerometer.....	79
6.4.2	Duration of testing .....	81
6.4.3	Interpretation of results .....	81
6.5	DGA results.....	82
6.6	Load analysis.....	83
6.7	Effect of sensor position .....	85
6.8	Spectrum analysis .....	86
6.9	Summary of Results .....	92
<b>CHAPTER 7 .....</b>		<b>93</b>
<b>CONCLUSION.....</b>		<b>93</b>
7.1	Further Work.....	93
<b>REFERENCES.....</b>		<b>95</b>
<b>Appendix A.</b>	<b>Project Specification .....</b>	<b>99</b>
<b>Appendix B.</b>	<b>MATLAB Code .....</b>	<b>100</b>
<b>Appendix C.</b>	<b>Arduino Code .....</b>	<b>113</b>
<b>Appendix D.</b>	<b>DGA Reports .....</b>	<b>116</b>
<b>Appendix E.</b>	<b>Load Profiles.....</b>	<b>122</b>
<b>Appendix F.</b>	<b>Risk Analysis .....</b>	<b>124</b>
<b>Appendix G.</b>	<b>ADXL345 Data Sheet.....</b>	<b>127</b>

# LIST OF FIGURES

Figure 2-1 Principle of AE (IEEE Std C57.127 2007) .....	23
Figure 2-2 Gas Generation Chart (Singh & Bandyopadhyay 2010) .....	25
Figure 2-3 PD Experiment (Kozako <i>et al.</i> 2009) .....	26
Figure 3-1 Signal capture and data flow .....	34
Figure 3-2 Basic accelerometer structure (Aggarwal 2010) .....	35
Figure 3-3 ADXL345 (Left), ADXL345 Development Board (Right) (element14) .	38
Figure 3-4 ADXL345 sensor functional block diagram (Analogue Devices 2009) ..	38
Figure 3-5 Arduino UNO (Left), Raspberry Pi (Right) (element14) .....	40
Figure 3-6 Simplified program flow chart .....	43
Figure 3-7 Experimental setup representation .....	44
Figure 3-8 Vibration motor construction (top), Uxcell vibration motor (bottom) (Microdrives 2016).....	45
Figure 3-9 Site 1 (Top Left), Site 2 (Top Right), Site 3 (Middle Left), Site 4 (Middle Right), Site 5 (Bottom Left), Site 6 (Bottom Right) .....	48
Figure 4-1 XBee communication Arduino to PC.....	51
Figure 4-2 Wireless shield UART selection switch.....	52
Figure 4-3 ZigBee mesh network example .....	53
Figure 4-4 Configuration of XBee using XCTU.....	55

Figure 4-5 Shore Hardness Scale (Smooth On 2012) .....	56
Figure 4-6 Sensor Terminated (Top Left), Casting Process (Top Right), Curing Process (Bottom Left), Finished Result (Bottom Right).....	58
Figure 4-7 Software Process Plan .....	59
Figure 4-8 Arduino IDE Programming Environment .....	60
Figure 4-9 New Matlab GUIDE (Top), Developed Matlab GUIDE (Bottom).....	61
Figure 4-10 Vibration Monitoring System User Interface .....	62
Figure 4-11 Before Initialisation (Left), Program Running (Right) .....	62
Figure 4-12 Serial Communication Parameters .....	63
Figure 4-13 Prior to Serial Connection (Left), Successful Serial Connection (Right) .....	64
Figure 4-14 Arduino IDE Serial Monitor Output .....	64
Figure 4-15 Real-time Vibration Measurement Display.....	65
Figure 4-16 Two Examples of Bad Reading.....	66
Figure 4-17 Real-time Signal Information (Left), Statistical Information (Right) ....	66
Figure 4-18 Histogram & PDF (Top), All Acceleration Data Plot (Bottom) .....	67
Figure 4-19 Fast Fourier Transform (Top), Power Spectral Density (Bottom) .....	68
Figure 4-20 Auto and Manual Export (Left), Export to directory (Right).....	69
Figure 4-21 Log File Output .....	69

Figure 4-22 Load Historical Data Files.....	70
Figure 4-23 Filter Selection .....	71
Figure 4-24 EMA Filter (Top), Low Pass Filter (Bottom) .....	71
Figure 6-1 ADXL345 initial test setup (Left), ADXL345 initial wiring (Right).....	72
Figure 6-2 Initial XBee communication .....	73
Figure 6-3 Zone substation transmission range testing.....	76
Figure 6-4 Vibration system and motor test setup .....	77
Figure 6-5 Portion of sampled signal .....	77
Figure 6-6 Frequency components of vibration motor signal.....	78
Figure 6-7 Proposed accelerometer placement (Borucki 2012).....	79
Figure 6-8 Site 5 rear wall mount (Top), Site 5 side wall mount (Bottom).....	80
Figure 6-9 STFT plot for Site 1 – 2D (Left), 3D (Right).....	82
Figure 6-10 Site 3 load profile .....	84
Figure 6-11 Site 4 load profile .....	85
Figure 6-12 Sites 1 and 2 sensor location comparison.....	86
Figure 6-13 Sites 1 to 3 Short Time Fourier Transform .....	87
Figure 6-14 Sites 4 to 6 Short Time Fourier Transform .....	88
Figure 6-15 Sites 1 to 6 Power Spectral Density .....	89
Figure 6-16 Sites 1 to 6 frequency peak comparison.....	90

Figure 6-17 Sites 3 and 4 frequency peak comparison ..... 91

# LIST OF TABLES

Table 2-1 Recommended DGA limits (Wang, Vandermaar & Srivastava 2002).....	24
Table 3-1 Desired sensor specification .....	36
Table 3-2 MEMS sensor comparison.....	37
Table 3-3 Development platform comparison .....	39
Table 3-4 Resource Analysis .....	40
Table 3-5 Vibration motor characteristics .....	45
Table 3-6 Dissolved Gas Analysis Condition Limits (IEEE Std C57.104 2009) .....	47
Table 3-7 Sites 1 to 6 comparison.....	47
Table 3-8 DGA Results, Sites 1, 2 & 3 .....	49
Table 3-9 Transformer Condition Assessment .....	49
Table 4-1 XBee Pro characteristics (Digi 2014).....	51
Table 4-2 Wireless Network Settings .....	54
Table 4-3 Encapsulation Resin Comparison .....	56
Table 4-4 Epoxy Resin ER2074 properties.....	57
Table 6-1 Direct USB connection testing .....	74
Table 6-2 XBee wireless connection testing.....	74
Table 6-3 Summary of DGA results .....	83
Table 6-4 Load profile summary.....	83

Table 7-1 Risk Matrix .....	125
Table 7-2 Hazards and Controls.....	125

# CHAPTER 1

## INTRODUCTION

Power transformers provide the crucial link between the generation, transmission and distribution of electricity to customers at different voltage levels. Broadly the study of power transformers is a key field in the power engineering discipline. Whilst the fundamental electrical principles have not changed since transformers were introduced the consumer dependence on efficient power networks has driven the investment and research in this area.

The life expectancy of a transformer is linked to the deterioration of both solid and liquid oil dielectric insulation over time. A transformers life expectancy is typically 25 to 35 years through design however in practice transformers can remain in service for over 60 years. The predominant causes of transformer insulation degradation are from electrical, thermal and mechanical stresses. Electrical stress is caused by over current or over voltage conditions which can lead to thermal stress from increased winding and hotspot temperatures. Mechanical stress is primarily a result of the electromagnetic constriction forces known as magnetostriction and is the main source of transformer noise.

Due to the critical role of transformers in the electricity network, power utilities place importance on the maintenance and condition monitoring of these assets. A traditional diagnostic method for transformer condition monitoring is through testing the insulating oil and is known as dissolved gas analysis (DGA). This type of testing involves a number of oil samples being taken over time and examining of the presence and concentration of certain types of dissolved gases. Depending on the type of gas and ratio in the sample conclusions can be drawn about the condition of a transformers internal insulation.

A possible result of the deterioration of insulation is the presence of partial discharge (PD) inside the transformer tank. The presence of PD is of concern and if



left unmonitored can result in a critical failure of the asset. Whilst the most common practice to determine transformer insulation condition is to analyse the presence of dissolved gases, it has also been extensively demonstrated that acoustic emission methods in the high frequency range can be used to determine a correlation of PD activity and the source location of PD. Presently the detection and location of PD is not considered an exact science (IEEE Std C57.127 2007) although acoustic methods provide another source of information to assist in condition assessment.

The primary source of transformer noise is from vibrations in the laminated iron core where electromagnetic attraction between the laminated sheets and constantly changing magnetic flux causes structural deformations of the magnetic material. It is recognised that vibration measurement is not a traditional method of analysis used for condition assessment of transformers. The Vibroacoustic Method (VM) is one suggested by Bartoletti *et al.* (2004) and consists of measuring mechanical vibrations for transformer condition assessment. Current literature on transformer vibration is limited and in depth studies are required before vibration characteristics can be used as a diagnostic method and predictive maintenance tool. This research aims to identify the validity of monitoring transformer vibroacoustic emissions in the low frequency range as a predictive maintenance tool for the precursor events that lead to PD and potential transformer failure.

## **1.1 Project Aim**

To date research on condition monitoring of transformers using acoustic emissions in the high frequency range has been extensively undertaken for the identification and location of PD in a transformer. Most research of PD in oil suggests in addition to the measurable electrical pulses, acoustic waves occur in the ultra-sonic range and electromagnetic waves up to the Ultra High Frequency (UHF) range. Developing a further understanding of partial discharge in transformers is believed to have a direct cost saving by enhancing risk management, replacement strategies and investment decisions. The successful measurement and analysis of acoustic noise signatures are a

tool in predictive maintenance and intervention strategies to prevent catastrophic failure of a transformer.

In contrast to this research the monitoring of transformer vibrations in the low frequency range is not a widely adopted condition monitoring method. It is theorised that by spectral analysis of the acoustic signal in the low frequency range and by looking at the changes in the specific frequency peaks over time a determination can be made to depict if these source changes are internal to the transformer or by external harmonic loads. Through this research a greater understanding of transformer vibration signatures is the objective.

The development of a low cost vibration monitoring system is required as part of this project. Modern acoustic emission methods for transformer condition assessment in the high frequency range require specialised piezoelectric sensors, signal conditioning and data acquisition units that are considerably expensive. Vibration condition monitoring systems are not applied to transformers and those that do exist for rotating plant are also expensive. As power utilities look to be more efficient and reduce capital expenditure the design of cost effective condition monitoring systems contributes to the field of maintenance engineering.

## **1.2 Project Objectives**

The specific project objectives can be summarised as follows:

- Develop an inexpensive real-time vibration measuring system
- Test the developed system using a controlled experiment
- Select suitable substations and analyse DGA results
- Monitor selected substations using developed system
- Analyse substation vibration signatures to determine a correlation with DGA results

### 1.3 Ethical Considerations

The consequences and ethics of this research project have been considered in terms of the improvements to the field of transformer condition assessment and the potential social and economic impacts of this work. Some of the relevant ethical principles to this research project are:

- Scientific integrity – adhering to professional values, and practices ensuring objectivity and clarity.
- Data integrity – quality of the procedure, documentation and reporting of results.
- Social responsibility – considering the impacts of the research on the environment and society.

This research requires access to organisational data from NSW electricity utility Ausgrid, for which approval has been granted. The data obtained from this organisation is not classified however some of the specific locations and names of substations have been changed. Data integrity is maintained and no changes have been made to results or measurements.

Social responsibility in this research requires the mitigation of health and safety risks. The risks which exist in the application of this work are due to the nature of working in close proximity to electricity. Whilst this risk exists for persons involved in working near transformers, it is intended that the methods explained are only used by adequately trained and experienced persons. The outcomes of this work are not expected to present any health and safety impacts to the environment or general public.

Transformers are an essential part of the distribution network and as population density is increased, transformers are installed closer to the general populace. The causes and remedies of transformer noise and vibrations has been the study of many researchers over many generations. Any consequential effects of this research to the environment or public are considered positive. The study of transformer noise and vibration is one

that only aids to decrease the impact of noise and improve the efficiency of power networks.

# CHAPTER 2

## BACKGROUND AND LITERATURE

### 2.1 Magnetostriction

Magnetostriction is the property of ferromagnetic materials which causes them to change shape when subject to a magnetic field. Transformers inherently undergo mechanical forces which are a result of the constantly fluctuating magnetic field permeating the iron core. Mechanical forces are produced when the magnetisable material inside a transformer changes configuration. The mechanical forces that result from these magnetic forces lead to periodic changes of length in the laminated core structure. Transformers are designed such that the core laminations are pressed together which suppresses these mechanical vibrations. Noise however is still generated by these forces and can be a significant impact to the environment, public and life of the asset (Transformers 2003).

Magnetostriction is characterised by the coefficient  $\epsilon$ , and can be represented by (Kulkarni & Khaparde 2004):

$$\epsilon = \frac{\Delta l}{l} \quad (1)$$

Where  $l$  and  $\Delta l$  are the length of the lamination sheet and its change. The magnetostriction coefficient depends on the instantaneous measure of flux density given by the following expression:

$$\epsilon(t) = \sum_{v=1}^n K_v B^{2v} \quad (2)$$

Where  $B$  represents instantaneous flux density and  $K_v$  is a coefficient depending on type of lamination. The magnetostriction force  $F$  is then given by:

$$F = \epsilon(t)EA \quad ( 3 )$$

Where  $E$  represents the modulus of elasticity and  $A$  is the cross sectional area of the lamination.

Early research into magnetostriction effects by George (1931) found vibrations to occur at frequencies which are multiples of the fundamental frequency (50Hz). These effects occur in the low frequency range and are tonal in nature. The vibrations occur at even harmonics of the power frequency and are dominated by that of the 2<sup>nd</sup> harmonic (100Hz). The 'IEEE Standard Test Code for Liquid-Immersed Distribution, Power, and Regulating Transformers' (2016) describes transformer audible noise being composed of three components:

- **Core sound** - Originates from transformer core consisting of primarily even harmonics 2<sup>nd</sup>, 4<sup>th</sup>, 6<sup>th</sup> and 8<sup>th</sup>.
- **Load sound** - Originates from vibrations of the windings and tank walls under load, dominated by the 2<sup>nd</sup> harmonic.
- **Cooling sound** - Typical broadband fan noise at the blade passage frequency.

Transformer noise however does not only occur at even harmonics, in practice transformer noise is found to be made up of frequencies of odd multiples of the fundamental frequency being 1<sup>st</sup>, 3<sup>rd</sup>, 5<sup>th</sup> and 7<sup>th</sup> harmonics. The magnitude of these transformer frequencies is dependent on the transformer construction and transformer load.

Other sources that accelerate insulation damage include severe load faults, lightning strikes, load induced current harmonics as well as transformation harmonics from the voltage transformation process. Further to the noise generated by magnetostriction is the potential degradation and accelerated aging causing paper to chaff and pressboard blocks to loosen between turns and coil groups.

## 2.2 Acoustic Signals

Transformers in normal operation emit acoustic signals and the study of these emissions is aimed at providing an indication of condition and insulation health. Acoustic signals from transformers are known from many studies to be generated from:

- Magnetostriction of the transformer magnetic materials and wound conductors.
- Partial discharge as a result of the mechanical and thermal stress applied to the components inside the transformer tank that result from corona discharge in insulation voids.
- Loosening of packing blocks due to displacement of windings
- Destruction of conductor paper insulation during fault conditions
- Shrinkage and decomposition of the insulation with age.

A definition from AS 60270 (R2015) describes partial discharge (PD) as an electrical discharge that does not completely bridge the insulation between conductors, or conductors and an earthed part of the transformer. PD forms from a concentration of local electrical stress either on or in the insulation and appears as short current pulses. PD is a term used to explain many forms of electrical discharge however these are generally categorised as follows:

- **Internal discharge** - Discharge formed in insulation cavities due to poor manufacture or aged insulation.
- **Surface discharge** - Discharge formed along the surface boundary of typically a solid type of insulation liquid or gas interface.
- **Corona** - Current discharge often initiated around sharp points of conduction generally at air or oil insulation interfaces.
- **Electrical treeing** - Discharge formed over time in a solid dielectric that begins to form permanent conducting tracks across an insulation dielectric surface, often in the pattern of a tree silhouette.

These signals propagate from the source in all directions travelling through intersecting mediums (i.e. oil, mechanical and insulation supports) until the signal arrives at the tank wall. Figure 2-1 shows the principle behind the AE method of detecting PD.

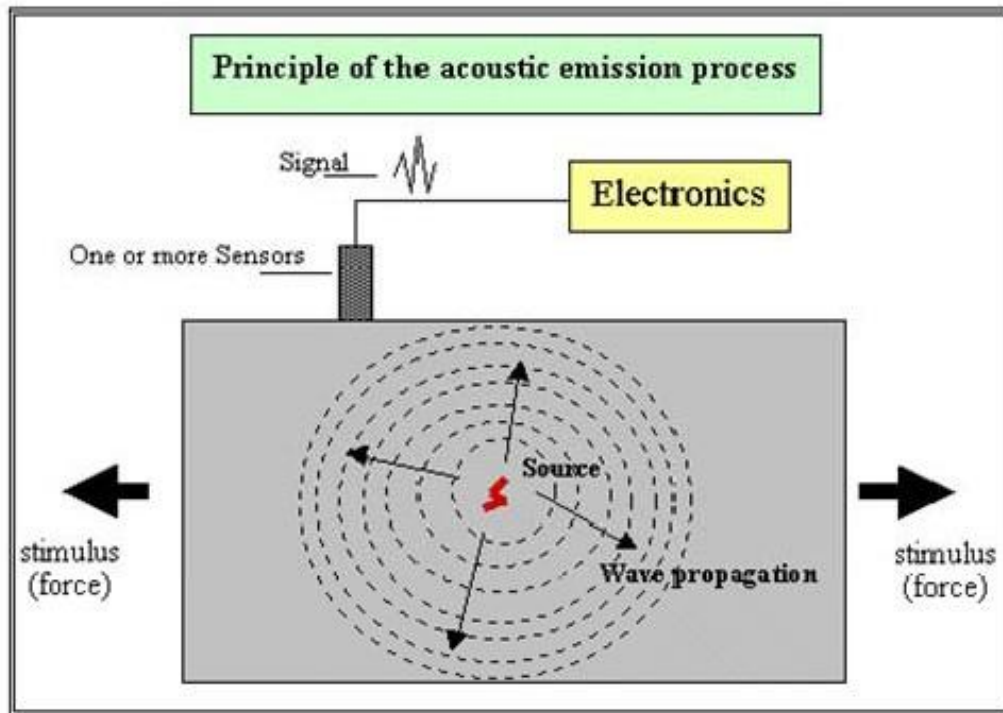


Figure 2-1 Principle of AE (IEEE Std C57.127 2007)

### 2.3 Traditional Condition Monitoring

There are many methods that can be employed for condition monitoring of transformers some of which can be categorised as chemical, electrical, thermal and acoustic. The formation of PD inside a transformer results in chemical changes to the insulating oil and produces electrical, thermal and acoustic emissions that can be detected by various means.



### 2.3.1 Chemical Detection

Oil testing methods such as DGA are conducted offline and can identify the presence of gases based on oil samples periodically taken over time. Wang, Vandermaar and Srivastava (2002) describe a characteristic of partial discharge as high levels of hydrogen with low levels of other gases. However, it is discussed that oil testing does not always provide sufficient information to determine insulation integrity. In addition to DGA, parameters of age, manufacturer and failure history are a vital part of the evaluation. Table 2-1 shows the typical gases tested, concentration thresholds and the age compensation that can be applied. DGA requires expert analysis to draw conclusions about insulation condition due to the complex and variable nature of chemical testing.

Table 2-1 Recommended DGA limits (Wang, Vandermaar & Srivastava 2002)

Table II. Recommend Limits of Dissolved Gases				
Gas	Dornenburg/Stritt	IEEE	Bureau of Reclamation	Age Compensated
Hydrogen	200	100	500	$20n + 50$
Methane	50	120	125	$20n + 50$
Ethane	35	65	75	$20n + 50$
Ethylene	80	50	175	$20n + 50$
Acetylene	5	35	7	$5n + 10$
Carbon Monoxide	500	350	750	$25n + 500$
TDCG* (total of above)		720		$110n + 710$
Carbon Dioxide	6000	2500	10000	$100n + 1500$
$n$ = years in service				
*Total dissolved combustible gas				

The two main causes of gas and chemical formation inside an oil immersed transformer are from thermal and electrical disturbances. The thermal decomposition of both oil and solid insulation exposed to arcing temperatures produces a wide range of gases. The rate at which these gases are generated are produced is dependant exponentially on temperature and volume of material at that temperature (IEEE Std C57.104 2009).

The gases and chemicals that form inside a power transformer generate at different temperatures as shown in Figure 2-2. Both hydrogen and methane begin to form at approximately 150°C, with ethane at 250°C and ethylene produced at 350°C. Traces of acetylene indicate temperatures of at least 500°C whilst large amounts of acetylene indicate temperatures over 700°C. In addition to temperature it should be noted that small quantities of hydrogen, methane and carbon monoxide are produced by the aging process and thermal decomposition of oil impregnated cellulose.

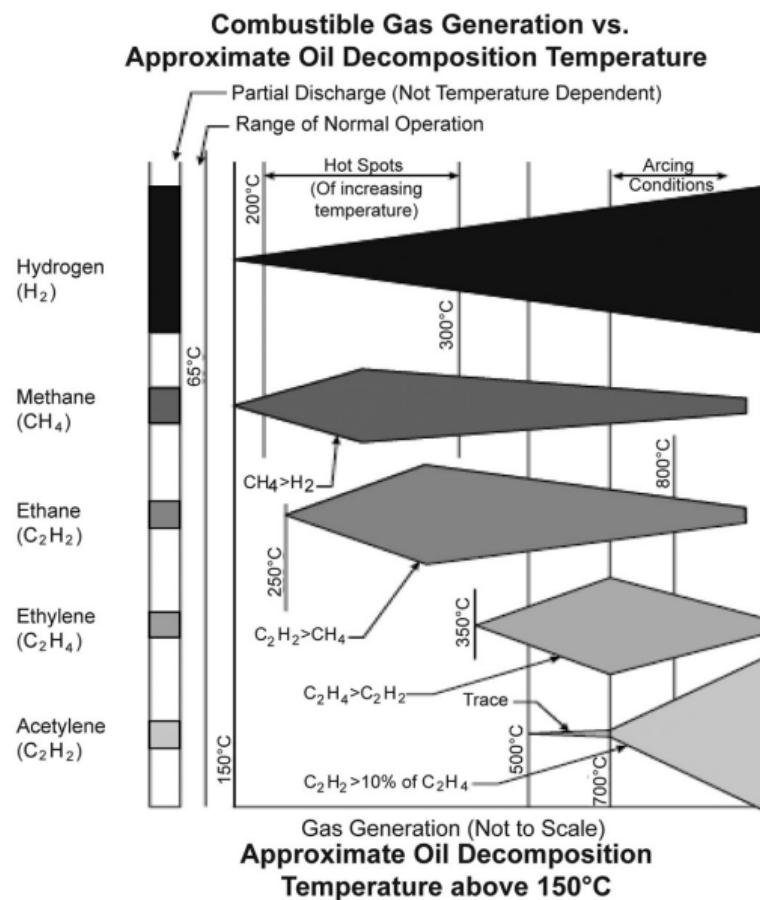


Figure 2-2 Gas Generation Chart (Singh & Bandyopadhyay 2010)

### 2.3.2 Acoustic Detection

Acoustic Emission (AE) methods use ultrasonic piezoelectric transducers to detect the AE generated by the various potential acoustic sources listed. Acoustic sensors can be installed internally or externally on the transformer tank wall to detect the emission. There are benefits of reduced interference and noise from installing the sensors internally although this is not always a practical approach. Installing sensors externally increases the flexibility of the system and is a less invasive approach, and allows for measurement while the transformer remains in operation. Externally mounted sensors require a coupling gel or grease to increase the accuracy of the acoustic measurements and reduce unwanted noise. The types of systems used to measure AE from PD include automated workstations, digital oscilloscopes and continuous online monitoring systems. Figure 2-3 shows an example PD test experiment with externally placed sensors using a digital storage oscilloscope coupled with a preamplifier circuit.

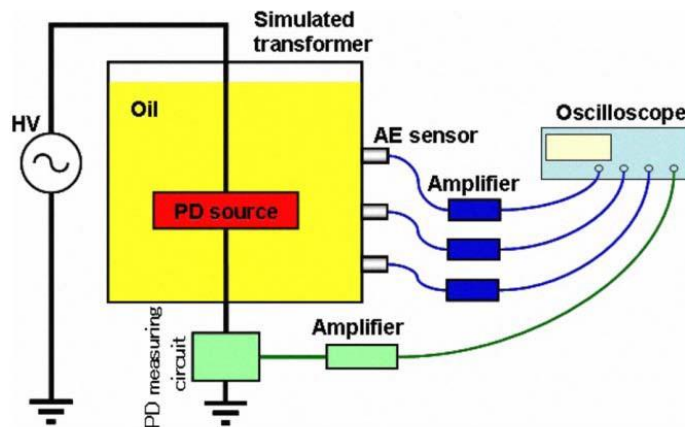


Figure 2-3 PD Experiment (Kozako *et al.* 2009)

### 2.3.3 Source location of partial discharge

A major advantage of AE methods is the possible correlated identification of the acoustic source location within the transformer. The short current pulse generated from PD, or the more cyclic increase in ‘hum’ frequencies of the transformer winding

becoming less restrained by the pressboard blocks has a particular shape, size and frequency. It is the spectral analysis of these signals which can be used to determine the propagation delay between the sensors.

Digital signal processing techniques are required to analyse AE and determine the source location of PD. It is identified in IEEE Standard (2007) that for accurate source location a variety of signal processing techniques can be employed including:

- **Time domain** - Examining the start of a signal in the time domain is the simplest approach.
- **Cross correlation** - Two acoustic sensors are used with one data source delayed in comparison to the other channel. Corresponding data points are multiplied to attain a correlation where the maximum will be given by the real time delay between the signals. A disadvantage of this method would be where there are two different waveforms recorded.
- **Signal mean** - Averaging can be applied to repetitive signals to eliminate stochastic noise. This method reduces the amplitude of random signals nearly to zero revealing the repetitive signal. A disadvantage of this method is that AE signals are not always repetitive in nature and can have varying amplitudes.
- **Fast Fourier Transform** - The signal is decomposed into its natural frequencies so that the spectral densities can be analysed. These densities can be modified mathematically to get an estimate of time delay and source location.
- **Wavelet Transform** - A suitable wavelet technique is employed to analyse the signal and frequency around a certain point in time. This can provide the estimated time delays and yield a more accurate acoustic source location than other methods.

## 2.4 Vibroacoustic Condition Monitoring

The research of transformer vibrations is primarily via the analysis of measured statistical data or through calculation in an established model. A vibroacoustic method of transformer condition assessment describes the measurement of vibrations under a transformers regular operation. This type of condition monitoring while widely adopted by industry for rotating plant is not an industry standard for assessment of transformers. At the core of this method is the analysis of acceleration values and amplitudes of the frequency components.

Borucki (2012) discusses a vibroacoustic method for the assessment of transformer core condition and highlights some of the issues of using this method. As a large variety of transformers are used in operation, the varying size, power and construction type can make determining an effective diagnostic criteria difficult. Another issue is the nonlinearity of the transformers load and induced oil circulation which can generate overlapping vibrations leading to erroneous interpretation of the results. For this research the vibration signals were measured during the transient state when switching a 200kVA transformer under laboratory conditions. The vibration signals were analysed using a Short Time Fourier Transform (STFT) and found to occur in the range 0Hz to 10kHz. It was found that the location of measurement transducer on the transformer tank had no significant influence on the registered signals.

Shengchang, Lingyu and Yanming (2011) further analysed transformer vibrations with respect to the variation of transformers and found that those of the same type have almost identical vibration profiles. Contrary to those findings by Borucki (2012) it was noted that sensor position was important and that transformers of different types could not be used to compare vibration signatures. It was stated that when vibration signatures are compared they must be normalised by the square of the applied voltage and loading current.

In the field of partial discharge measurement Solin, Yolanda and Siregar (2009) used a vibration monitoring technique and determined that the vibration signatures were not

clear enough to detect PD in momentary windows of monitoring. As PD magnitude is influenced by temperature and location of the source it was theorised that only by continuously monitoring a transformer over time could a correlation between PD and vibration signature be determined.

Saponara *et al.* (2015) recognised a key issue in the study of transformer predictive maintenance was the development of a system of tracking mechanical degradation. This work implemented a distributed network of measuring nodes where vibration measurements were taken in the range 100Hz-1kHz. The developed system used capacitive MEMs accelerometers where processing the signal in the frequency domain was done via software using Fast Fourier Transform (FFT). It was recognised in industrial cases where high level background noise is more than 70dB that vibration measurement was the only viable online method to detect mechanical degradation.

## **2.5 Signal Processing**

Stone (2005) highlights that there is much literature on the subject of signal processing and removal of noise although there is little corroboration to which is the best method. Various methods to process and differentiate signals from noise include statistical analysis, neural networks, fuzzy logic, wavelet transformation, fractal analysis and time vs frequency clustering. Statistical analysis involves using the mean, standard deviation, kurtosis and skew to approximate the shape of the signal. The following sections briefly outline some of the key methods used in most literature for processing of vibroacoustic signals.

### **2.5.1 Shannon Nyquist Sampling Theorem**

The Shannon Nyquist Sampling Theorem is an important concept in digital signal processing. The theorem was derived by Harold Nyquist and Claude Shannon and forms a cornerstone of modern signal processing. This theory discovered that aliasing of the signal occurred when the sampling frequency was less than at least twice that of the highest frequency of the signal, this frequency is referred to as the ‘Nyquist

frequency'. More in depth this theorem states that a function of time  $f(t)$  that contains no frequency components greater than  $\omega_c$  is thus band limited and can be constructed by the values of  $f(t)$  at a set of sampling points spaced by  $T < \pi/\omega_c$  seconds (Luo, Ye & Rashid 2010). This signal can be constructed by:

$$f(t) = \sum_{k=-\infty}^{+\infty} e(kT) \frac{\sin v(t, kT)}{v(t, kT)} \quad (4)$$

Where  $v(t, kT) \equiv (\omega_s - \omega_s kT)/2$

### 2.5.2 Fast Fourier Transform (FFT)

The Discrete Fourier Transform (DFT) and Fast Fourier Transform (FFT) are essential mathematical tools to decompose a discretely sampled signal into its frequency components. The Fourier Transform (FT) is the transformation of a continuous time signal and can be defined as:

$$X(\omega) = \int_{-\infty}^{\infty} x(t) e^{-j\omega t} dt, \quad \omega \in (-\infty, \infty) \quad (5)$$

The DFT replaces the infinite integral with the finite sum:

$$X(\omega_k) \equiv \sum_{n=0}^{N-1} x(t_n) \cdot e_k^{-j\omega_k t_n}, \quad k = 0, 1, 2, \dots, N-1 \quad (6)$$

The FFT algorithm has the primary advantage of significantly reduced computation compared to that of DFT. In general, the discrete Fourier coefficients of a signal sampled ' $n$ ' times has  $O(n^2)$  computational complexity. Comparatively when  $n$  is an integer of power 2, the FFT delivers a reduce order of complexity  $O(n \log(n))$ .

### 2.5.3 Window Function

Discrete blocks of digitised time are required by the FFT process and are referred to as 'FFT bins'. To prevent erroneous values, it is necessary to compress the values at

the beginning and end of the cycle. As a signal can only be measured for a specific time period the FT makes the assumption that the signal is repetitive and resulting discontinuities can be introduced. Spectral leakage is related to the spreading in the frequency spectrum, where the signal which should be at one frequency although leaks into all other frequencies (Bores 2012). This leakage is related to the discontinuities at the end of each measurement time and may be reduced by an appropriate window function. The window function in effect multiplies the signal by a function that approaches zero at either end. There are many different types of window functions and to select an appropriate function an estimate of the frequency content of the signal is required.

From the literature the common window functions applied are the Hamming and Hann functions which are sinusoidal in shape. Shreve (1995) highlights that the Hamming window provides better frequency resolution at the expense of amplitude. In comparison the Kaiser-Bessel window is ideal for separating close frequencies as there is less spectral leakage into the side bins however the resolution is less than with Hamming.

#### **2.5.4 Power Spectral Density (PSD)**

The results of vibroacoustic measurement were processed by Zmarzly *et al.* (2014) using the Power Spectral Density function. PSD is useful in showing the strength of variations in energy, which in this case is acceleration as a function of frequency. Random vibrations are those which are not predictable at any point in time unlike that of a sinusoidal vibration. The amplitude of random vibrations cannot be expressed as a function of time mathematically although statistical analysis can determine the probability of occurrence at a specific amplitude. The PSD is the FT of the autocorrelation function and is of use in the analysis of random vibrations.

The autocorrelation of two signals  $s_1(t)$  and  $s_2(t)$  with time delay  $\tau$  is given by (MIT 2010):



$$R_c(\tau) = \langle s_1(t)s_2(t + \tau) \rangle \quad ( 7 )$$

The PSD of the stationary stochastic process defined by the Wiener-Khinchin theorem is then:

$$S(f) = \int_{-\infty}^{\infty} R_c(\tau) e^{-j\omega\tau} d\tau \quad ( 8 )$$

This process is the same for a discrete time process where PSD is given by the DFT of the discrete autocorrelation function:

$$S_x(f) = \sum_{n=-\infty}^{n=\infty} R_x(n) e^{-j\omega n}, \quad -\frac{1}{2} \leq f \leq \frac{1}{2} \quad ( 9 )$$

## 2.6 Review of Information

It is clear from the literature that acoustic measurement techniques to assess transformer condition are not an exact science or widely adopted by industry. Typically, most power utilities rely upon the long standing and proven methods such as chemical testing (DGA) which usually require the transformer to be out of service to take samples. It is evident that only by trend analysis over time can the changes in ‘hum’ frequencies of the vibroacoustic response be used in condition diagnostics. The changes in this acoustic response of the transformer is theorised to be a predictive maintenance tool in the identification of deformation due to faults, damage to magnetic core material, and lessening of restraint of coils by press board blocks and end of winding sheet insulation.

# CHAPTER 3

## METHODOLOGY

Transformer oil with high levels of hydrogen dissolved gas is considered to have a partial discharge occurring within the tank. The project aims to determine a correlation between the high levels of certain gases in oil and the vibroacoustic emissions that should be present. The refined project objectives are:

- Develop a real-time vibration measuring system using non-commercial grade and cost effective equipment.
- Test the developed system using a controlled experiment
- Monitor substations to determine correlation between vibration signatures and DGA results

This project involves the development of a cost effective measurement system which forms a crucial part of this project. The vulnerability to noise is a major issue with vibration measurements and to determine if the device operates as expected a controlled experiment is required. The controlled experiment will simulate a known vibration signal using a vibration motor. Following a confirmed working system, a selected set of transformers will be monitored to determine if there is a correlation between DGA and results from vibroacoustic testing.

### 3.1 Measurement System Hardware

A system needs to be developed that is capable of close to real time data processing. The components need to be carefully selected such that the sampling rate at minimum satisfies that of the Nyquist frequency. From the literature it is evident that vibrations in the range of 100Hz-400Hz is the target bandwidth. The system will require four main components including a sensor, signal conditioning circuitry, microcontroller and connection mechanism to a computer as shown in the data flow in Figure 3-1.

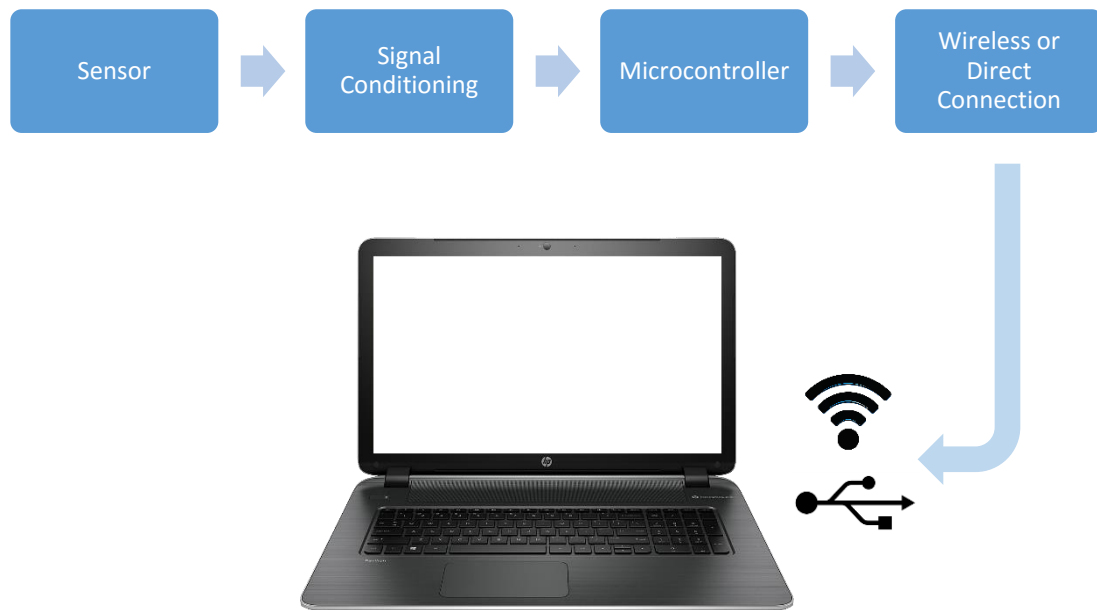


Figure 3-1 Signal capture and data flow

### 3.1.1 Sensor Selection

The choice of sensor is important to obtain valid results with requirements for stable performance and good frequency response. Conventional piezoelectric sensors are used in industry for vibration based condition monitoring however come at a high cost. The sensors alone can cost thousands of dollars and require signal conditioning amplifiers which are considerably more expensive. The recent advances in embedded accelerometers make for a much cheaper alternative and these often have built in signal conditioning.

Micro-ElectroMechanical Systems (MEMS) are a small low powered and low cost accelerometer that have enabled innovation in smartphones and modern electronic devices. Advancements in MEMS performance and accuracy have seen industrial applications specifically in vibration measurement. MEMS utilise semiconductor technology with single chip components to provide a low mass sensor with high

sensitivity and shock resistance. External acceleration is measured via the changes in capacitance of a proof mass between fixed electrodes as shown in Figure 3-2.

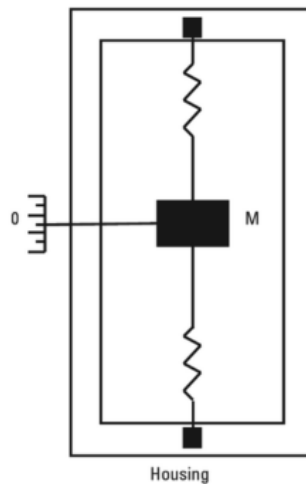


Figure 3-2 Basic accelerometer structure (Aggarwal 2010)

The advantage of these types of sensors is that they can generally measure a wide band from 0Hz (DC) to 32kHz, although most inexpensive MEMS have a range of 0 to 1kHz. In addition to good low frequency response MEMS sensors have the advantage of good temperature sensitivity. A disadvantage of capacitive accelerometers is the sensitivity to electromagnetic interference and reduced resolution due to the unit size and plate surface area. To avoid erroneous results a suitable casing is required to reduce susceptibility to interference. Important characteristics to consider in the selection of a suitable MEMS sensors with multiple axis are:

- **Bandwidth** – Operating capability of the sensor in Hz
- **Operating Temperature** – Operating temperature range in °C
- **Measurement range** – The acceleration range in  $g$
- **Sensitivity** - Acceleration change expressed as a ratio due to output signal.  
For digital sensors in LSB/g or for analogue in mV/g.
- **Noise density** – Noise generated per power unit of bandwidth in  $mg/\sqrt{Hz}$

- **Cross axis sensitivity** – Measure of effects on an axis when acceleration is applied to a differing axis in %.

Each transformer will have a vibration profile, when this vibration is linear a single axis sensor can be used however a tri axis sensor will add more flexibility as the vibration direction can be detected. Therefore, only those MEMS sensors with three axis measurement points have been considered.

A list of basic specifications has been determined for the desired application in Table 3-1. The acceleration range has been specified based on findings by Saponara et al. (2015). Bandwidth is an important factor in determining which sensor to use. For digital MEMS sensors the bandwidth is limited by half the data rate of the signal conditioning circuitry, to satisfy the Nyquist frequency. Operating temperature is also of importance due to the high temperatures experienced during transformer peak loads.

Table 3-1 Desired sensor specification

Specification	Min	Max
Bandwidth	50Hz	1kHz
Interface	Digital or Analogue	N/A
Operating Temperature	-10°C	70°C
Acceleration range	0.5g	5g
Noise Density	0g/ $\sqrt{Hz}$	10mg/ $\sqrt{Hz}$
Cross Axis Sensitivity	-2%	2%
Cost	0	\$150

Taking into consideration these important characteristics, commonly available sensors have been compared in Table 3-2. These sensors all come supplied on a development board which provides some minor circuitry and wire connection points. All the sensors listed operate within a range of  $-40^{\circ}C$  to  $+85^{\circ}C$  and are considered suitable.

Table 3-2 MEMS sensor comparison

Sensor	Band. width. Hz	Interface	Acc. Range	Sensitivity	Noise Density mg/ $\sqrt{\text{Hz}}$	Cross Axis Sens.	Cost
ADXL345	6.25 to 1600	SPI / I2C	$\pm 2\text{g}$ to $\pm 16\text{g}$	3.9mg/LSB 31.2mg/LSB	3.9 31.2	$\pm 1\%$	\$84
ADXL343	0.1 to 1600	SPI	$\pm 2\text{g}$ to $\pm 16\text{g}$	3.9mg/LSB 31.2mg/LSB	4.2 34.3	$\pm 1\%$	\$60
ADIS16209	0 to 50	SPI	$\pm 1.7\text{g}$	0.24mg/LSB	0.19	$\pm 2\%$	\$161
ADXL375	0 to 1000	SPI / I2C	$\pm 200\text{g}$	49mg/LSB	5	$\pm 2.5\%$	\$60
LIS331AL	0 to 1000	Analogue	$\pm 2\text{g}$	145mV/g	0.3	$\pm 2\%$	\$71
BMA150	25 to 1500	I2C	$\pm 2\text{g}$ to $\pm 8\text{g}$	256mg/LSB	0.5	$\pm 2\%$	\$42

From the analysed MEMS sensors, the ADXL345 shown in Figure 3-3 has been chosen as it meets all desired criteria. The ADXL345 is a small and thin 3mm x 5mm x 1mm package and has a selectable measurement range of  $\pm 2\text{g}$ ,  $\pm 4\text{g}$ ,  $\pm 8\text{g}$  and  $\pm 16\text{g}$ . It is envisaged that for this application  $\pm 2\text{g}$  will be used, with testing required validate the correct range. The digital communication protocols I<sup>2</sup>C and SPI are available and it is envisaged that SPI will be the simplest to implement for this application. An embedded 32 level First In First Out (FIFO) buffer as shown in Figure 3-4 is used to store information that cannot be read immediately. This type of buffering is a useful way of storing the data that arrives asynchronously and allows a decreased interaction between the microcontroller and the sensor thus saving considerable power. Due to the sensitive structure of the development board, suitable encapsulation of the accelerometer is required for thermal, mechanical and water resistant protection. The device can be set in a suitable electrical epoxy resin once the appropriate connections have been made.

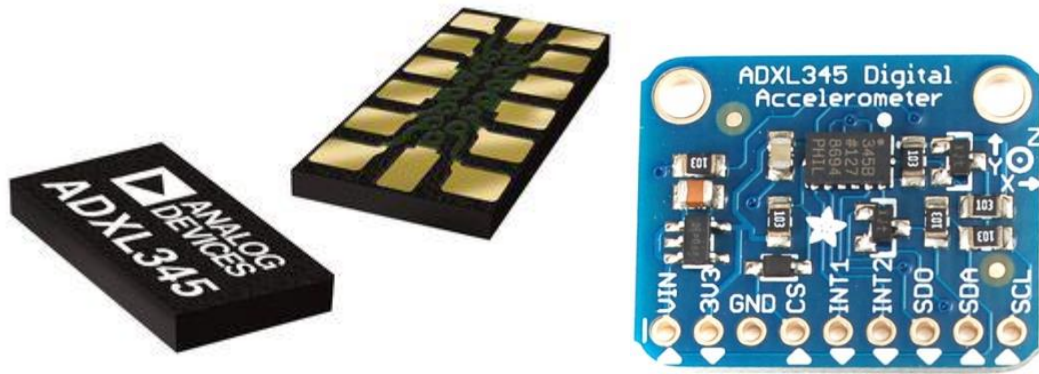


Figure 3-3 ADXL345 (Left), ADXL345 Development Board (Right) (element14)

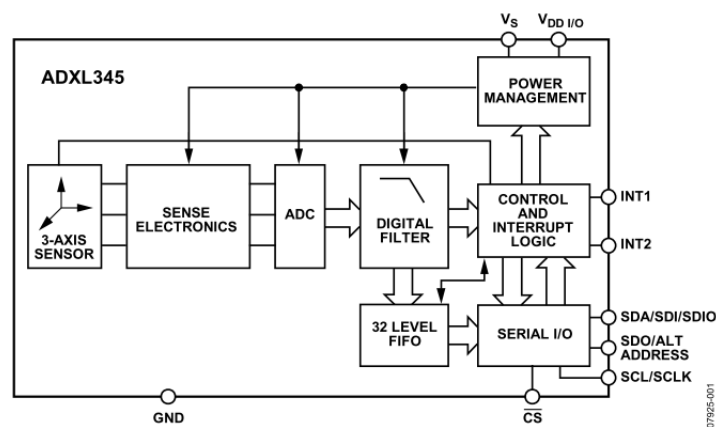


Figure 3-4 ADXL345 sensor functional block diagram (Analogue Devices 2009)

### 3.1.2 Microcontroller

A small, cost effective and efficient microcontroller is required to process the signal. The two most commonly used development platforms are the Raspberry Pi and Arduino. The Arduino is a microcontroller that includes an on board Analogue to Digital Converter (ADC) which makes it ideal for applications involving external sensors. In comparison, the Raspberry Pi is a functional minicomputer and requires an operating system. A core comparison of these development platforms is shown in Table 3-3.

Table 3-3 Development platform comparison

Attribute	Arduino UNO	Raspberry Pi 3
Architecture	ATmega328P	ARM Cortex A53
Storage	32kB	microSD Card
Clock Speed	16MHz	1.2GHz
RAM	2kB	1GB
USB	✓	✓
SPI	✓	✓
USART	✓	✓
I2C	✓	✓
ADC	✓	-
Operating System	-	Linux
Language	C, C++	C++, Java, Python
Cost	\$49	\$56

The Arduino by this comparison can be assumed to be inferior however for the proposed application it is still considered suitable. Both the Arduino and Raspberry Pi can be interfaced with a laptop via direct serial connection (USB) or wirelessly using the ZigBee communication protocol and a wireless XBee shield. This data can be directly analysed using the MATLAB programming environment.

The Arduino has less overheads in comparison with the Raspberry Pi as it simply executes the written code as the firmware interpretes it without an operating system. The Raspberry Pi programming environment can be considered more complex due to the Linux environment and Python language. The clear advantages of the Raspberry Pi are the processing power and operating system functionality however the hardware connections are not as distinct in comparison with the Arduino. The main purpose of an Arduino is for sensor applications with greter flexibility for inputs and outputs. After consideration of both platforms the Arduino as shown left in Figure 3-5 is the chosen development microcontroller for this application.



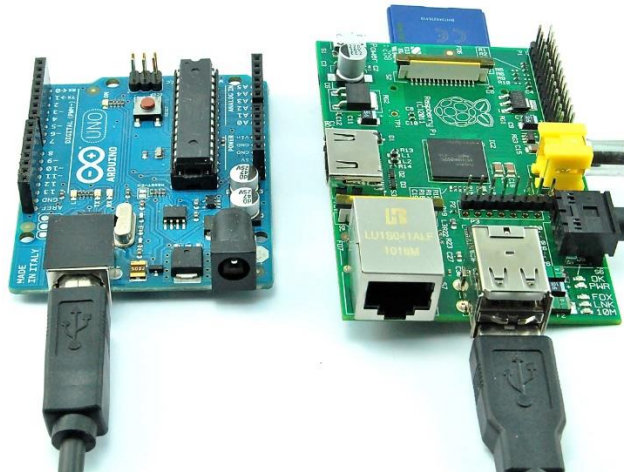

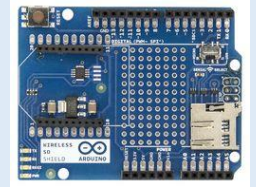



Figure 3-5 Arduino UNO (Left), Raspberry Pi (Right) (element14)

### 3.1.3 Resource Analysis

Hardware resources required for the build of the measurement system are considered in Table 3-4.

Table 3-4 Resource Analysis

Resource	Image	Source	Qty	Comments	Cost
Arduino UNO		Element14	1	MCU development platform	\$49
Arduino prototype board, wireless and SD card shield		Element14	1	For connection of XBee wireless modules and SD card	\$28
Accelerometer ADXL345		Element14	1	Tri axis accelerometer mounted on PCB	\$84

Resource	Image	Source	Qty	Comments	Cost
PRO power 0.055mm <sup>2</sup> 6 core screened cable		Element14	10m	Cable for connection from sensor to Arduino	\$28
XBee PRO wireless module		Element14	2	Wireless module for communication between PC and Arduino	\$106
XBee Explorer USB		Australian Robotics	1	Serial base unit for XBee. For programming and communicating between XBee and PC.	\$39
DC Vibration Motor		Zoxoro Australia	1	DC vibration motor for testing sensor response	\$30
Lithium rechargeable battery and charger		Little Bird Electronics	1	Rechargeable battery supply for Arduino	\$57
Arduino enclosure		Little Bird Electronics	1	Enclosure to house Arduino	\$25
Electrolube Epoxy, White		Element14	250g	Epoxy resin for electrical encapsulation and potting	\$30

**TOTAL: \$476**

### 3.2 Measurement System Software

To capture the data from the ADXL345 a suitable program is to be developed to communicate between the microcontroller and sensor. Firmware for the sensor is to be created in the Arduino IDE programming environment and uploaded to the microcontroller. The sensor will communicate in SPI with the microcontroller sending the measurement readings as ASCII characters to the microcontroller at a high data rate. The microcontroller is to perform minimal on board processing of the measurements as to not slow the data flow. To maintain real time data capture the signal processing is to be performed on a laptop computer with suitable processing capabilities.

A Graphical User Interface (GUI) is to be developed in MATLAB for real time processing. The idea behind a user interface is from commercial vibration monitoring systems which offer real time processing. An advantage of vibration condition monitoring is that the user can make decisions about the health of an asset often instantly without the need for post processing. The user should be able to have instant access to the vibration data and be able to make assessments without returning to the office to analyse the results.

Signal processing of the acquired vibration signal is to be performed by the software developed. As the proposed sensing is not time coherent the non-zero values at the start and end of sensing will cause spectral leakage, degrading the resolution when using FFT. The application of a window function in MATLAB can be used in addition to FFT for analysis. Whilst analysing the signal using FFT is for a specific moment in time it is important that the user be updated with the frequency components in real time also. With the above taken into consideration the simplified program flow chart is shown in Figure 3-6.

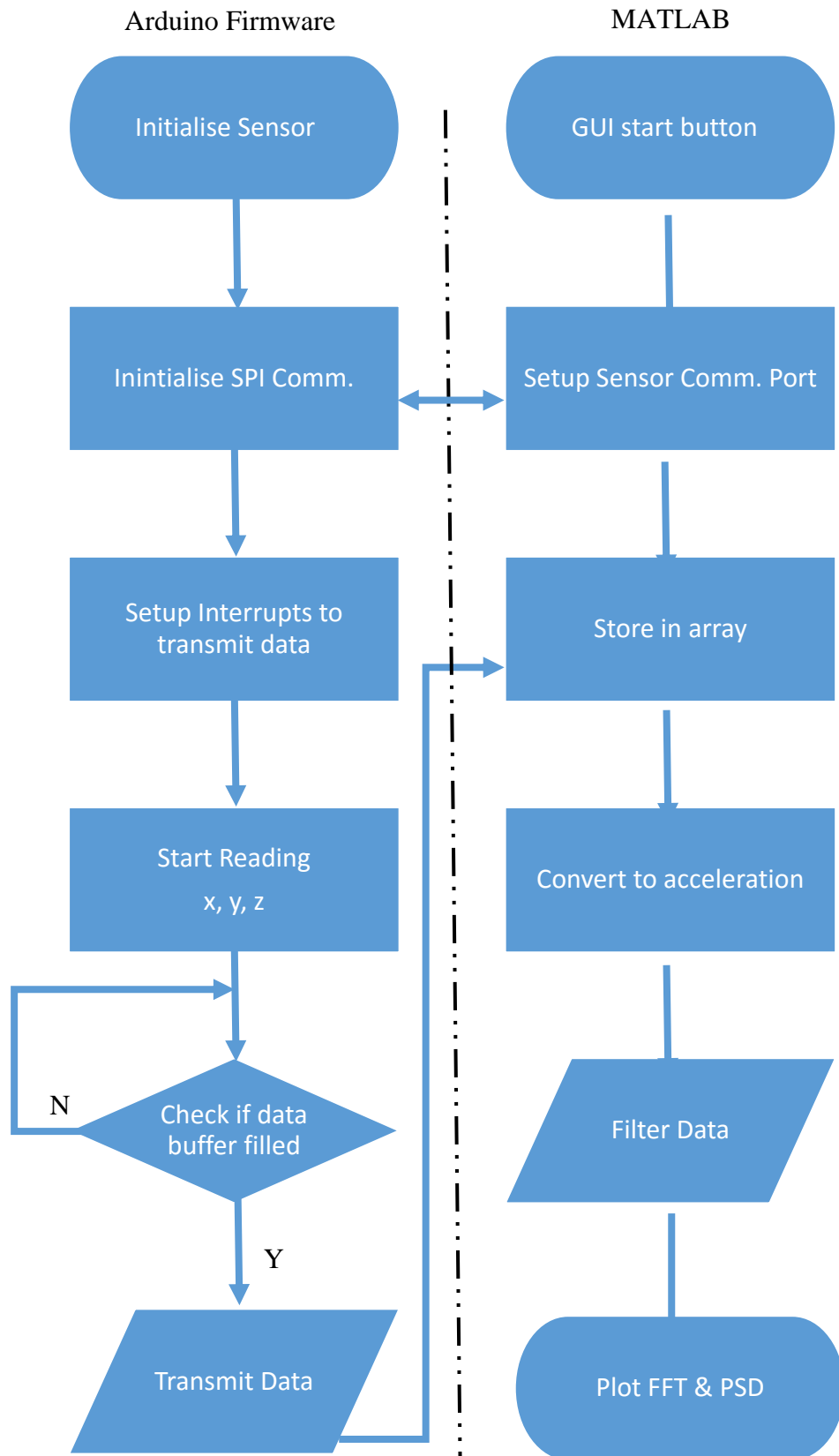


Figure 3-6 Simplified program flow chart

### 3.3 Controlled Experiment

A controlled experiment will simulate the vibrations at a particular frequency to ensure that the sensors are operating correctly. This experiment utilises a DC magnetic vibration motor which will simulate vibrations at a known frequency. The sensor is attached to the vibration motor with a suitable coupling gel and connected to the microcontroller. A series of tests are to be conducted and results analysed in real time and post processing applied. The measurement set up is shown in Figure 3-7.

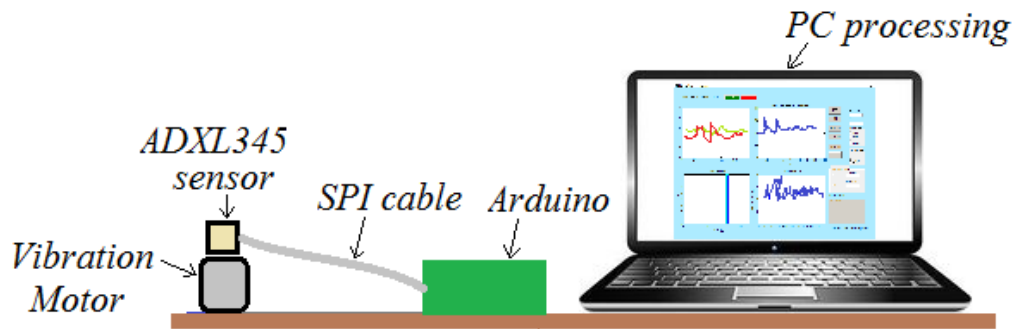


Figure 3-7 Experimental setup representation

A vibration motor has a large range of applications and has been used by researchers including Saponara et al. (2015) to validate accelerometer readings to a known source. A cylinder type vibration motor has a DC motor of similar type construction to that shown in Figure 3-8. The motor vibrates due to the off centred mass attached to the end of the rotating shaft. The vibration force can be adjusted by the mass connected to the shaft and the frequency is a function of the motor speed in revolutions per minute given by the following equations.

$$f_{vibration} = \frac{MotorRPM}{60} \quad (10)$$

$$F_{vibration} = mr\omega^2 \quad (11)$$

Where  $m$  = mass,  $r$  = offset distance,  $\omega$  = speed of motor

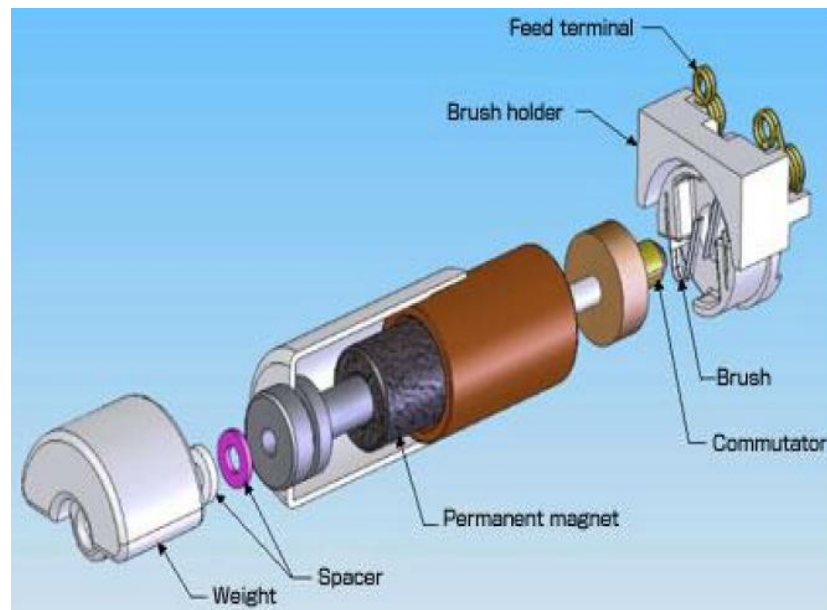


Figure 3-8 Vibration motor construction (top), Uxcell vibration motor (bottom)  
(Microdrives 2016)

Table 3-5 outlines the manufacturer specifications for the chosen vibration motor.

Table 3-5 Vibration motor characteristics

Attribute	Uxcell Vibration motor
Voltage	DC 6-24V
Speed	2 – 10000 RPM
Dimensions	25 x 38 mm
Vibration frequency	1 to 167 Hz
Vibration Size	10 x 8mm

### 3.4 Field Testing

Test reports for substations where DGA reveals high levels of H<sub>2</sub> are analysed with assistance from experts in this field to obtain a suitable list of monitoring sites. Following testing, the developed measurement system will be installed at the selected locations and monitored for a period of time. Data will need to be reviewed between installation at new locations to determine if there are any fundamental flaws with the system and that the results are as expected. In addition to a site with insulation degradation a location is selected which is assumed to have no degradation. The site where insulation integrity is maintained is measured to provide a baseline for comparison.

#### 3.4.1 Condition Analysis

Challenges were encountered in the selection of suitable sites due to the lack of records and history kept on substation DGA results. Survey results were made available from 2016 data although no past history was obtained for specific sites. There are difficulties in assessing DGA results if a location has no previous measurement history. A four level criteria developed by IEEE Std C57.104 (2009) is recommended where historical readings are not available. This method has been adopted which uses concentrations to make determinations on the condition as follows:

- **Condition 1** – Indicates the transformer is operating satisfactorily
- **Condition 2** – Indicates greater than normal combustion levels. Action should be taken to establish a trend.
- **Condition 3** – Indicates a high level of decomposition. Immediate action should be taken to establish a trend.
- **Condition 4** – Indicates excessive decomposition. Continued operation could result in failure.

The four condition criteria utilises the concentration levels in Table 3-6.

Table 3-6 Dissolved Gas Analysis Condition Limits (IEEE Std C57.104 2009)

Status	Dissolved key gas concentration limits [ $\mu\text{L/L}$ (ppm) <sup>a</sup> ]							
	Hydrogen (H <sub>2</sub> )	Methane (CH <sub>4</sub> )	Acetylene (C <sub>2</sub> H <sub>2</sub> )	Ethylene (C <sub>2</sub> H <sub>4</sub> )	Ethane (C <sub>2</sub> H <sub>6</sub> )	Carbon monoxide (CO)	Carbon dioxide (CO <sub>2</sub> )	TDCG <sup>b</sup>
Condition 1	100	120	1	50	65	350	2 500	720
Condition 2	101–700	121–400	2–9	51–100	66–100	351–570	2 500–4 000	721–1920
Condition 3	701–1800	401–1000	10–35	101–200	101–150	571–1400	4 001–10 000	1921–4630
Condition 4	>1800	>1000	>35	>200	>150	>1400	>10 000	>4630
NOTE 1—Table 1 assumes that no previous tests on the transformer for dissolved gas analysis have been made or that no recent history exists. If a previous analysis exists, it should be reviewed to determine if the situation is stable or unstable. Refer to 6.5.2 for appropriate action(s) to be taken.								
NOTE 2—An ASTM round-robin indicated variability in gas analysis between labs. This should be considered when having gas analysis made by different labs.								

### 3.4.2 Site Selection

Six sites have been selected for field testing based on available DGA reports and are shown in Figure 3-9 as well as compared in the following Table 3-7. The sites chosen are of differing manufacturers, voltage ratios and age with differing insulation condition.

Table 3-7 Sites 1 to 6 comparison

Attribute	Site 1	Site 2	Site 3	Site 4	Site 5	Site 6
Commissioned year	1979	1970	1994	1994	2007	2011
Age in Years as of 9/16	38	46	22	22	9	5
Primary / Secondary (kV)	33/11	33/11	132/11	132/11	66/11	132/11
Nameplate Rating (ONAN)	15MVA	15MVA	25MVA	25MVA	20MVA	30MVA
Manufacturer	Tyree	Standard Waygood	Asea Brown Broveri	Asea Brown Broveri	Wilson	Wilson
Type of Insulation	Oil	Oil	Oil	Oil	Oil	Oil
Vector Group	DYN1	DYN1	YND1	YND1	DYN1	YND1
No of Pumps	1	2	1	1	1	1
No of Fans	6	4	4	4	4	4





Figure 3-9 Site 1 (Top Left), Site 2 (Top Right), Site 3 (Middle Left), Site 4 (Middle Right), Site 5 (Bottom Left), Site 6 (Bottom Right)

The DGA results of these sites are summarised in Table 3-8.

Table 3-8 DGA Results, Sites 1, 2 &amp; 3

Component (ppm)	Formula	Site 1	Site 2	Site 3	Site 4	Site 5	Site 6
Hydrogen	H <sub>2</sub>	213	81	196	28	2.8	6.3
Oxygen	O <sub>2</sub>	1160	969	21000	9310	31900	31400
Nitrogen	N <sub>2</sub>	45600	78500	72500	55500	66300	66800
Methane	CH <sub>4</sub>	92	147	27	4	0.8	0.9
Carbon Monoxide	CO	809	1400	622	746	40	83
Carbon Dioxide	CO <sub>2</sub>	3340	4770	4260	1010	424	534
Ethylene	C <sub>2</sub> H <sub>4</sub>	207	49	38	< 1	0.5	0.6
Ethane	C <sub>2</sub> H <sub>6</sub>	38	117	2	< 1	0.08	0.1
Acetylene	C <sub>2</sub> H <sub>2</sub>	23	11	239	< 1	0	0
Propane	C <sub>3</sub> H <sub>8</sub>	56	132	8	< 1	0.1	0.5
Total Dis. Comb. Gas	TDCG	1438	1937	1131	778	44	91

Through application of the condition criteria shown in Table 3-9, it is evident that Sites 1-3 have serious decomposition. Comments from an expert chemist in is that the DGA results indicate discharges of high energy are probably present at these locations. As a product of the poor results and historical results at site 1 it is planned that the substation be replaced before the end of 2017. Sites 2 and 3 are being routinely tested to monitor any further deterioration in condition. In comparison both sites 5 and 6 results are considered satisfactory and are to act as a baseline measurement.

Table 3-9 Transformer Condition Assessment

Component	Hydrogen (ppm)	Methane (ppm)	Acetylene (ppm)	Ethylene (ppm)	Carbon Monoxide (ppm)	Carbon Dioxide (ppm)	Total Dissolved Combustable Gas (ppm)
Known As	H <sub>2</sub>	CH <sub>4</sub>	C <sub>2</sub> H <sub>2</sub>	C <sub>2</sub> H <sub>4</sub>	CO	CO <sub>2</sub>	TDCG
Site 1	Condition 2	Condition 1	Condition 3	Condition 4	Condition 3	Condition 2	Condition 2
Site 2	Condition 1	Condition 2	Condition 3	Condition 1	Condition 4	Condition 3	Condition 3
Site 3	Condition 2	Condition 1	Condition 4	Condition 1	Condition 3	Condition 3	Condition 2
Site 4	Condition 1	Condition 1	Condition 1	Condition 1	Condition 3	Condition 1	Condition 2
Site 5	Condition 1	Condition 1	Condition 1	Condition 1	Condition 1	Condition 1	Condition 1
Site 6	Condition 1	Condition 1	Condition 1	Condition 1	Condition 1	Condition 1	Condition 1

### 3.5 Risk Assessment

Risks associated with physical safety are assessed and categorised in line with workplace procedures and safe work method statements (SWMS). As part of workplace safety policy before commencing work a hazard assessment check (HAC) form will be required to document worksite specific hazards. This document is to be completed in association with reading the relevant SWMS for the task.

A strategy employed to mitigate risk is applying a hierarchy of controls with the most effective control being elimination and least effective control is the use of personal protective equipment (PPE). Working through the list of controls is a method of reducing the level of risk to the lowest possible, these are:

- |                  |  |
|------------------|--|
| • Eliminate      | Removal of the hazard completely                     |
| • Substitute     | Change process or item to reduce risk                |
| • Isolate        | Use preventative measures                            |
| • Engineer       | Use mechanical aids, barriers etc                    |
| • Administrative | Develop safe work procedures                         |
| • PPE            | Use protective equipment, e.g. gloves, hard hat etc. |

The installation of an acoustic measuring device requires substation access to mount the device on the transformer walls. Gaining access to substations is part of current employment duties and whilst considered a common task in the work place various hazards are introduced and need to be assessed. Risks are standardised using the risk matrix in and common risks associated with working in substations are identified in Appendix F.

# CHAPTER 4

## VIBRATION MONITORING SYSTEM

### 4.1 Hardware Development

#### 4.1.1 Wireless communication

For the monitoring system to be suitable for installation a wireless network connection is required. XBee modems are Arduino compatible and are purpose built on a development board for easy connection with the use of a wireless Arduino Shield as shown in Figure 4-1.

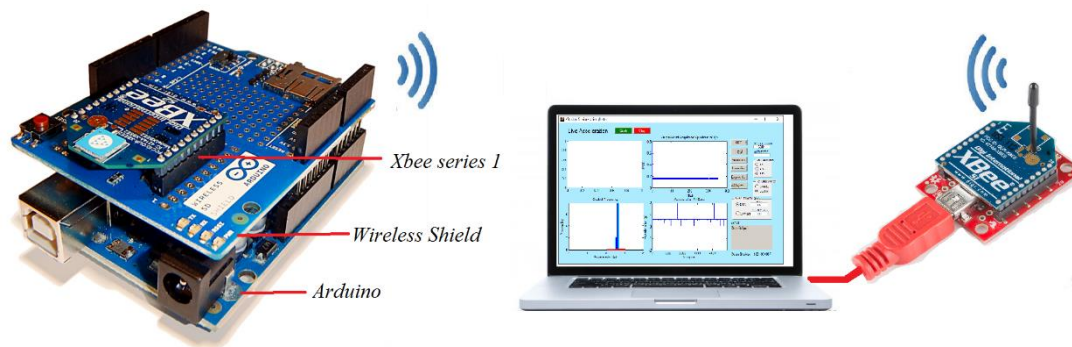


Figure 4-1 XBee communication Arduino to PC

Table 4-1 outlines some of the key characteristics of the XBee Pro.

Table 4-1 XBee Pro characteristics (Digi 2014)

Performance	XBee Pro 802.15.4
RF Data Rate	250kbps
Indoor Urban Range	100 m
Outdoor Range	1.6 km
Transmit Power	60 mW
Receiver Sensitivity	-100 dBm
Serial Data Interface	3.3 V CMOS UART

Performance	XBee Pro 802.15.4
Configuration	API or AT
Frequency Band	2.4 GHz

The Arduino utilises a single hardware UART which is used for either programming the board or serial communication to a PC. An important component of the wireless shield is the MICRO/USB switch. This switch controls the selection between serial communication for software and hardware. To upload a program to the Arduino the DIP switch is in the USB position. To communicate with the PC wirelessly the switch is changed to the Micro position as shown in Figure 4-2.

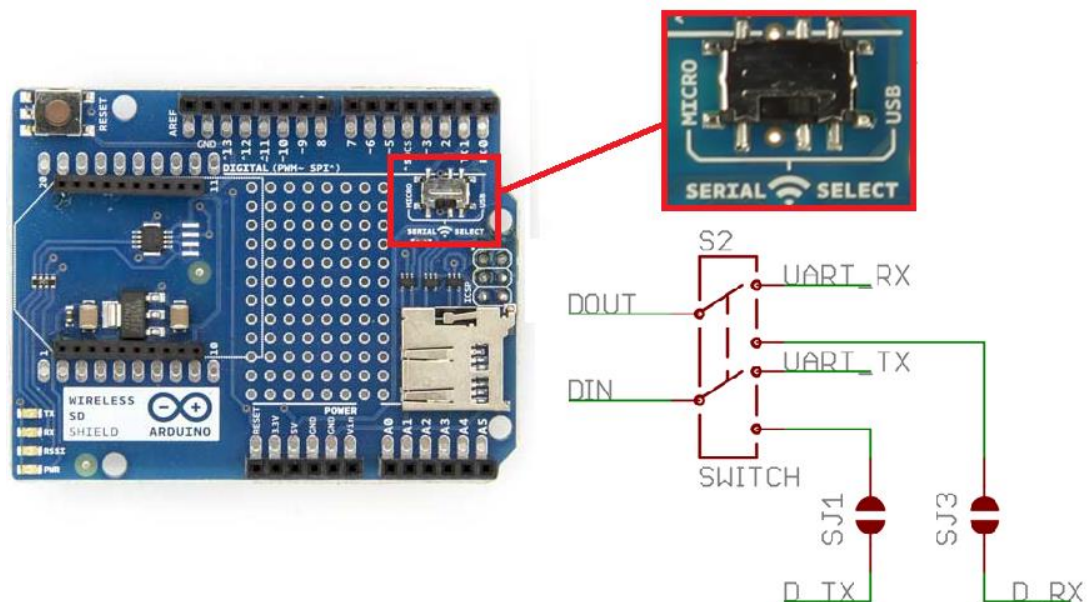


Figure 4-2 Wireless shield UART selection switch

The XBee family of RF modules utilise the ZigBee communication protocol for data transmission. The ZigBee protocol is based on the 802.15.4 standard for wireless communication by IEEE which was developed for low power consumption and battery applications. The standard specifies the access control for low data rate area networks and the physical layer structure. This standard specifies that communication should occur in 5MHz channels from 2.45 to 2.480 GHz. The maximum over the air data rate



is 250 kbps however due to the overheads of this protocol the theoretical maximum is only half this. ZigBee caters for mesh networking which is ideal for this application where the distance between two points say A and B may be out of range, an intermediate radio at point C can be used to forward a message as shown in Figure 4-3.

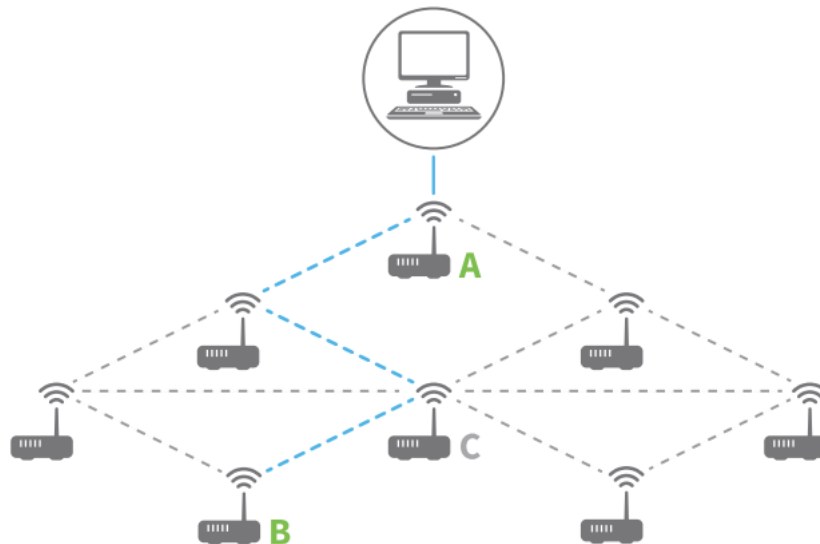


Figure 4-3 ZigBee mesh network example

XBee modules support both AT (transparent) and API serial interfaces. When operating in transparent mode any data sent to the XBee is immediately sent to the module identified by the destination address. For this mode no packet information is required, the data is simply sent to the TX of the transmission XBee and received on the RX of the receiving XBee. Transparent mode is generally used in point to point communication links where data is sent to a single coordinator. In comparison API is a more complicated option however provides sophisticated ability to transmit packets, and allows for changes to the parameters without entering command mode which sends the module to sleep. For this mode data must be formatted in frames with destination and payload information. An advantage of this mode is that the end devices can enter a sleep mode until data is ready for transmitting. For this application the AT mode of operation has been chosen as the communication at this stage is only required between two modules.

Configuring of the XBee modules for wireless communication using AT mode requires the setting of key fields utilising the programming software XCTU developed by Digi. The following key fields are to be set:

- **Channel (CH)**– This setting controls the frequency band.
- **Personal Area Network (ID)** – The network ID in hexadecimal between 0 and 0xFFFF. Communication between two XBees can only occur if they have the same network ID.
- **Destination Address (DH DL)**– Determines which source address the XBee can send data to. To transmit data one XBee must have the same source as the other XBee destination address.
- **Source Address (MY)**– Determines which destination address the XBee can send data to. To transmit data one XBee must have the same destination as the other XBee source address.
- **Interface Data Rate** – The baud rate to transfer data.

Table 4-2 outlines the settings applied to the XBee modules for communication.

Table 4-2 Wireless Network Settings

Setting	Acronym	XBee 1 Coordinator (Arduino)	XBee 2 End Device (PC)
Channel	CH	C	C
PAN ID	ID	0x12F7	0x12F7
Destination Address High	DH	0x00	0x00
Destination Address Low	DL	0x01	0x00
16-bit Source Address	MY	0x00	0x01
Serial Number High	SH	13A200	13A200
Serial Number Low	SL	41022723	40F27D79
Interface Data Rate	BD	115200	115200

The configuration platform for programming the XBee modules is XCTU which allows programming through a graphical user interface as shown in Figure 4-4.

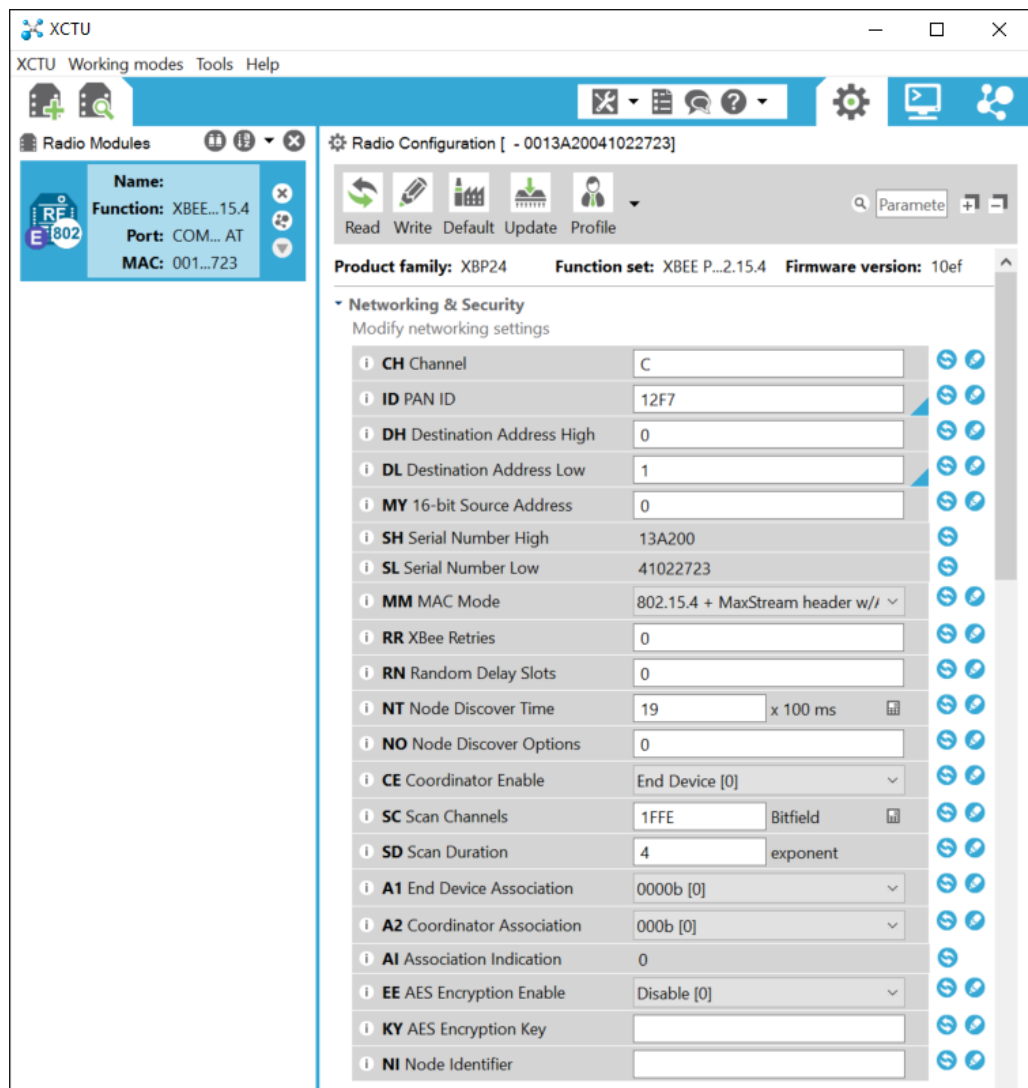


Figure 4-4 Configuration of XBee using XCTU

### 4.1.2 Sensor Encapsulation

The ADXL345 sensor in its development board form is not suitable for mounting on surfaces and measuring vibrations. To safely house the sensor electrical encapsulation is required for electromagnetic, thermal and mechanical protection. There are varying



resin types that can be used for encapsulation including epoxy, polyurethane and silicon resins which have varying cured properties as shown in Table 4-3.

Table 4-3 Encapsulation Resin Comparison

Attribute	Epoxy	Polyurethane	Silicon
Hardness	Hard	Medium	Soft
Adhesion	Excellent	Excellent	Fair
Chemical Resistance	Excellent	Average	Poor
Moisture Resistance	Excellent	Average	Poor
Tensile Strength	Medium	Medium	Low
Tear Strength	High	High	Low
High Temp Operation	Good	Poor	Excellent
Electrical Insulation	Excellent	Fair	Excellent

As the purpose of the sensor device is to measure vibrations the hardness is of significant importance in choosing a resin compound. A soft compound will exhibit a dampening effect on the vibrations and potentially skew the results. As the epoxy resin comes in a wide variety of hardness and has overall good performance it has been chosen as the encapsulation compound. There are differing scales for measuring hardness, the Shore Harness Scale is used for rubbers and plastics. Figure 4-5 shows the Shore Harness Scale with typical examples of products and their values.



Figure 4-5 Shore Hardness Scale (Smooth On 2012)

The epoxy resins that are manufactured by Electrolube come in a variety of chemical compositions with varying properties. The hardness of the Epoxy resin ranges from D50 to D90. A general purpose Epoxy resin ER2074 has been chosen due to its good overall performance and hardness value of D80. The key characteristics of this resins are detailed in Table 4-4.

Table 4-4 Epoxy Resin ER2074 properties

Attribute	ER2074
Shore Hardness	D80
Temperature Range (°C)	-40 to +130
Colour	White
Tensile Strength (MPa)	82
Water Absorption (10 days @ 20°C)	< 0.5%

For encapsulation a mould is required that can be used for casting the sensor. A 40mm hard plastic plumbing end cap is used to house the sensor during the curing process. Two ADXL345 sensors are terminated to a six core screened cable and suspended in the mould and allowed to cure for twenty-four hours as shown in Figure 4-6.

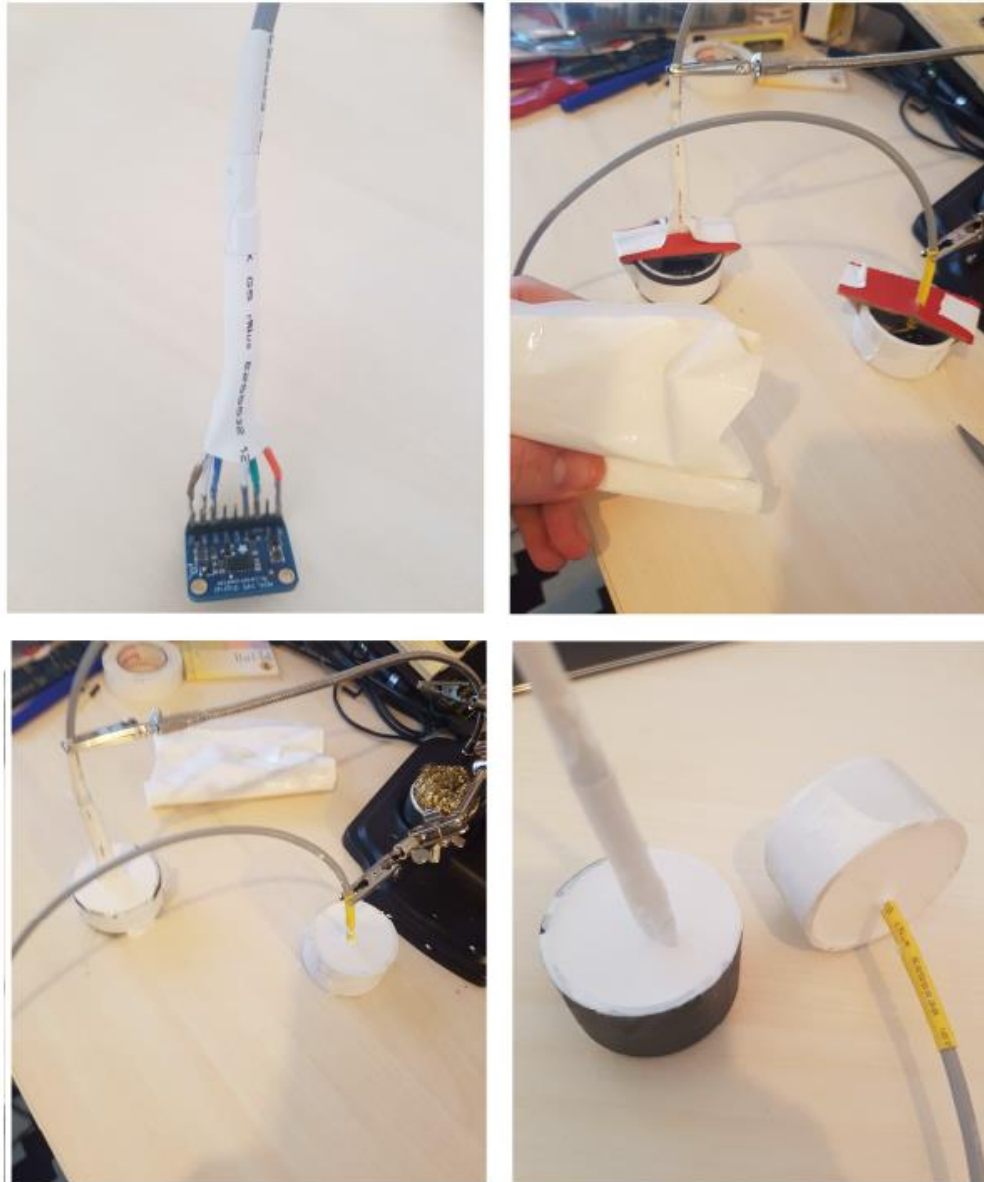


Figure 4-6 Sensor Terminated (Top Left), Casting Process (Top Right),  
Curing Process (Bottom Left), Finished Result (Bottom Right)

## 4.2 Software Development

A major objective of this project is the development of a vibration monitoring system that can analyse historical data and monitor vibrations in real-time. For the system to

be an effective tool the creation of a user friendly software program forms a crucial component. The main process involved in the program is shown in Figure 4-7.

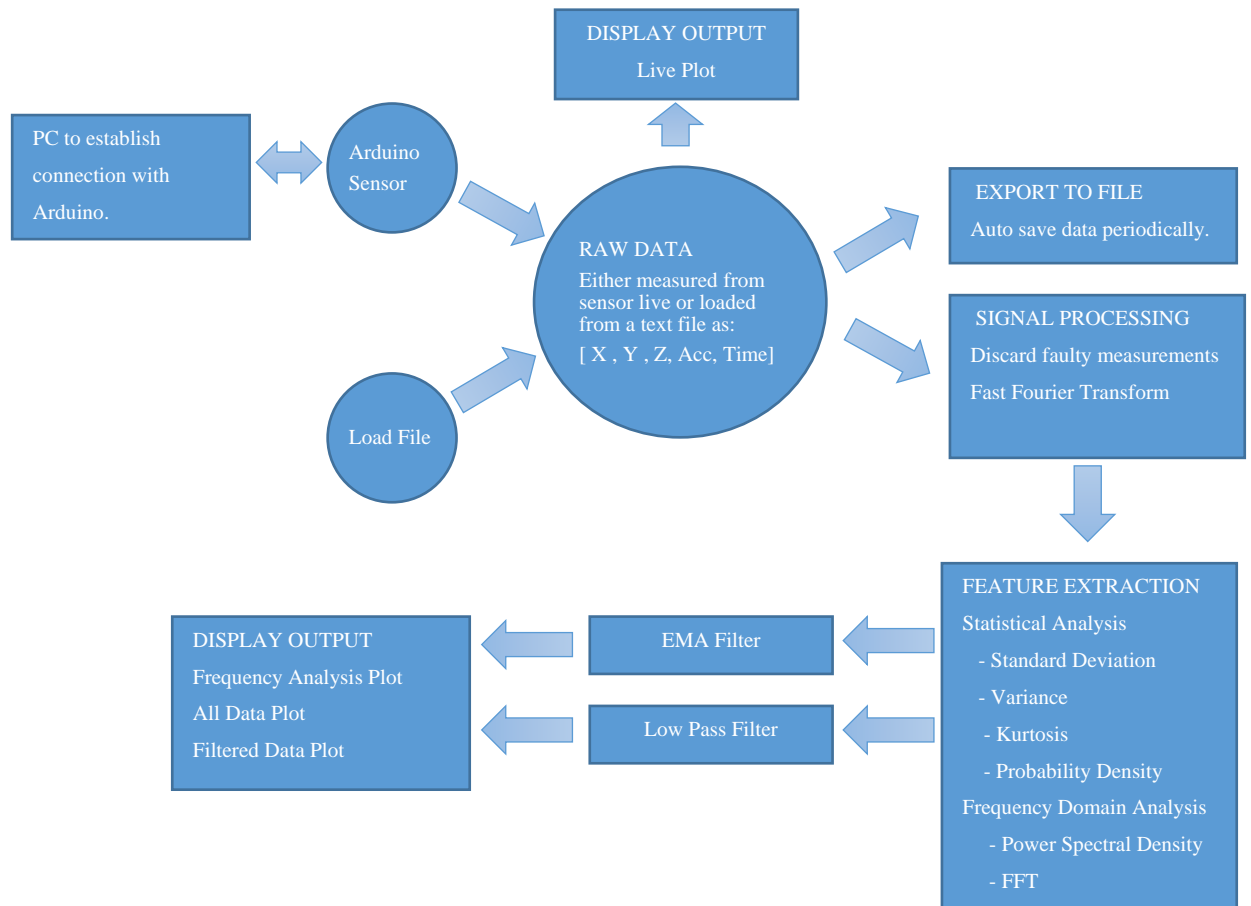


Figure 4-7 Software Process Plan

#### 4.2.1 Programming Software

An Arduino program utilises an open source C and C++ programming environment. A program is known as a ‘sketch’ and can be compiled using the Arduino IDE programming environment as shown in Figure 4-8.

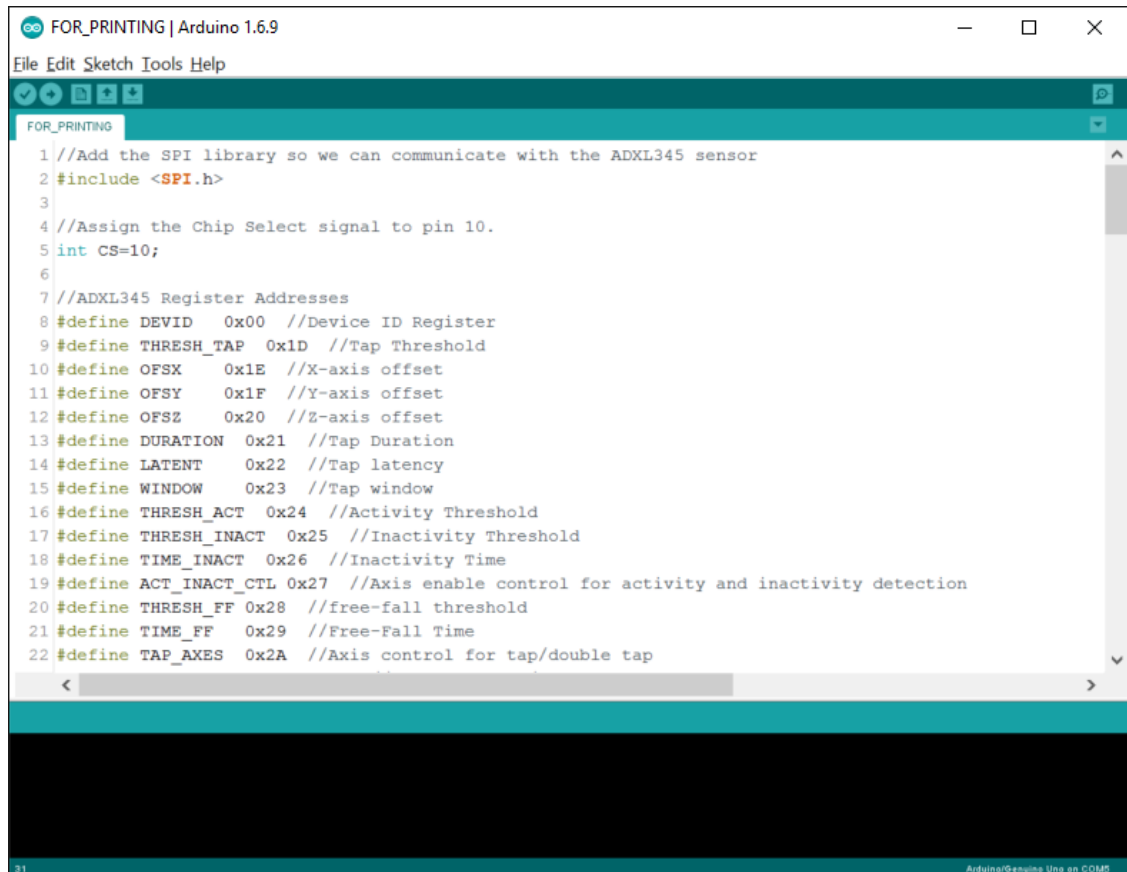


Figure 4-8 Arduino IDE Programming Environment

There are many different programming packages and environments available for data acquisition over a serial interface. The two main programs considered for this task were Matlab and LabVIEW due to availability and prior knowledge. LabVIEW is widely used as a data acquisition tool however the large cost involved with purchasing a professional licence for general users makes Matlab the preferred and chosen option.

The Matlab R2013a Student version has been used with the program designed utilising the Graphical User Interface Development Environment (GUIDE). GUIDE allows the developer to design a custom user interface that employs Matlab functions. The GUIDE layout editor is shown in Figure 4-9.

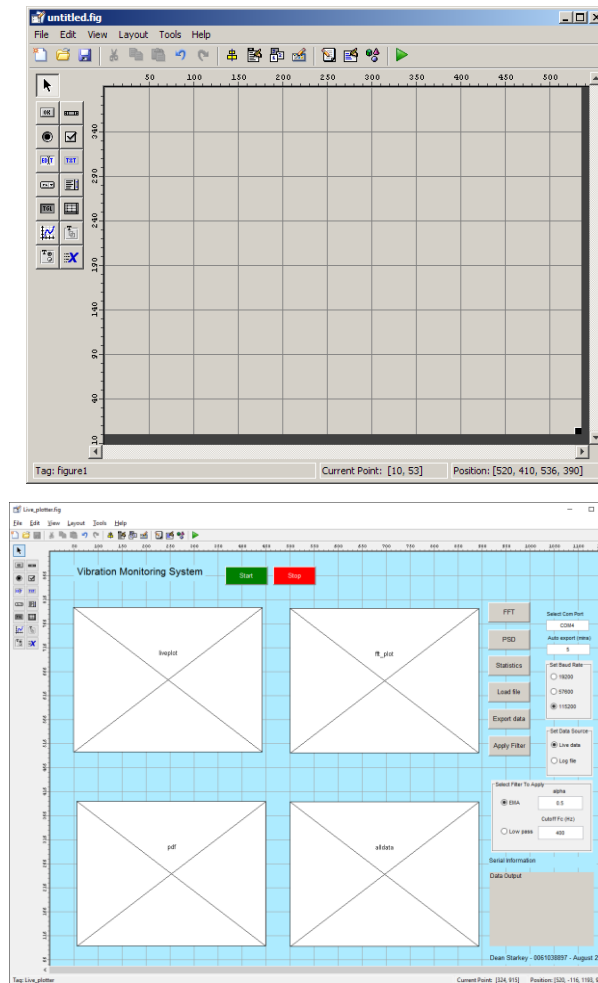


Figure 4-9 New Matlab GUIDE (Top), Developed Matlab GUIDE (Bottom)

## 4.2.2 GUI Layout and Structure

The user interface needs to be able to display vibration measurements in real-time as well as perform feature extraction. The interface is on a single screen that is split into four main windows as shown in Figure 4-10. The top left window is for real time monitoring of the vibration magnitudes in the x, y and z planes of the accelerometer. The chosen measurement range for the accelerometer is +2G to -2G with a scrolling horizontal time axis. The top right window is for spectral analysis in the frequency domain. This screen can be toggled by the user for Power Spectral Density or Fast Fourier Transform. The bottom left window provides the histogram and probability

density function for the data. The bottom right window shows all acceleration data which is calculated off the x, y and z real-time measurements. The right hand panel of the user interface allows the user to change configuration and various parameters.

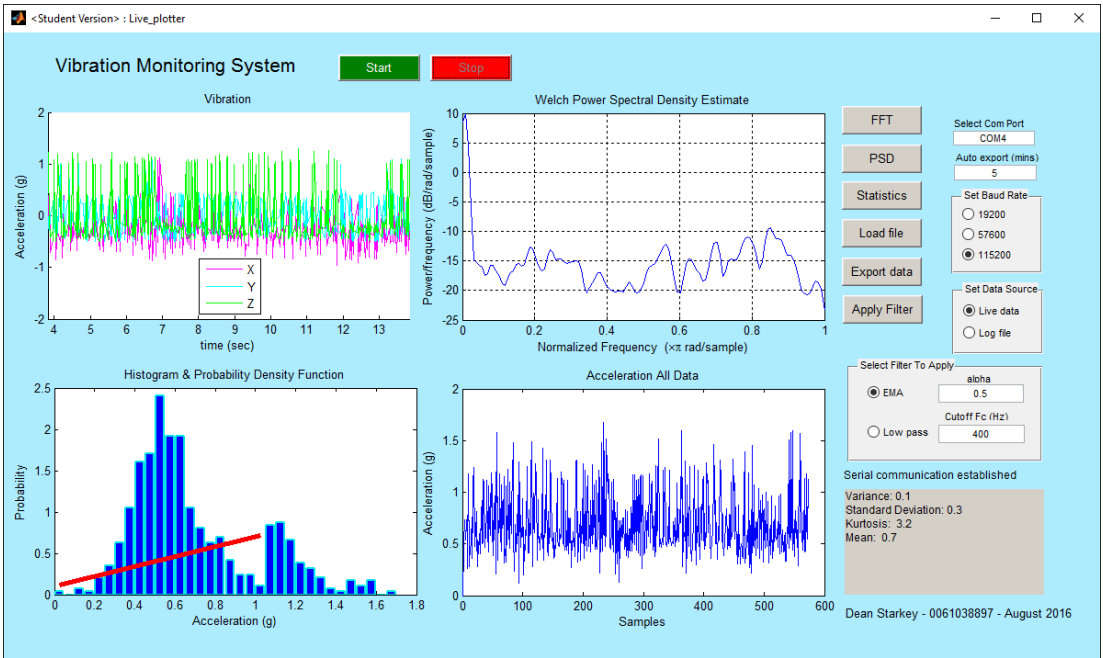


Figure 4-10 Vibration Monitoring System User Interface

### 4.2.3 Program Initialisation

The measurement process is initiated and terminated by the start and stop buttons on the user interface. Once the start button has been pressed the program will initialise and begin to establish a serial connection between the Arduino and Matlab, the word ‘Running’ is displayed on the button until the process is stopped as shown in Figure 4-11.

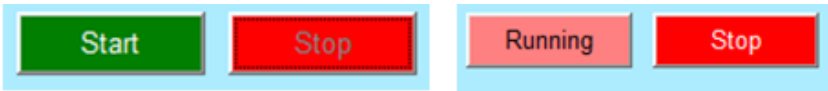


Figure 4-11 Before Initialisation (Left), Program Running (Right)

The following serial communication parameters are then set:

- **Com Port** – The port the computer expects to receive and transmit data over. In this case for wireless communication the device is connected to COM5 and for direct USB the device is connected to COM4.
- **Input buffer size** – The total number of bytes that can be stored in the input buffer during a read operation. A 1MB buffer is set for this application.
- **Flow control** – Data flow control, configured to ‘none’ as handshaking is not to be used
- **Baud rate** – As determined by the user with options of 19200, 57600 and 115200
- **Data bits** – Set to eight data bits, one stop bit no parity bit

By default, the interface is set to utilise live acceleration data. The serial communication parameters are set in the program in conjunction with variable settings specified by the user on the right hand panel as shown in Figure 4-12.

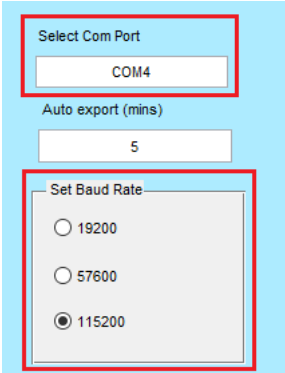


Figure 4-12 Serial Communication Parameters

In the Arduino program a while condition constantly performs a read operation until the character ‘a’ is received from the Matlab program. The Matlab program sends the character ‘a’ then similarly pauses until the Arduino has sent a corresponding character ‘a’ to Matlab. Once this has been completed the serial connection is established and the user is notified through a change on the screen as shown in Figure 4-13. The serial connection is also closed in a similar manner once the stop button has been pressed.



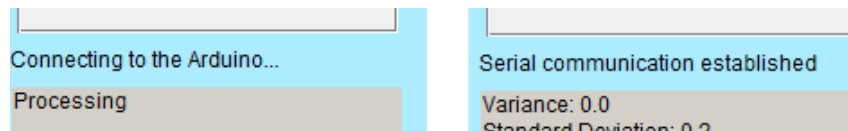


Figure 4-13 Prior to Serial Connection (Left), Successful Serial Connection (Right)

#### 4.2.4 Process Measurement

The Arduino processor continuously reads the data registers from the sensor. The sensor stores 10-bit acceleration values stored as 8 bit bytes which are combined by the processor as integers and sent to the end terminal for processing. The Arduino does minimal on board processing to increase the data rates. The output from the Arduino to the end terminal is “*x, y, z, time(ms)*” in ASCII with a line feed operation forming a continuous column vector as shown in Figure 4-14.

```

COM4 (Arduino/Genuino Uno)
30, 64, -48, 2
32, 64, -50, 2
32, 64, -52, 3
36, 64, -48, 3
32, 64, -48, 4
34, 64, -50, 4
30, 66, -48, 5
34, 64, -40, 5

```

Figure 4-14 Arduino IDE Serial Monitor Output

Matlab reads the ASCII data from the Arduino utilising the serial ‘fscanf’ function. The values are read in the specified format and stored into a vector. The acceleration data in the x, y and z planes has to be converted from a unit less number to acceleration. The resolution at the chosen  $\pm 2G$  range is 10 bits therefore the planar acceleration and total acceleration is given by:

$$C = \left( \frac{4}{2^{10}} \right) = 3.9mg/LSB$$

Where  $C$  is the conversion constant:

$$\begin{bmatrix} x \\ y \\ z \end{bmatrix} (g) = C \begin{bmatrix} x \text{ reading} \\ y \text{ reading} \\ z \text{ reading} \end{bmatrix} \quad (12)$$

$$\text{Resultant acceleration } (g) = \sqrt{x^2 + y^2 + z^2} \quad (13)$$

The calculated x, y and z plane acceleration values are displayed in real-time to the top left window of the user interface. The output is on a horizontal scrolling time display as shown in Figure 4-15.

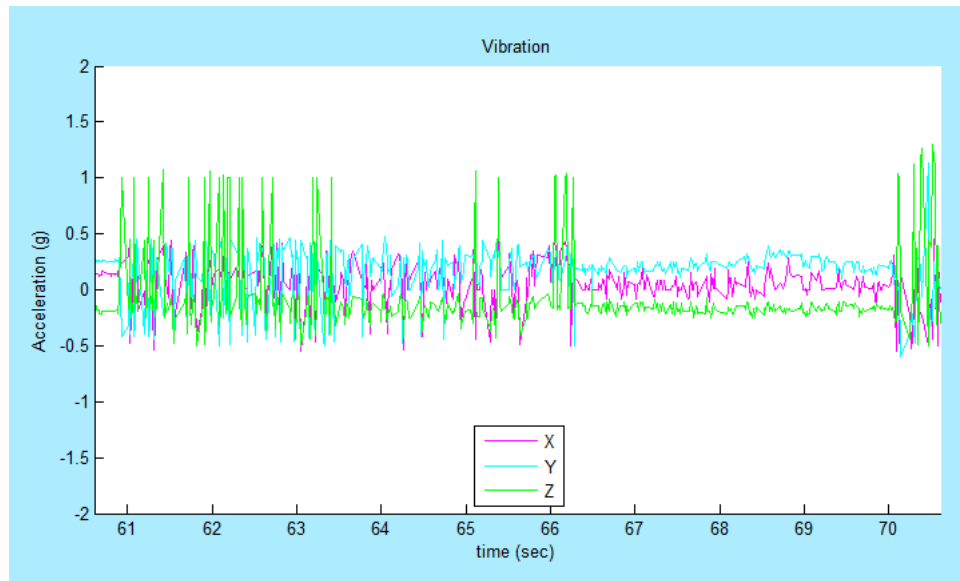


Figure 4-15 Real-time Vibration Measurement Display

As part of the measurement process serial communication errors do occur. It is important for the user to know when communication errors occur as this can potentially skew data results. The program is set to read in the specified format, however when a

failure in the format occurs this is counted as a ‘bad reading’ and displayed to the interface. A typical example of format failed readings is shown in Figure 4-16.

y38, 64, -48, 1	32, 64, -42, 1200
32, 66, -48, 2	34, 64, -44, 1201
36, 66, -54, 2	36, 64, -44,
32, 64, -50, 3	36, 66, -54, 1203

Figure 4-16 Two Examples of Bad Reading

#### 4.2.5 Feature Extraction

Signal feature extraction is the most crucial component of this application for the user to draw conclusions from the measurement results. During live data streaming the sampling frequency is updated based on a one-hundred-point mean difference in sampling time. As data errors are important to identify the bytes available, number of failed readings and calculated data accuracy are displayed to the user. When the bytes available in buffer is close to zero the buffer overflows and subsequent data is lost. Statistical information is also shown when the ‘Statistics’ option is selected from the user interface as shown in Figure 4-17.

Bytes avail. in buffer: 1009	Variance: 0.1
Bad reads: 2	Standard Deviation: 0.3
Samp. freq. (Hz): 885	Kurtosis: 3.2
Data Accuracy (%): 98.02	Mean: 0.7

Figure 4-17 Real-time Signal Information (Left), Statistical Information (Right)

Further analysis in the time domain is provided through the histogram and all acceleration data plot shown in Figure 4-18. All acceleration data is shown to allow the user identify specific acceleration events in time. The histogram and probability density function provide useful statistical information about the distribution of data.

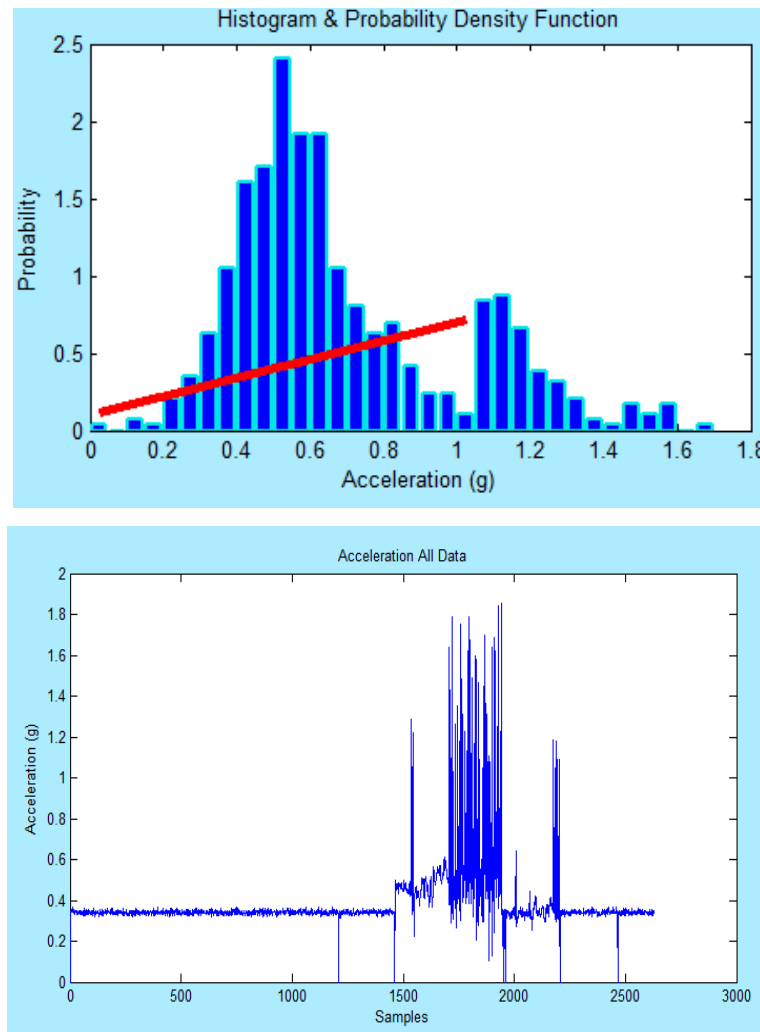


Figure 4-18 Histogram & PDF (Top), All Acceleration Data Plot (Bottom)

Random vibrations are composed of a continuous spectrum of frequencies whilst natural frequencies occur in a system which oscillates when not subject to external force. Shifts which occur in the natural harmonic frequencies can be caused by a change in the condition of a structure. The purpose of analysis in the frequency domain is to extract the unknown frequency components of the signal and identify any discerning trends. Two methods are used for this being the Fast Fourier Transform and Power Spectral Density which are shown in Figure 4-19. The FFT is applied periodically during live data streaming every 50,000 samples. This ensures that the program speed is not compromised whilst providing real-time frequency data.

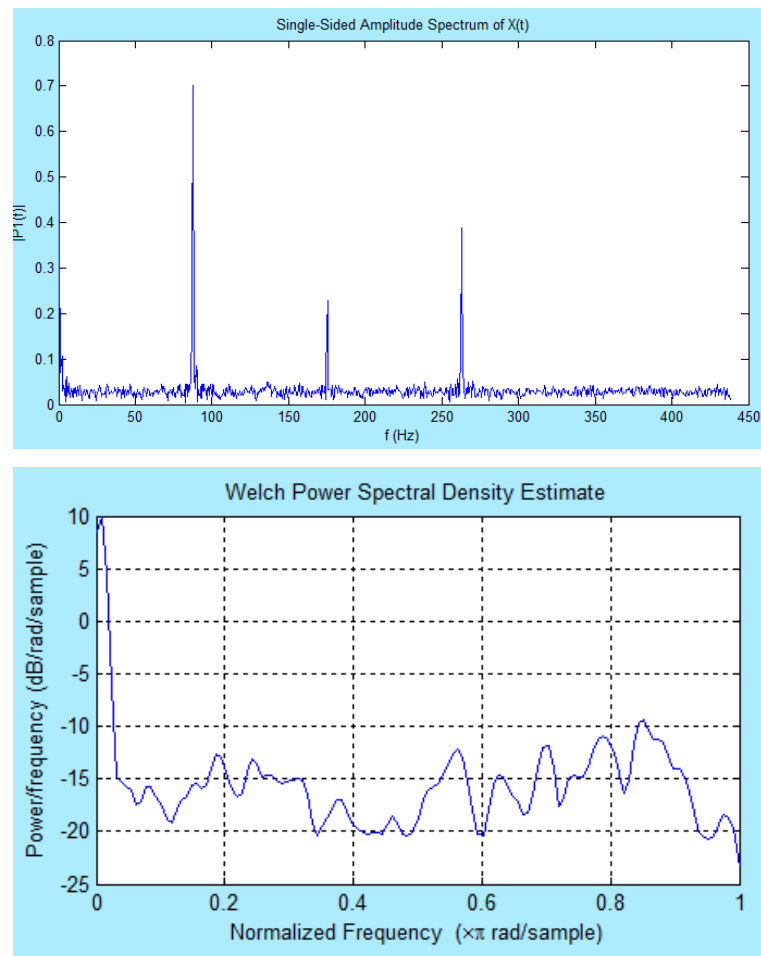


Figure 4-19 Fast Fourier Transform (Top), Power Spectral Density (Bottom)

#### 4.2.6 Exporting and Loading Data

Matlab allocates memory to a variable and stores a contiguous block of memory for a data array. When working with large data sets, if the array is increased beyond the available memory capabilities an error occurs and data can be corrupted. As the data rates in this application approach 1000 samples per second a continuous monitoring program will fill the available memory. In order to counter this an auto export function was incorporated to the user interface which will output a text file to after the desired number of minutes as shown in Figure 4-20. Additionally, the data can be exported at any time using the manual export button. The source of the data displayed on the interface can be selected by toggling the ‘Set Data Source’ options.

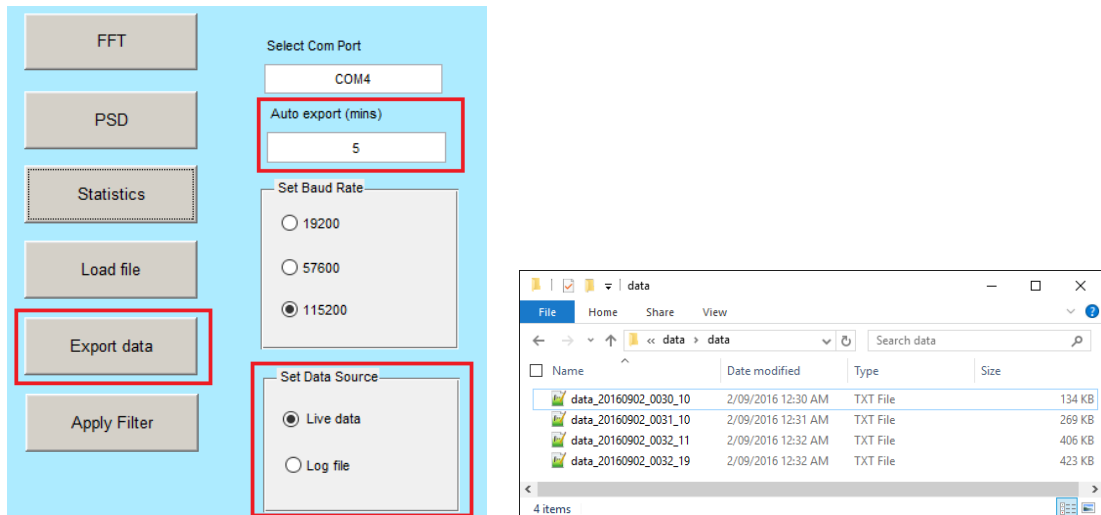


Figure 4-20 Auto and Manual Export (Left), Export to directory (Right)

The exported data displays the log date and time in the header information and includes the sampling frequency as shown in Figure 4-21.

Data Log: 02-Sep-2016 00:30:10					
Sampling frequency (Hz): 876.1					
X axis (g)	Y axis (g)	Z axis (g)	Acc. (g)	Time (ms)	
0.000000	0.000000	0.000000	0.000000	0	
0.132813	0.226563	-0.179688	0.318210	2	
0.132813	0.257813	-0.140625	0.322307	2	
0.132813	0.250000	-0.156250	0.323347	3	
0.125000	0.250000	-0.187500	0.336573	3	
0.140625	0.250000	-0.171875	0.334390	4	
0.125000	0.250000	-0.171875	0.328125	4	
0.132813	0.265625	-0.187500	0.351215	5	
0.125000	0.250000	-0.156250	0.320217	5	
0.117188	0.250000	-0.148438	0.313475	6	
0.125000	0.250000	-0.179688	0.332284	7	
0.132813	0.250000	-0.179688	0.335301	8	
0.132813	0.250000	-0.156250	0.323347	9	
0.125000	0.250000	-0.164063	0.324101	10	
0.148438	0.250000	-0.171875	0.337749	11	
0.117188	0.250000	-0.171875	0.325229	13	
0.148438	0.250000	-0.171875	0.337749	14	
0.125000	0.257813	-0.156250	0.326353	15	
0.148438	0.250000	-0.179688	0.341791	16	

Figure 4-21 Log File Output

Additional functionality was added to the user interface to allow for data to also be imported from a text file. This allows historical log files to be opened and analysed which is of importance when logging data continuously for long periods. The ‘Load File’ button when operated will open up a file explorer and allow the user to select a particular file of interest as shown in Figure 4-22.

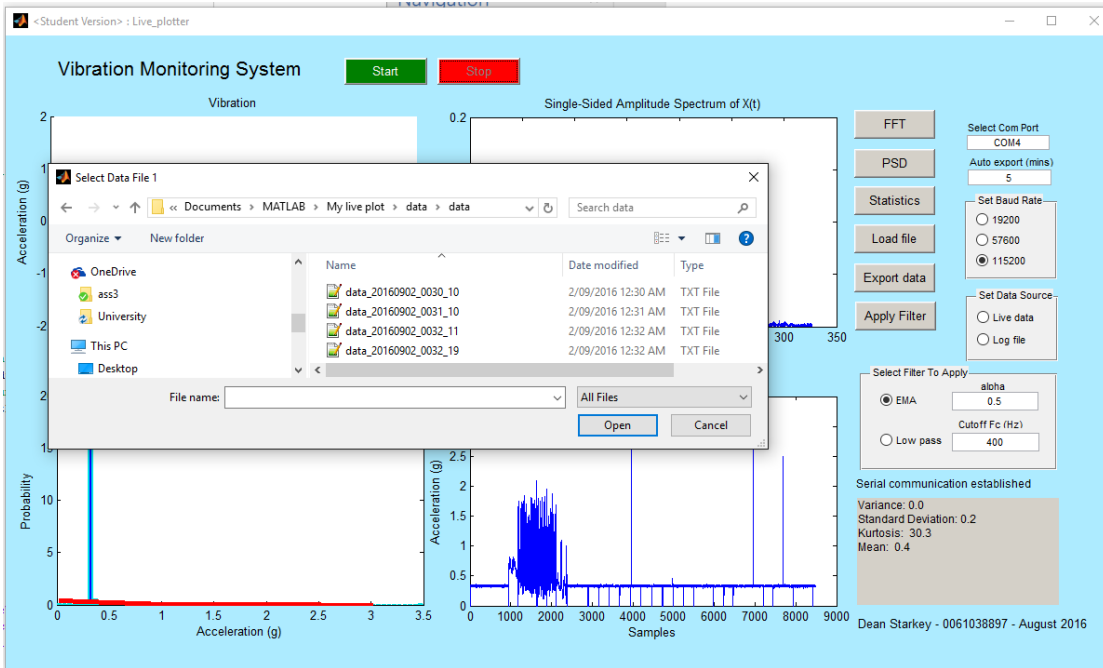


Figure 4-22 Load Historical Data Files

#### 4.2.7 Filtering Data

Two options for filtering data have been provided with the user able to select between an exponential moving average and first order Butterworth low pass filter. The low pass filter has its cut off frequency selectable from the user interface as shown in Figure 4-23. The exponential average filter allows the user to adjust the smoothing coefficient which can be varied between  $0 < \alpha < 1$ . By applying the filter, a new window is opened for the user to examine the results as shown in Figure 4-24.

Select Filter To Apply

☐ EMA

alpha

0.5

☒ Low pass

Cutoff Fc (Hz)

400

Figure 4-23 Filter Selection

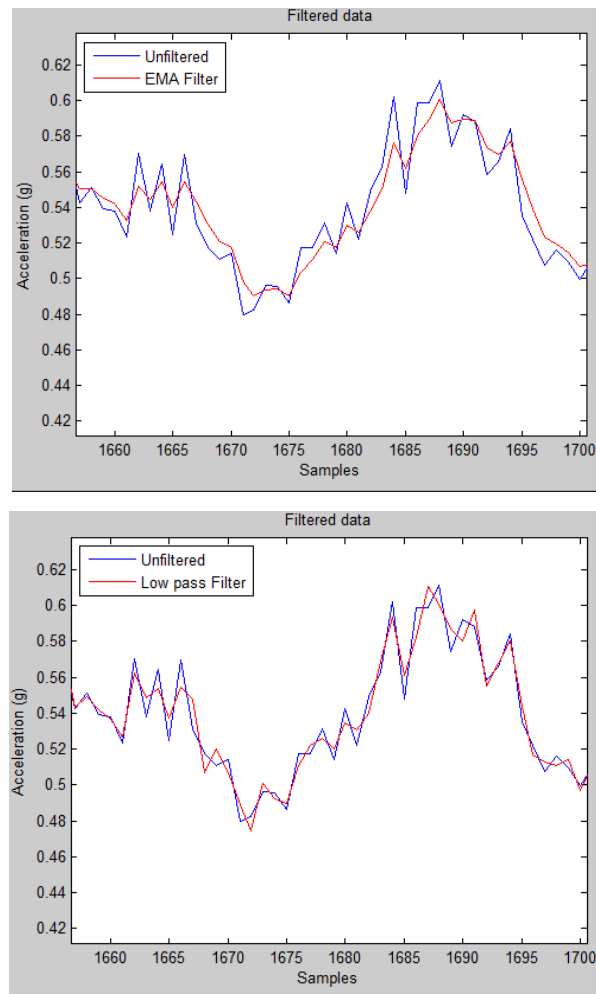


Figure 4-24 EMA Filter (Top), Low Pass Filter (Bottom)



# CHAPTER 6

## TESTING AND RESULTS

### 6.1 Initial System Testing

Initial testing of the proposed measurement system consisted of connecting the ADXL345 as shown in Figure 6-1. The accelerometer is connected in SPI configuration and the Arduino is loaded with firmware. The Arduino is proven to read the accelerometer and can interface with MATLAB storing the resultant acceleration values into an array.

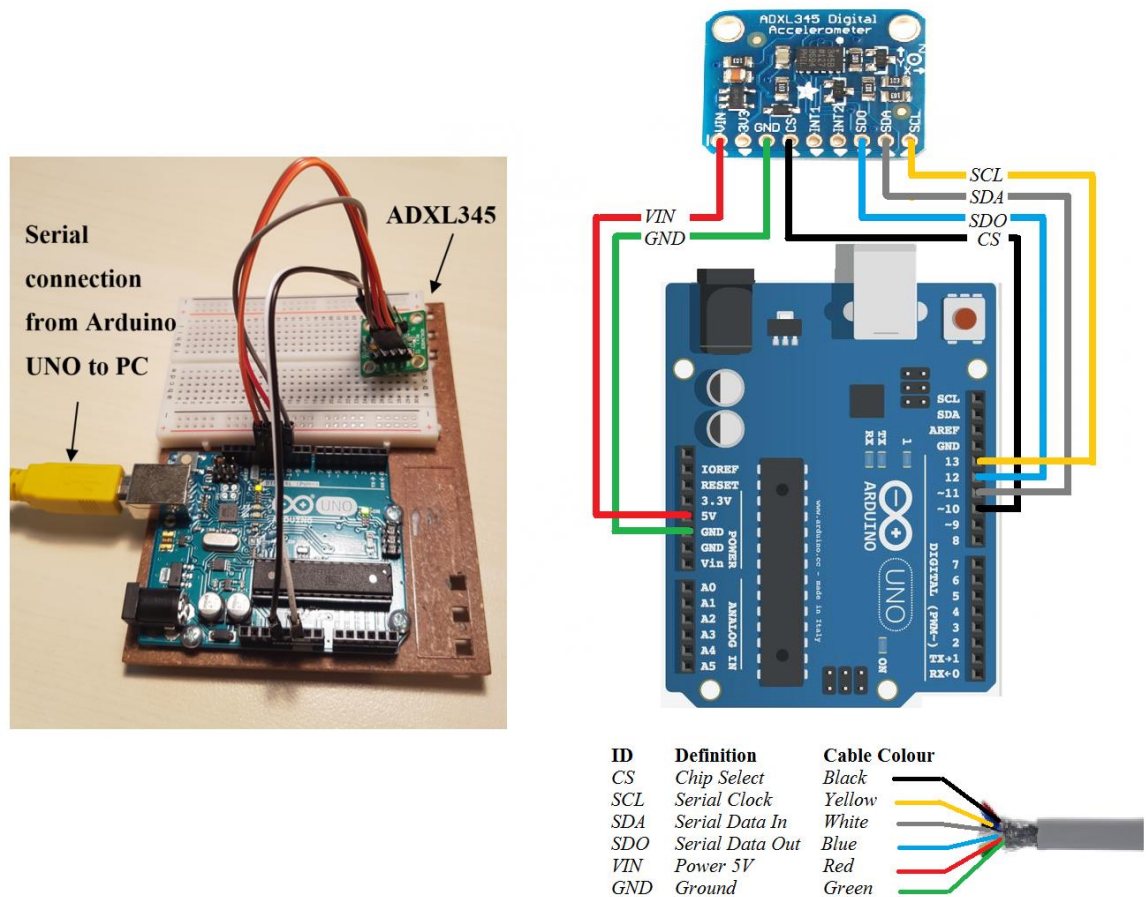


Figure 6-1 ADXL345 initial test setup (Left), ADXL345 initial wiring (Right)

## 6.2 Wireless testing

The Arduino is interfaced for wireless connection using XBee radios, where the Arduino is connected to XBee 1 via a wireless shield and XBee 2 connected to the computer via an XBee Explorer dongle. The XBee radios are first connected at 9600 baud and programmed to send ASCII characters from the computer serial monitor to the Arduino serial monitor as shown in Figure 6-2.



**Computer Serial Monitor**



**Arduino Serial Monitor**

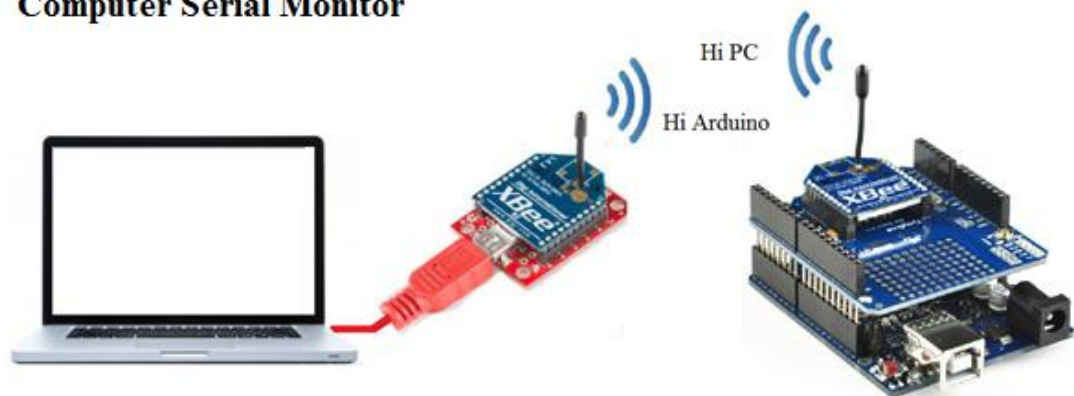


Figure 6-2 Initial XBee communication

### 6.2.1 Transmission data accuracy

Following confirmed communication between XBee 1 and 2, the desired function of transferring acceleration values from the sensor to the PC is tested. During testing some erroneous values are found to be present in the serial monitor when communicating wirelessly. Further investigation into this issue found data accuracy was compromised when communicating wirelessly. The data accuracy is calculated upon the number of failed transmissions where the expected format is not receipted by the terminal computer. To adequately compare transmission accuracy, the mean was taken for the first 10000 acceleration samples over 10 iterations. This was completed indoors of a residential home for different baud rates and compared to a direct USB connection as shown in Table 6-1 and Table 6-2.

Table 6-1 Direct USB connection testing

Baud Rates	USB connection		
	Mean Sampling Frequency (Hz)	Mean Samples Dropped	Data Transmission Accuracy
19200	135	1	99.99%
57600	423	2	99.98%
115200	883	4	99.96%

Table 6-2 XBee wireless connection testing

Baud Rates	XBee wireless connection		
	Mean Sampling Frequency (Hz)	Mean Samples Dropped	Data Transmission Accuracy
19200	126	79	99.21%
57600	394	155	98.45%
115200	744	235	97.65%

It is evident that communication via direct USB connection results in good data accuracy with minimal samples being lost. In comparison the wireless connection sees an approximate linear increase in data inaccuracy with increased baud rate. It is evident that 19200 and 57600 baud are not suitable for a 100Hz to 400Hz bandwidth as they do not meet the minimum Nyquist frequency to avoid aliasing the signal.

Increased data errors were obtained when connecting wirelessly compared with the USB. It is documented by the manufacturer that this phenomenon is due to baud rate mismatch. The baud rate in bits per second (bps) sets the speed of serial communication which on the Arduino can be 300, 600, 1200, 2400, 4800, 9600, 14400, 19200, 28800, 38400, 57600 or 115200. The requirement for communication between the Arduino and computer is that both devices are operating at the same baud. Through investigation it was found that the XBee radio has a digital oscillator which does not achieve a baud of 115200. The baud generated by the XBee is closer to 111000 and the mismatch in these baud rates results in poor signal quality and lost readings. When operating at slower speeds such as 9600 baud the mismatch is much less with wireless and direct connection producing similar transmission accuracy.

### **6.2.2 Transmission Range Testing**

A typical urban zone substation has outdoor transformers and primary switchgear with indoor secondary switchgear and control equipment. The measurement device is designed to be installed on the wall of a transformer and data streamed to a nearby terminal computer inside the substation switch room. Substation switch rooms are generally of brick or concrete construction with a distance of approximately 20 to 50m to the transformers. To simulate this the device is first tested in a residential home and found to communicate within the same data transmission accuracy levels as previously tested. Following this the device is installed at a real substation as shown in Figure 6-3 and tested for data transmission accuracy. The device is found to operate as expected within the confines of the substation perimeter fence up to a distance of 100m.



Figure 6-3 Zone substation transmission range testing

### 6.3 Controlled Experiment

To test the developed system is operating as expected a known vibration source is introduced and spectral analysis performed to determine the present frequency components in the signal as per the simulated setup shown in Figure 6-4. As per the vibration motor manufacturer specifications at 24V DC supply the motor operates at 10000 RPM and at an induced vibration frequency of approximately 167Hz. The results from the test setup are shown in the portion of sampled data and resulting Fast Fourier Transform plot shown in Figure 6-6.



Figure 6-4 Vibration system and motor test setup

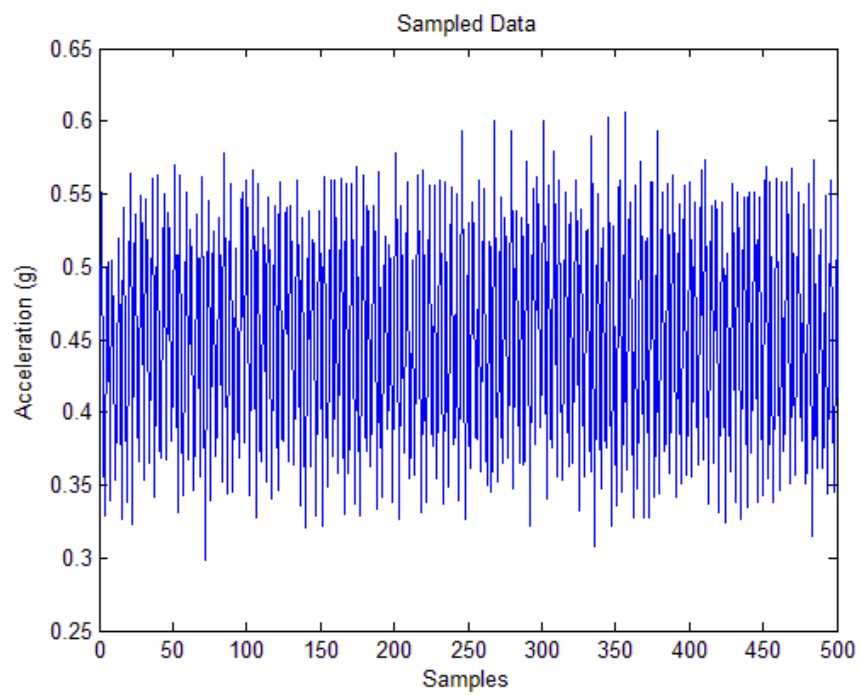


Figure 6-5 Portion of sampled signal

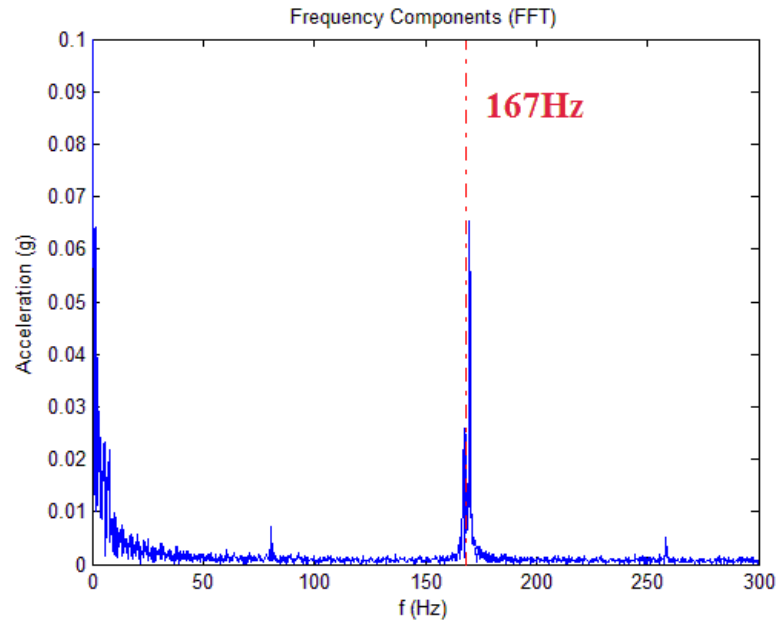


Figure 6-6 Frequency components of vibration motor signal

It is evident that the primary frequency component of the vibration motor is close to that of the manufacturer specifications. The identified frequency peak has been measured at approximately 169Hz. There is also added harmonics which are expected from the motor which is not a pure source of vibrations. From multiple tests it is concluded that the designed system is operating as expected and capable of identifying frequency components with reasonable accuracy.

## 6.4 Field Testing

Following the identification of a working measurement system field testing was performed. The chosen 6 sites were monitored for similar durations and sensors located in similar locations depending on the construction of the transformer. Vibrations signatures were identified for each transformer and spectrum analysis performed to identify the presence of harmonics and changes of these frequency peaks with transformer loading.

#### 6.4.1 Location of accelerometer

Transformer vibration signatures are suggested by Shengchang, Lingyu and Yanming (2011) to be comparable in only cases where transformer construction is identical. Boczar (2005) identified that the sensor location had little impact on the magnitude of the first 8 harmonics and as such this would be tested looking at two locations on the transformer. The sensor is installed close to the centre of the rear and side transformer walls as shown in Figure 6-7.

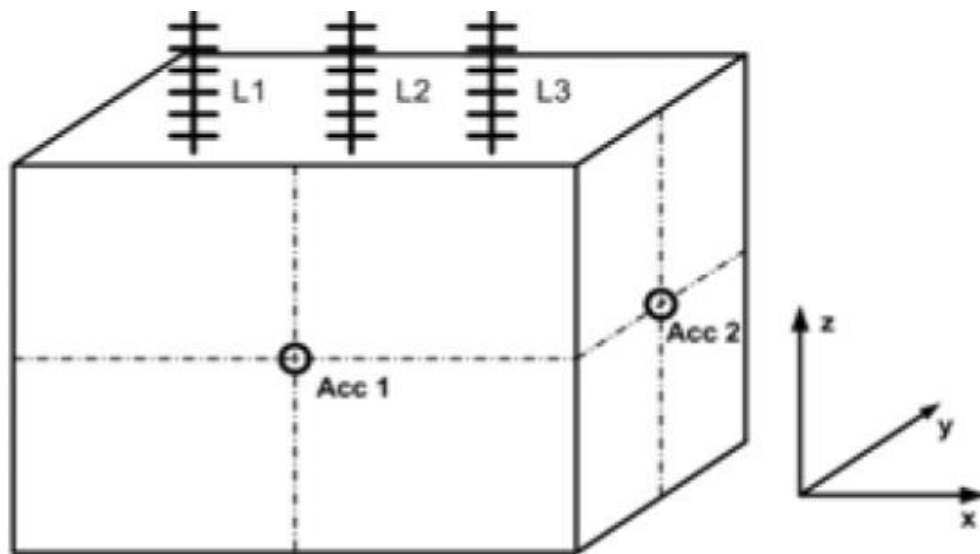


Figure 6-7 Proposed accelerometer placement (Borucki 2012)

The sensor is not mounted along a structural rib, oil pipe, or near the on load tap changer as to not reduce or obscure vibration signals. An example of the measuring device installed at location 5 is shown in **Error! Reference source not found..**





Figure 6-8 Site 5 rear wall mount (Top), Site 5 side wall mount (Bottom)

### **6.4.2 Duration of testing**

The monitoring system is set to automatically save vibration data logs in 5 minute intervals for post processing. Due to access and time restrictions each transformer was monitored for a period of at least 2 hours. This included 2 hours at 2 different locations on the transformer tank as previously specified. The transformer load profile is measured and averaged at intervals by the substation distribution monitoring equipment and processed following the installation to assist in analysis of the results. The load measurements have all been taken at the transformer secondary terminals at 11kV. Due to the varying age and type of monitoring equipment installed at the substation the load measurement intervals are varied from 2 minutes to 15 minutes.

### **6.4.3 Interpretation of results**

As suggested by Shengchang, Lingyu and Yanming (2011) normalisation of vibration magnitudes against the square of the applied voltage is required when drawing comparisons for vibration signatures on identical constructed transformers. Only at site 3 and site 4 locations are the transformer manufacture, model and construction identical. These transformers are both parallel connected to the same 132kV bus and vibration magnitudes are considered equal for comparison at these locations.

The frequency components of the 5-minute sampled signal are extracted and first analysed. The Short-Time Fourier Transform is performed to evaluate the changes in the frequency content over time. A spectrogram plot is produced where:

- The sampled signal is divided into sections of length 500
- Hamming window function applied
- 300 samples overlap between adjoining sections
- 500 sampling points evaluated to calculate the Discrete Fourier Transform.

An example of the produced plot is shown in Figure 6-9 below. The plot can be viewed in both two and three dimensions. The spectrogram allows for analysing frequency drift with time.

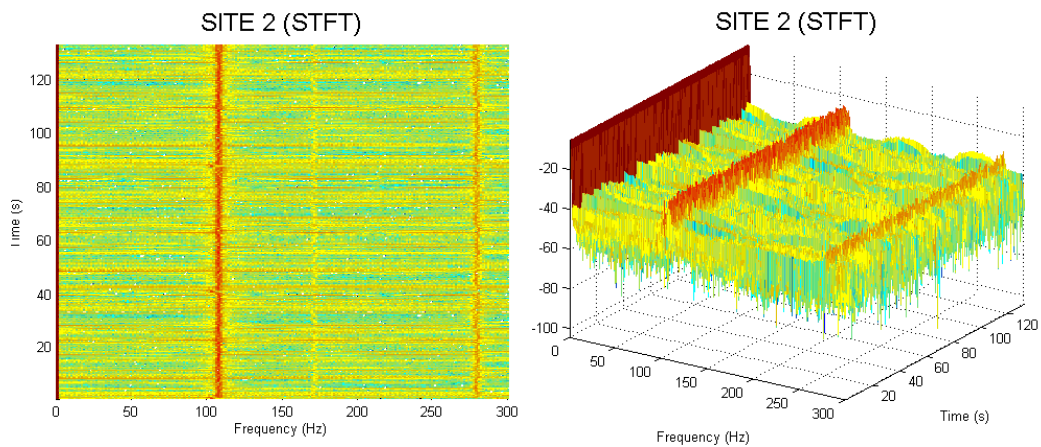


Figure 6-9 STFT plot for Site 1 – 2D (Left), 3D (Right)

Further momentary windows of shorter duration are then analysed across the 5-minute sample period and compared to ensure consistency. Power spectral density plots are performed to a common reference power to analyse spectral components.

## 6.5 DGA results

Site 1 has the most decomposition of all sites analysed. High levels of ethylene, acetylene and carbon monoxide indicate severe overheating and the presence of high energy discharges. Site 2 has similar high levels of decomposition with high levels of carbon monoxide indicating hotspots inside the transformer and likely electrical faults present. Site 3 has levels of acetylene that indicate low energy discharges present with levels of carbon dioxide and carbon monoxide noted to have significantly increased since previous results. Site 4 has high levels of carbon monoxide present however historical records indicate that the level has not changed significantly and is below the actionable threshold. Sites 5 and 6 are fairly new substations and as expected have

satisfactory results to be used as a baseline for comparison. A summary of the DGA results for the chosen sites is shown in Table 6-3.

Table 6-3 Summary of DGA results

Site	Age (yrs)	Worst Condition	Worst Component	Scientist Comments
Site 1	38	Condition 4	Ethylene	Discharges of high energy are likely present
Site 2	46	Condition 4	Carbon Monoxide	Mixtures of electrical and thermal faults are likely present
Site 3	22	Condition 4	Acetylene	Electrical discharge of low energy is likely present
Site 4	22	Condition 3	Carbon Monoxide	Similar to previous results, levels stable and acceptable in service parameters
Site 5	9	Condition 1	N/A	Test results satisfactory
Site 6	5	Condition 1	N/A	Test results satisfactory

## 6.6 Load analysis

The load on the transformer has a direct relationship to the vibration signature and magnitude of vibrations due to increased flux in the transformer core. It is therefore important when assessing the vibration signatures to assess the load profiles. This is to identify if any significant changes in vibration magnitude are due to load or changes in the core. Following installation at sites 1 to 6, the load profiles for the period of installation have been attained and are summarised in Table 6-4.

Table 6-4 Load profile summary

	Install	Recovered	Voltage	Max Load	Min Load	Average load
Site 1	18/09/2016 10:49	18/09/2016 13:00	11kV	359A	339A	348A
Site 2	18/09/2016 13:00	18/09/2016 15:00	11kV	386A	362A	372A
Site 3	17/09/2016 9:00	18/09/2016 11:00	11kV	217A	161A	193A
Site 4	17/09/2016 11:10	17/09/2016 13:10	11kV	332A	282A	311A
Site 5	13/09/2016 10:40	13/09/2016 12:40	11kV	243A	221A	232A
Site 6	13/09/2016 12:45	13/09/2016 14:45	11kV	21A	20A	20.5A

Sites 1, 2, 5 and 6 exhibited reasonably linear load profiles during the period of installation with the load remaining reasonably consistent. The load profiles at locations 3 and 4 show larger variations in load as shown in Figure 6-10 and Figure 6-11. All load profiles are included in the attached Appendix E for reference.

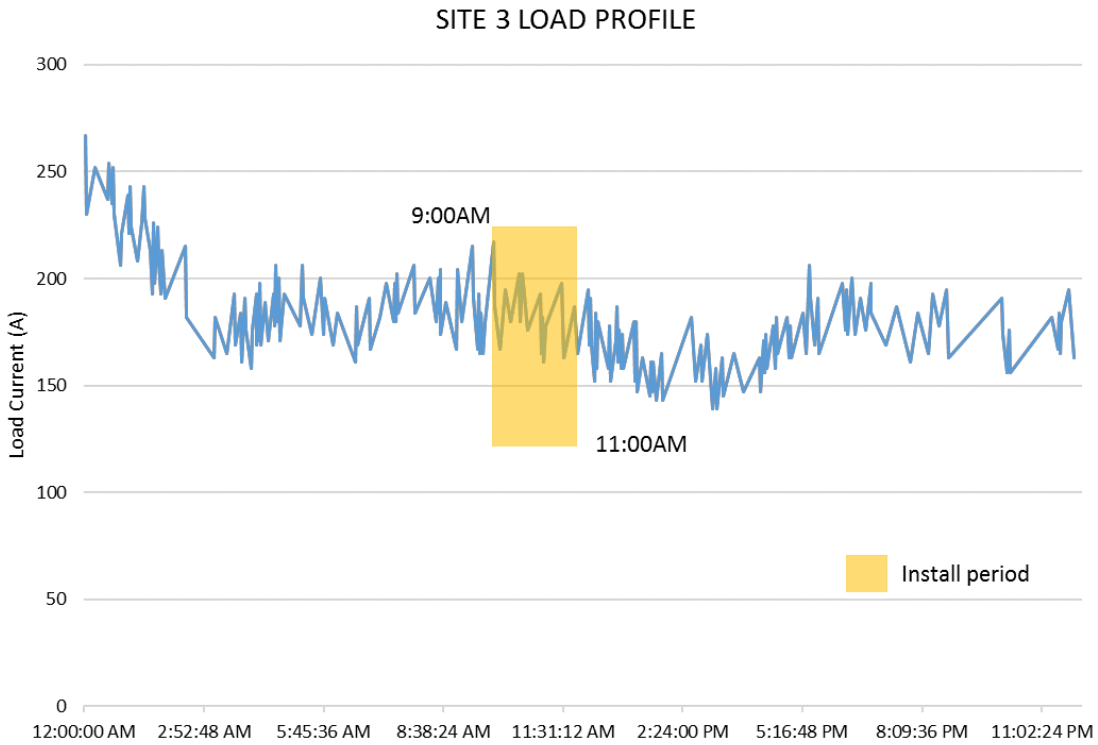


Figure 6-10 Site 3 load profile

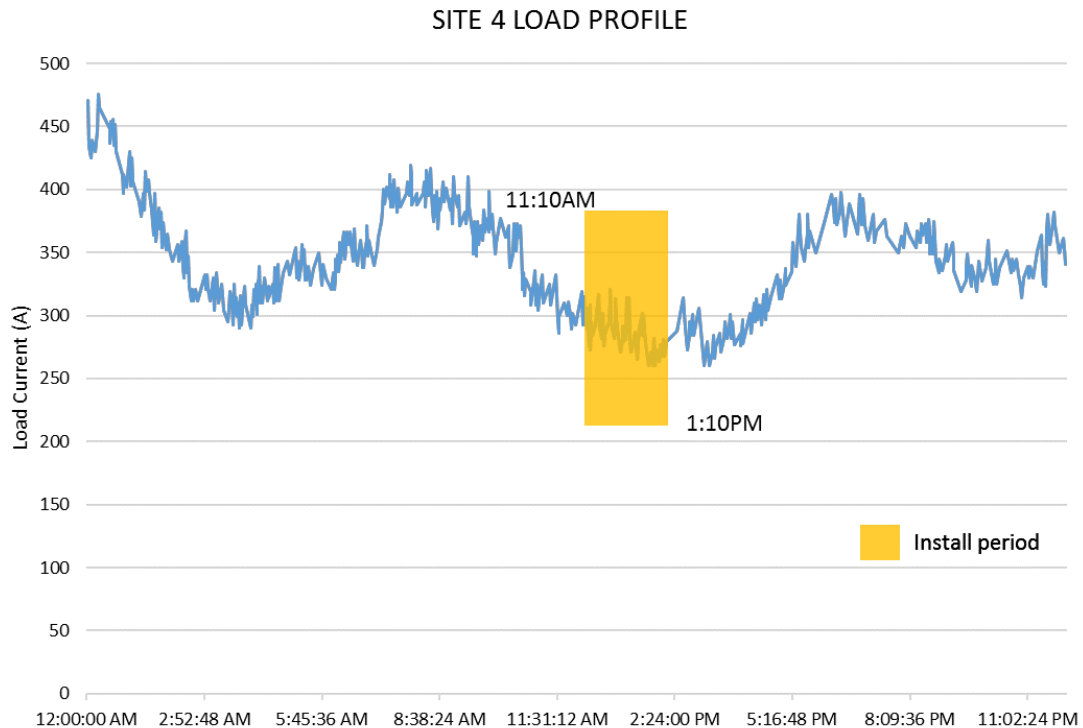


Figure 6-11 Site 4 load profile

It has been noted that during the time of installation at site 6 the transformer was abnormally lightly loaded. Upon further investigation it was found that the load side feeders were abnormally switched during the period of installation which reduced the load on the supplying transformer.

## 6.7 Effect of sensor position

At all locations the rear transformer wall resulted in larger vibration magnitudes. Attenuation of the vibration magnitude is present when the sensor is mounted on the side wall however only slight with the frequency component maintained. In all cases the vibration magnitude when side mounted was within 80% of the recorded rear mounted vibration magnitude. The effect of sensor position is shown at site 1 and 2 locations in Figure 6-12. The markings indicate the peak frequency components

identified from Power Spectral Density (PSD) plots. From this it can be seen that there is a marginal difference in magnitude at all identified frequencies.

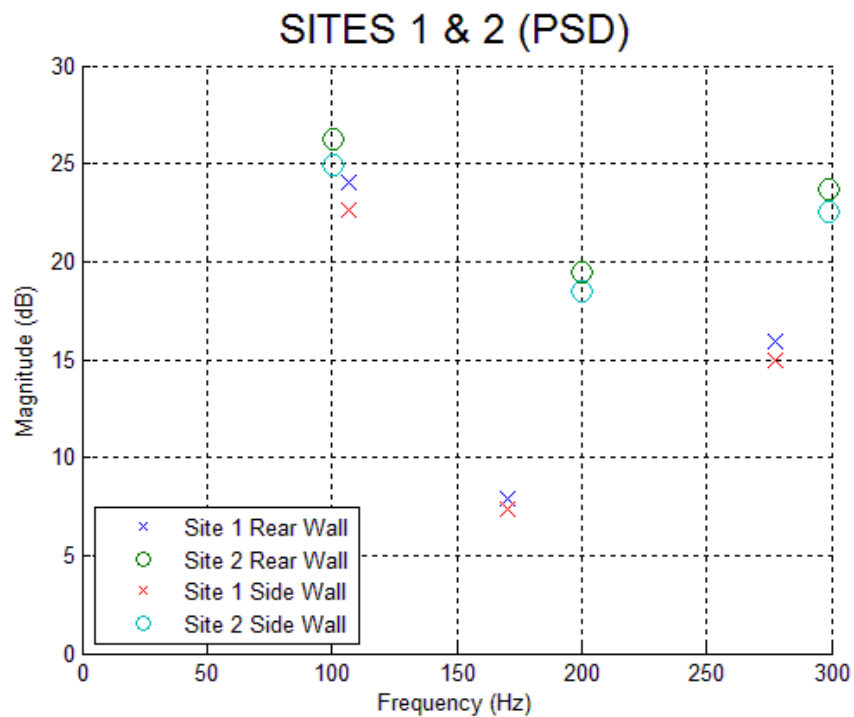


Figure 6-12 Sites 1 and 2 sensor location comparison

## 6.8 Spectrum analysis

The STFT spectrograms produced for all sites show that frequency components are uniform in all locations with no discernible frequency drift experienced during the monitored periods. Figure 6-13 shows the STFT for sites 1 to 3 which were identified as having damage insulation from DGA analysis. From this it can be seen that sites 1 and 2 have present frequency components at three specific and consistent frequencies. By comparison sites 3 to 5 have only two identifiable frequency components. Sites 3 and 4 exhibited the biggest variation in load during the time of installation however this has not correlated to variation in frequency or magnitude. Figure 6-14 shows the STFT for sites 4 to 6. From this it can be seen that sites 4 and 5 have two consistent



frequency components whilst location 6 has no discernable frequency components detected.

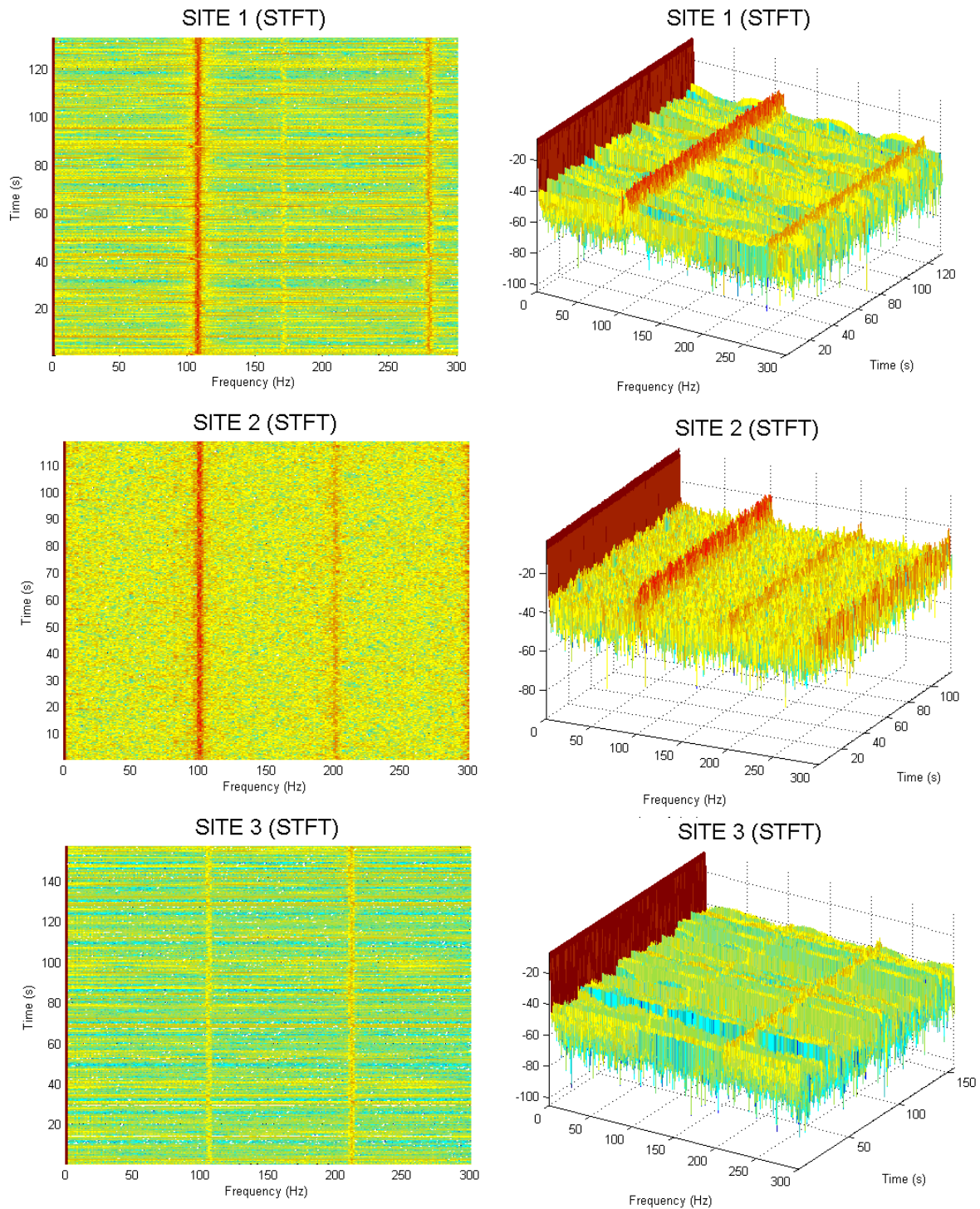


Figure 6-13 Sites 1 to 3 Short Time Fourier Transform



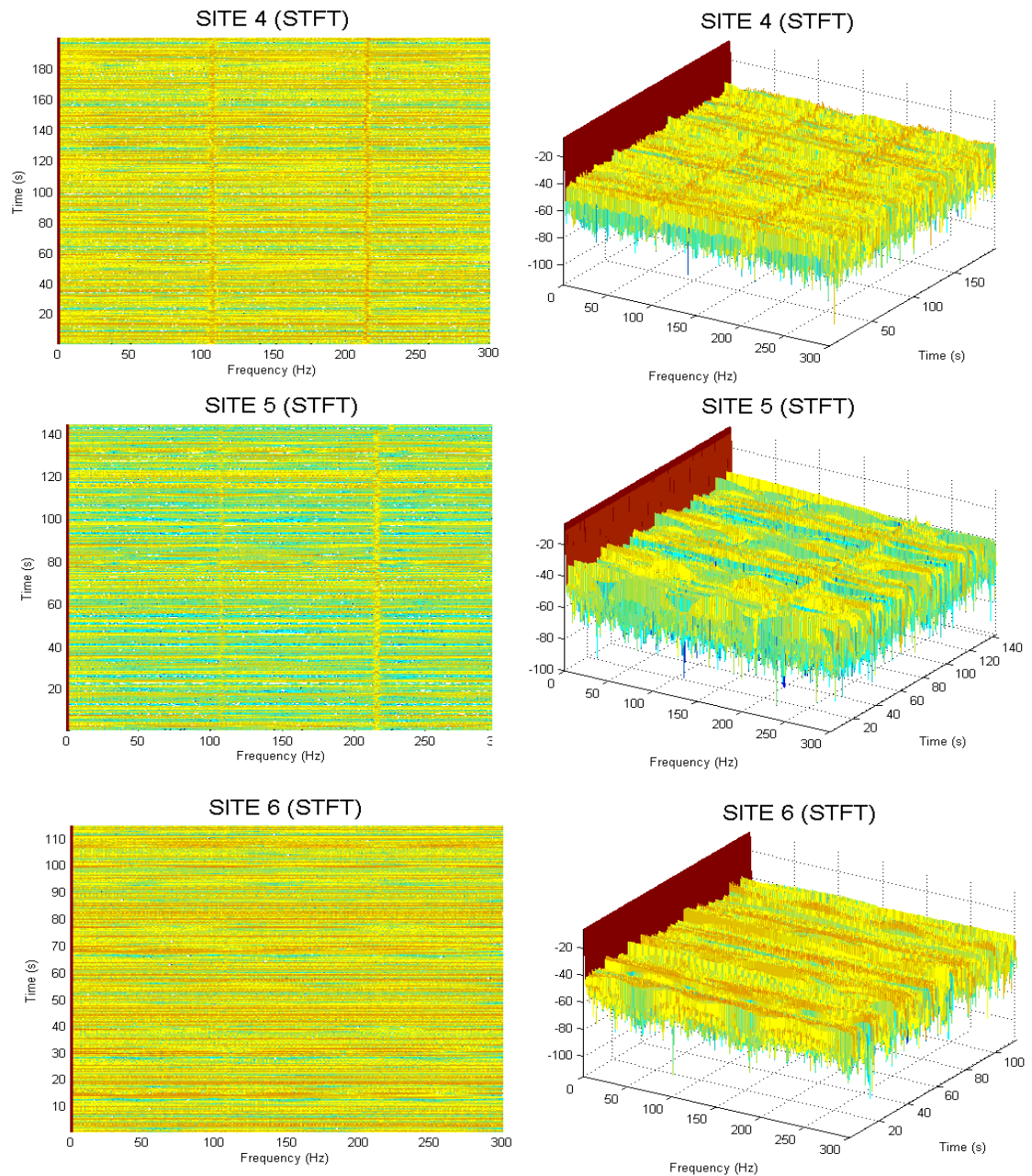


Figure 6-14 Sites 4 to 6 Short Time Fourier Transform

As there is minimal drift in frequency components across all sites during installation the power spectral density estimates are shown in Figure 6-15 to highlight the consistent frequency peaks and magnitudes at each location.

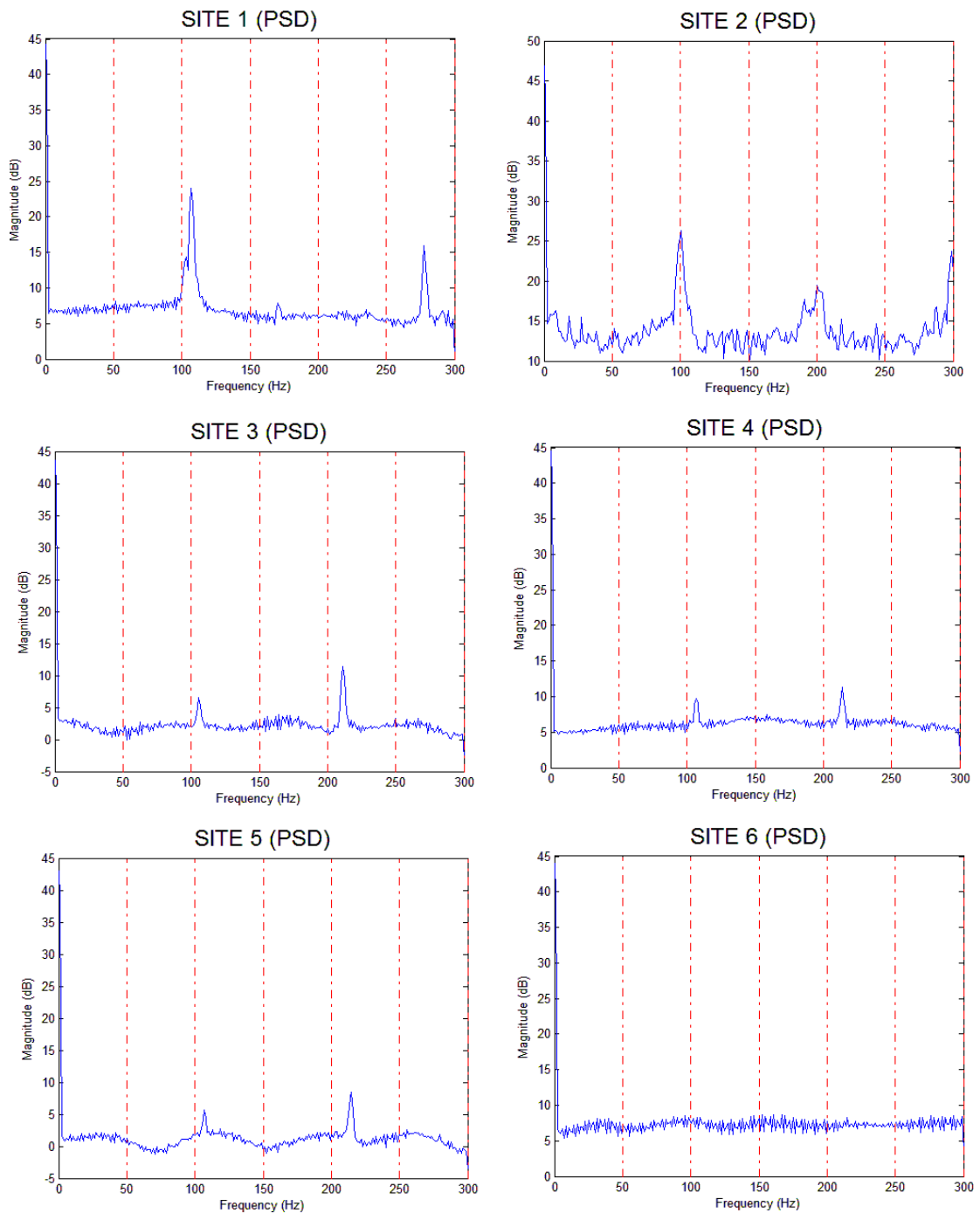


Figure 6-15 Sites 1 to 6 Power Spectral Density

Sites 1 and 2 which are of the poorest condition per DGA results, have significantly higher magnitudes in vibration. In contrast with this there was no noticeable frequency components at site 6. This is assumed to be due to several factors including being a

new transformer, lightly loaded at the time of measurement and the insufficient sensitivity of the measuring device for this particular location.

From analysis of power spectral density at different locations it is obvious to recognise the similarities in the data. For comparative analysis the specific frequency peaks have been overlayed for all six sites as shown in Figure 6-16. Sites 1 and 2 with the poorest DGA results and of greatest age have the largest vibration magnitudes and are the only sites with a visible 300Hz component. At sites 1 and 2 the dominant frequency component is 100Hz, this is contrary to sites 3 to 5 which have a dominant 200Hz component.

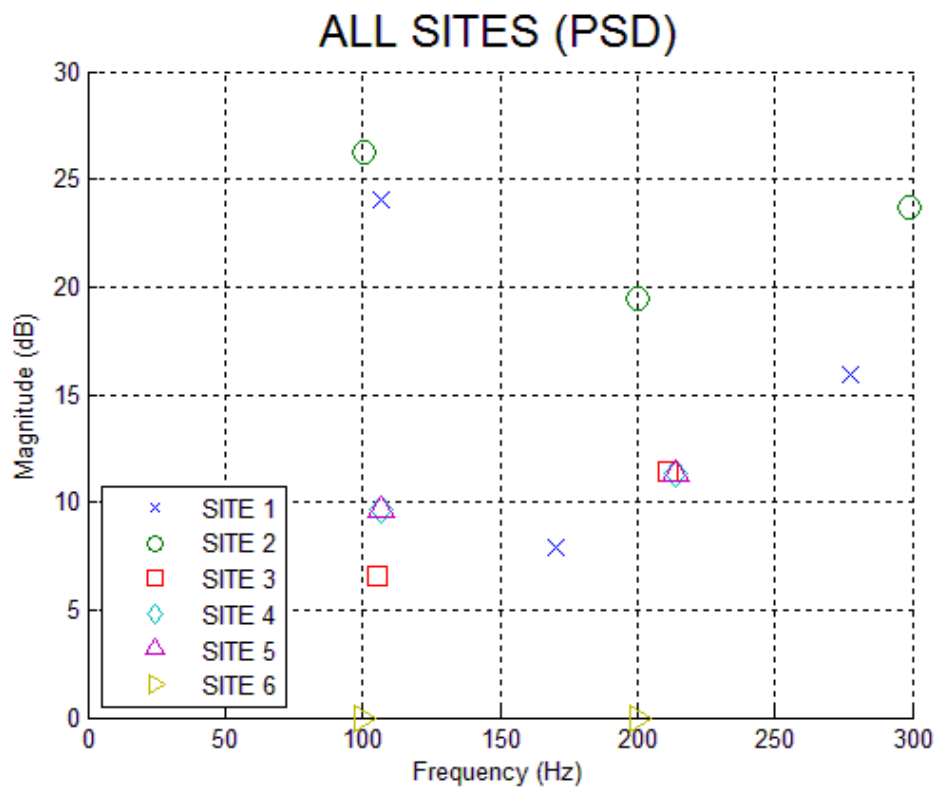


Figure 6-16 Sites 1 to 6 frequency peak comparison

Due to the differing transformer construction types conclusions cannot be drawn from the frequency spectra comparison above. However, both sites 3 and 4 are of the same

manufacturer, model and commissioned in the same year which allows a better basis for comparison. Site 3 has been identified to have the presence of low energy discharges in the transformer tank in contrast with site 4 which has satisfactory results. Figure 6-17 shows the frequency peaks comparison between sites 3 and 4. From the load analysis site 4 was noted to have over 160% loading in comparison with site 3 which is evident in the presence of a higher magnitude 100Hz component. There is however no discernible difference in the 200Hz component and without the presence of additional harmonics it is concluded that analysis of the vibration spectra at specific moments in time cannot determine the presence of transformer faults.

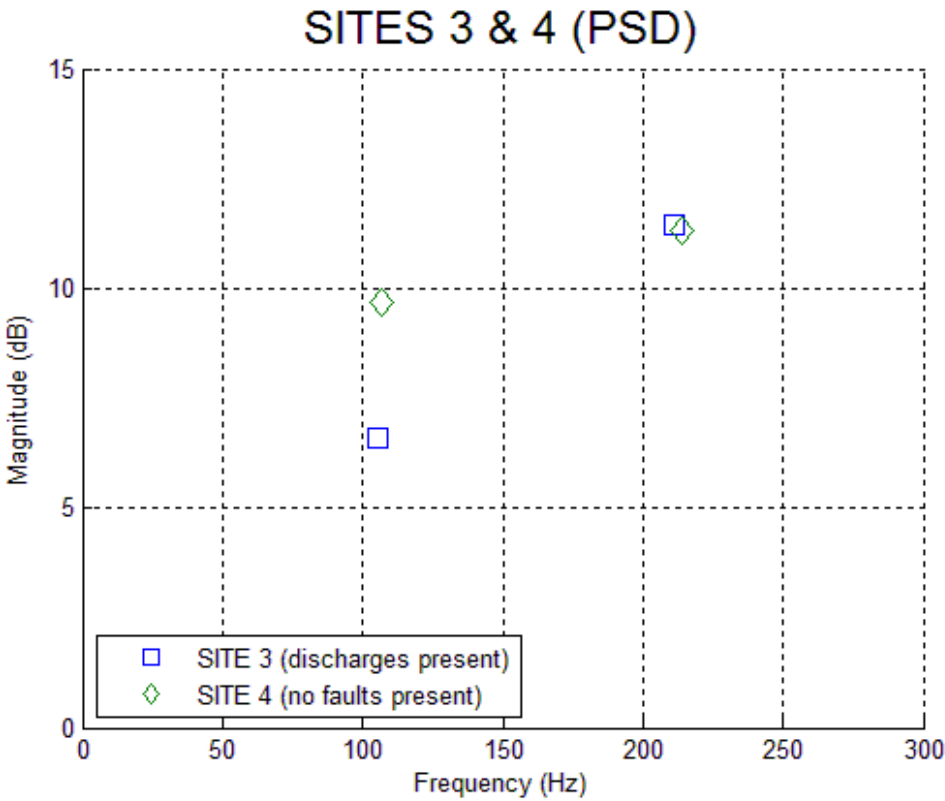


Figure 6-17 Sites 3 and 4 frequency peak comparison

## 6.9 Summary of Results

The vibration monitoring system developed was tested via means of testing wireless data transmission and by introduction of a known vibration source. The system was found to act with reduced data accuracy when transmitting wirelessly at 115200 baud. This reduction in transmission accuracy is related to the baud rate mismatch from the XBee hardware. For the majority of testing in the field a direct hardware connection was used to increase the data accuracy. This however would not be feasible for long term installation on the transformer.

Following a developed vibration monitoring system, six zone transformers were selected for field testing and DGA reports analysed. Sites 1 to 3 were of reasonably poor condition as per DGA analysis with site 1 of the poorest condition being earmarked for replacement before the end of 2016. Sites 4 to 6 were found to have satisfactory DGA results and were used as a baseline for comparison.

The sites were monitored for at least 2 hours at two different locations on the transformer tank being the centre of the rear and side walls. This comparison found that sensor position made negligible difference for identifying the frequency components in the vibration signature. There was however a slight attenuation in the vibration magnitude when mounted on the transformer side wall. This attenuation was within 80% of the rear wall magnitude in all locations and as such the sensor position was not considered to have a large impact when using the vibroacoustic method.

The results were analysed using the Short Time Fourier Transform to pick up on any specific frequency drift that may aid in identifying the type of transformer fault. However, from the signatures obtained there is not enough variation in magnitude or frequency components to suggest that this method can identify the type of fault present. The measurement system developed was able to identify the vibration signature at each location however the overall sensitivity of the developed system needs to be improved to identify the discrete changes in the signal.

# CHAPTER 7

## CONCLUSION

A vibroacoustic method has been investigated for transformer condition assessment. This required the design of an effective vibration measurement system using non-commercial grade and cost effective equipment. The design system utilised a Micro Electro Mechanical (MEMs) capacitive accelerometer connected to an Arduino UNO microprocessor and communicated to a computer terminal wirelessly in real time. A contribution of this project is the hardware and software design for a cost effective real time vibration monitoring system. The developed system is something that can be used across multiple engineering disciplines to examine the vibration signatures of both rotating and stationary plant.

The vibroacoustic method of transformer condition assessment is still considered experimental and this work has contributed to the greater understanding of transformer vibration signatures outside of laboratories. For this method it was found that sensor position had little impact on the magnitude of vibration signal and frequency components present. It was determined that the condition of the transformer insulation was not identifiable from the momentary windows of operation. It is envisaged that assessment of transformer condition can only be made once an understanding of each individual transformer vibration signature is known. The differing transformer construction types and sizes makes comparison between transformers difficult and accurate assessment is only likely through monitoring the changes in the vibration signature of a transformer over longer periods.

### 7.1 Further Work

The development of cost effective vibration monitoring systems is extremely beneficial to those who do not have access to expensive commercial equipment. As

capacitive MEMs devices are further developed for integration in the phone market opportunity exists to apply this technology to sensing applications.

For further work the system developed in this project can be finely tuned and compared to a commercially available product to test the system accuracy and reinforce its suitability. This system is currently bound by the limits of the available hardware. An upper frequency limit beyond 500Hz is not likely whilst using the Arduino UNO due to the speed of the processor and serial communication.

The vibroacoustic method of transformer condition assessment is largely experimental. Further research and real world testing is required before it can be used to diagnose transformer faults. It is suggested that longer installation and monitoring is conducted than has been feasible in this project. Sites should be monitored for at least a month to gauge an accurate model of the individual transformers vibration signature. From the understanding of a transformers unique signature the changes in the frequency components over a period of time is suggested to provide useful information for condition assessment. It is not imagined that this method will replace traditional and trusted methods such as DGA. It is however envisaged that this method can be used to compliment traditional methods for a more accurate condition assessment.

# REFERENCES

Aggarwal, P 2010, *MEMS-based Integrated Navigation*, Artech House, viewed 9 May 2016, <[https://books.google.com.au/books?id=IfLdaZ\\_evpgC](https://books.google.com.au/books?id=IfLdaZ_evpgC)>

Analogue Devices 2009, *ADXL345 - Digital Accelerometer Data Sheet*, <[www.analog.com](http://www.analog.com)>

AS 60270 R2015, *High-voltage test techniques - Partial discharge measurements*, Standards Australia, viewed 8 May 2016,

Bartoletti, C, Desiderio, M, Carlo, DD, Fazio, G, Muzi, F, Sacerdoti, G & Salvatori, F 2004, 'Vibro-acoustic techniques to diagnose power transformers', *IEEE Transactions on Power Delivery*, vol. 19, no. 1, pp. 221-229, viewed 15 May 2016,

Boczar, T 2005, 'Time-frequency analysis of the acoustic emission pulses generated by multi-source partial discharges in oil', in *Proceedings of IEEE International Conference on Dielectric Liquids, 2005. ICDL 2005.*, pp. 265-268. viewed 23 April 2016.

Bores 2012, 'FFT Window Functions - Limits on FFT analysis', viewed 20 May 2016, <[www.bores.com/courses/advanced/windows/files/windows.pdf](http://www.bores.com/courses/advanced/windows/files/windows.pdf)>

Borucki, S 2012, 'Diagnosis of Technical Condition of Power Transformers Based on the Analysis of Vibroacoustic Signals Measured in Transient Operating Conditions', *IEEE Transactions on Power Delivery*, vol. 27, no. 2, pp. 670-676, viewed 16 May 2016,

element14, *Analogue devices EVAL-ADXL345*, viewed 21 May 2016, <<http://au.element14.com/analog-devices/eval-adxl345z/adxl345-inertial-imems-eval-board/dp/2301487>>



George, RB 1931, 'Power Transformer Noise Its Characteristics and Reduction', *Transactions of the American Institute of Electrical Engineers*, vol. 50, no. 1, pp. 347-352, viewed 14 May 2016,

'IEEE Standard Test Code for Liquid-Immersed Distribution, Power, and Regulating Transformers', (2016, *IEEE Std C57.12.90-2015 (Revision of IEEE Std C57.12.90-2010)*), pp. 1-120,

IEEE Std C57.104 2009, *IEEE Guide for the Interpretation of Gases Generated in Oil-Immersed Transformers*, IEEE Std C57.104-2008 (Revision of IEEE Std C57.104-1991), viewed 31 August 2016,

IEEE Std C57.127 2007, *IEEE Guide for the Detection and Location of Acoustic Emissions From Partial Discharges in Oil-Immersed Power Transformers and Reactors*, IEEE Std C57.127-2007 (Revision of IEEE Std C57.127-2000), viewed 10 October 2015,

Kozako, M, Yamada, K, Morita, A, Ohtsuka, S, Hikita, M, Kashine, K, Nakamura, I & Koide, H 2009, 'Fundamental study on partial discharge induced acoustic wave propagation in simulated transformer composite insulation system', in *Proceedings of Properties and Applications of Dielectric Materials, 2009. ICPADM 2009. IEEE 9th International Conference on the*, pp. 477-480. viewed 13 October 2015, <<http://ieeexplore.ieee.org.ezproxy.usq.edu.au/stamp/stamp.jsp?tp=&arnumber=5252386>>.

Kulkarni, SV & Khaparde, SA 2004, *Transformer Engineering: Design and Practice*, CRC Press, viewed 22 May 2016, <<https://books.google.com.au/books?id=qy4QT0BIV0MC>>

Luo, FL, Ye, H & Rashid, MH 2010, *Digital Power Electronics and Applications*, Elsevier Science, viewed 16 May 2016, <[https://books.google.com.au/books?id=R44dbJu\\_cYgC](https://books.google.com.au/books?id=R44dbJu_cYgC)>

Microdrives, P 2016, *The Limits of Vibration Frequency for Miniature Vibration Motors*, viewed 29 August 2016, <<https://www.precisionmicrodrives.com/tech-blog/2012/11/22/limits-vibration-frequency-miniature-vibration-motors>>

MIT, O 2010, *Introduction to Communication, Control, and Signal Processing*, MIT, viewed 21 May 2016, <[ocw.mit.edu/courses/electrical-engineering.../MIT6\\_011S10\\_chap10.pdf](http://ocw.mit.edu/courses/electrical-engineering.../MIT6_011S10_chap10.pdf)>

Saponara, S, Fanucci, L, Bernardo, F & Falciani, A 2015, 'A network of vibration measuring nodes with integrated signal processing for predictive maintenance of high power transformers', in *Proceedings of Intelligent Signal Processing (WISP), 2015 IEEE 9th International Symposium on*, pp. 1-4. viewed 5 May 2016,

Shengchang, J, Lingyu, Z & Yanming, L 2011, 'Study on transformer tank vibration characteristics in the field and its application', *Przegląd Elektrotechniczny*, vol. 87, no. 2, pp. 205-211, viewed 18 May 2016,

Shreve, D 1995, 'Signal Processing for Effective Vibration Analysis', *IRD Mechanalysis*, viewed 21 May 2016, <[http://www.irdbalancing.com/downloads/sigcond2\\_2.pdf](http://www.irdbalancing.com/downloads/sigcond2_2.pdf)>

Singh, S & Bandyopadhyay, MN 2010, 'Dissolved gas analysis technique for incipient fault diagnosis in power transformers: A bibliographic survey', *IEEE Electrical Insulation Magazine*, vol. 26, no. 6, pp. 41-46, viewed 30 August 2016,

Solin, IK, Yolanda, O & Siregar, R 2009, 'Partial discharge measurement and vibration monitoring on power transformer case study on power transformer with

high level noise (75.22 dB)', in *Proceedings of 2009 IEEE 9th International Conference on the Properties and Applications of Dielectric Materials*, pp. 521-524. viewed 5 May 2016,

Stone, GC 2005, 'Partial discharge diagnostics and electrical equipment insulation condition assessment', *Dielectrics and Electrical Insulation, IEEE Transactions on*, vol. 12, no. 5, pp. 891-904, viewed 1 October 2015,  
<<http://ieeexplore.ieee.org.ezproxy.usq.edu.au/stamp/stamp.jsp?tp=&arnumber=1522184>>

Transformers 2003, *Transformers*, 2nd edn, Tata McGraw-Hill,  
<https://books.google.com.au/books?id=rWgarr659pgC>>

Wang, M, Vandermaar, AJ & Srivastava, KD 2002, 'Review of condition assessment of power transformers in service', *Electrical Insulation Magazine, IEEE*, vol. 18, no. 6, pp. 12-25, viewed 2 October 2015,  
<<http://ieeexplore.ieee.org.ezproxy.usq.edu.au/stamp/stamp.jsp?tp=&arnumber=1161455>>

Zmarzly, D, Boczar, T, Fracz, P & Borucki, S 2014, 'High voltage power transformer diagnostics using vibroacoustic method', in *Proceedings of 2014 IEEE International Power Modulator and High Voltage Conference (IPMHVC)*, pp. 561-564. viewed 21 May 2016,

# APPENDIX A. PROJECT SPECIFICATION

For: Dean Starkey

Title: Partial Discharge in Transformers and Acoustic Noise Signature Correlation

Major: Electrical Engineering – Power Engineering

Supervisors: Andreas Helwig and Narottam Das

Sponsorship: Nil

Enrolment: ENG4111 – EXT S1, 2016  
ENG4112 – EXT S2, 2016

Project Aim: To develop, test and apply acoustic detection methods to identify partial discharge in transformers in the low frequency range.

**Programme: Issue A, 11<sup>th</sup> March, 2016**

1. Research background information relating to partial discharge in transformers and acoustic emissions.
2. Develop an acoustic emissions measuring device using non commercial grade and cost effective equipment.
3. Test the acoustic emissions measuring device using a controlled experiment.
4. Analyse results to determine the validity of acoustic noise detection in the lower frequency range.

*If time and resources permit:*

5. Monitor substations to determine correlation between acoustic emissions and gas analysis.

## APPENDIX B. MATLAB CODE

```
%=====
%
%           REAL-TIME VIBRATION MONITORING
%           UTILISING
%           ARDUINO & ADXL345
%
%           DEAN STARKEY - USQ
%           AUGUST 2016
%=====

%   This program reads live data from ADXL345 accelerometer to the
%   PC over serial communication either wirelessly or through USB.
%   The data is logged and saved to excel and displayed live to the GUI.

%=====
% Author:      Dean Starkey
% Student ID:   0061038897
% Created:      August 2016
% Assoc m files: 'Close_ports.m', 'Open_ports.m', 'Live_plotter.m'
% Version:      1
%-----
%               START OF CODE

%% Variables Declarations
% Define global variables
global xdata;
global ydata;
global zdata;
global tdata;
global acceleration;

% Set data variables
xdata      = 0;           % X plane - acceleration measured by ADXL345
ydata      = 0;           % Y plane - "
zdata      = 0;           % Z plane - "
tdata      = 0;           % Values of time in 'ms' from Arduino processor
acceleration = 0;         % Calc. value of acc. in 'g' (1g = 9.8ms^-2)
time       = 0;           % Time starts at 0
i          = 0;           % loop count
j          = 0;           % Loop count
scrollWidth = 10;         % A 10s scroll width for live plotting
delay      = 0.00005;     % Small delay for stability required
min        = -2;          % Min 'g' for plot
max        = 2;           % Max 'g' for plot
miss_read  = 0;           % Count # of miss reads for accuracy assessment
keep_going = true;        % Allows stop button to reset value
convert_g  = 4/1024;      % 10 bit resolution over a +/-2g range, to
                           % convert to Gs we use the equation:
                           %      xg = Measurement * (G-range/(2^10))

% Set serial variables
buffer      = 2^10;        % Total number of bytes stored in the software
                           % buffer during a read operation. 2^20 = (1MB).
flowcontrol = 'none';      % Data flow control (handshaking) is not used.
parity      = 'none';      % Parity checking not performed
databits    = 8;           % Transmit 8 bits at a time
stopbits    = 1;           % Transmit 1 stop bit
timeout     = 10;          % A 10s time out for serial connection
```

```

%% Initialisation
% Close open serial ports in Matlab
Close_ports()

% Open serial port
s = Open_ports(buffer, flowcontrol, parity, databits, ...
    stopbits, timeout, handles);

% Establish serial communication
Est_serial(handles)

% Assign plot to correct axes figure in gui
axes(handles.liveplot);
hold(handles.liveplot, 'on');
graph1 = plot(time, xdata, 'm-');
graph2 = plot(time, ydata, 'c-');
graph3 = plot(time, zdata, 'g-');

% Format the plot
title(handles.liveplot, 'Vibration')
xlabel(handles.liveplot, 'time (sec)')
ylabel(handles.liveplot, 'Acceleration (g)')
legend('X', 'Y', 'Z', 'location', 'S')

% Start time & set warning counter to map object
tic;
warningCounter = containers.Map();
%get(handles.mins, 'String')
mins = str2double(get(handles.mins, 'String'));
%% MAIN LOOP
while keep_going

% Set amount of minutes afterwhich data is exported to file
finalTime = datenum(clock + [0, 0, 0, 0, mins, 0]);

% Read and process data for # of mins before continuing
while keep_going && datenum(clock) < finalTime
    % See if stop button has been pressed
    Stopbutton_data = get(handles.Stopbutton, 'UserData');

    % When pressed Stopbutton_data.stop returns 1, stop the loop
    keep_going = ~Stopbutton_data.stop;

    % Take Measurement
    stream = fscanf(s, '%f,%f,%f,%f');

    % Count unsuccessful fscanf reads by counting warnings
    [msgstr, msgid] = lastwarn;
    if ~isempty(msgstr);
        if isKey(warningCounter, msgstr)
            warningCounter(msgstr) = warningCounter(msgstr)+1;
        else
            warningCounter(msgstr) = 1;
        end
    end
    lastwarn(''); % Reset lastwarn
    bad_read = warningCounter.values; % Set counter to cell value

    if (~isempty(stream))

```

```

i = i + 1;
time(i) = toc;

if (numel(stream) == 4)
    xdata(i) = stream(1, 1)*convert_g;
    ydata(i) = stream(1, 2)*convert_g;
    zdata(i) = stream(1, 3)*convert_g;
    tdata(i) = stream(1, 4);
else
    miss_read = miss_read + 1;
    continue;
end

% Every 100 iterations update GUI with freq. bad samples etc
if mod(i,100)==1 && length(tdata)>100
    % Calculate the sample freq. based on a 100 point rolling mean
    samp_f = mean(diff(tdata(i-100:i))*1e-3)^-1;

    % Monitor bytes available in buffer
    bytes_avail = s.BytesAvailable;

    % Put pertinent info into string to display on GUI
    data_str = sprintf(['Bytes avail. in buffer: %2d\n'...
                        'Bad reads: %1d\n'...
                        'Samp. freq. (Hz): %.0f\n'], ...
                        bytes_avail, bad_read{1}, samp_f);

    % Output to GUI
    set(handles.text_output,'String',data_str);
    % Every 50000 iterations update FFT plot
    if mod(i,50000)
        myfft(xdata,samp_f,handles)
    end
end

% Update live plot every 10th iteration
if mod(i,10)==1
    if(scrollWidth > 0)
        axes(handles.liveplot);
        selindex = time > time(i) - scrollWidth;
        set(graph1,'XData', time(selindex), 'YData', xdata(selindex));
        set(graph2,'XData', time(selindex), 'YData', ydata(selindex));
        set(graph3,'XData', time(selindex), 'YData', zdata(selindex));
        axis([time(i) - scrollWidth time(i) min max]);
    else
        set(graph1,'XData', time, 'YData', xdata);
        set(graph2, 'XData', time, 'YData', ydata);
        set(graph3, 'Xdata', time, 'YData', zdata);
        axis([0 time(i) min max]);
    end
end
end
pause(delay);
end
end

% Log data to file now that we have been processing for # of mins
acceleration = sqrt(xdata.^2+ydata.^2+zdata.^2);
data = [xdata;ydata;zdata;acceleration;tdata]';
end

% Calculate acceleration based on magnitude of x, y & z
acceleration = sqrt(xdata.^2+ydata.^2+zdata.^2);

```

```

data          = [xdata;ydata;zdata;acceleration;tdata]';

% Update the gui with data for processing
set(handles.Live_plotter,'UserData',data);
guidata(hObject,handles);

% Close open serial ports in Matlab
Close_ports()

%-----
%                               END OF MAIN SCRIPT
end

%-----
%                               FUNCTIONS
function Close_ports()
%-----
% Description: Close and delete any and all open serial ports in MATLAB
%
% Inputs: None
%
% Output: None
%
% Author:          Dean Starkey
% Student ID:      0061038897
% Created:         August 2016
% Assoc m files:   'Arduino_real_time.m'
% Version:         1
%-----
% Get info on all open serial ports
com_objs = instrfindall;

if ~isempty(com_objs)
    fclose(com_objs); % Close the open COM port connection
    delete(com_objs); % Delete the serial object
end

function Est_serial(handles)
%-----
% Description: Open serial ports using input parameters from gui
%
% Inputs: handles structure
%
% Output: None
%
% Author:          Dean Starkey
% Student ID:      0061038897
% Created:         August 2016
% Assoc m files:   'Arduino_real_time.m'
% Version:         1
%-----

% Send character 'a' to Arduino
fprintf(s,'%c', 'a');

% Assign any letter besides a
a = 'b';

while (a ~= 'a')
    % Continuously read from the serial port until letter 'a' is read

```



```

        a = fread(s, 1, 'uchar');
        % Allow program to exit if communication not being established
        if Stopbutton_data.stop == 1;
            a = 'a';
        end
    end
end

% Output message to gui
set(handles.serial_info,'String','Serial communication established');

end

function Export_data( data )
%-----
% Description:    Function stores data set in .txt file
% Syntax:        Export_data(data)
%
% Inputs:        data - complete data set for X, Y, Z, time & Acc
%
% Outputs:       None
%
% Author:        Dean Starkey
% Student ID:    0061038897
% Created:       August 2016
% Assoc m files: 'Arduino_real_time.m'
% Version:       1
%-----

% Column data
x = data( : , 1 );
y = data( : , 2 );
z = data( : , 3 );
a = data( : , 4 );
t = data( : , 5 );

% Calculate sampling frequency
f1 = mean(diff(t(1:100))*1e-3)^-1; % (Hz)

% Get the current date and time in decimal form
clock_now = clock; % [year month day hour minute seconds]
stamp = datestr(clock_now, 0); % 'dd-mmm-yyyy HH:MM:SS'
clock_now(6) = round(clock_now(6)); % Round to the nearest second
timestring = ''; % Setup date string

% Put time into string to name the file 'data_yyyyddmm_hhmm_ss'
for i = 1:1:6
    timestring = [timestring,num2str(clock_now(i),'%02d')];
    if i==3 || i==5 % Add underscore
        timestring = [timestring,'_'];
    end
end

% Create the "data" directory in the current location if not already
if exist('data')~=7 % If "data" does not yet exist
    mkdir('data'); % Create it
end

% Open new file
file_name = ['data/data_',timestring,'.txt'];

```

```

fidl = fopen(file_name,'wt');

% Print credits and information to top lines of file
fprintf(fidl,['Data Log:\t']);
fprintf(fidl,'%s\n\n', stamp);
fprintf(fidl, 'Sampling frequency (Hz): %5.1f\n',f1);

% Print column headins
fprintf(fidl,'X axis (g)\tY axis (g)\tZ axis (g)\tAcc. (g)\tTime (ms)\n');

% For every row data set print to file and include time string
for i=1:length(data)
    % Output data to file
    fprintf(fidl,'%9f\t%9f\t%9f\t%9f\t%9.0f\n', ...
        x(i), y(i), z(i), a(i), t(i));
end

% Close file once complete
fclose(fidl);
%-----
end

function GF_data = G_filter( data, type, fs, handles )
%-----
% Description: Apply filters to data set
%
% Inputs: data = raw acceleration data, column vector
%         type = filter type eg. 'EMA', 'Low Pass'
%         fs   = sampling frequency (Hz)
%         handles structure
%
% Output: None
%
% Author:      Dean Starkey
% Student ID:  0061038897
% Created:     August 2016
% Assoc m files: 'Arduino_real_time.m'
% Version:     1
%-----

% For EMA set alpha from value in GUI
alpha = str2num(get(handles.EMA_alpha,'String'));

% For Low pass get cutoff freq. from GUI
fc = get(handles.fc,'String');

% Put pertinent info into string to display on GUI
data_str = sprintf(['Filter applied:   %s\n'...
    'Number of samples: %2d\n'...
    'Samp. freq. (Hz):   %0f\n'], ...
    type, length(data), fs);
% Output to GUI
set(handles.text_output,'String',data_str);
switch type
    case 'EMA'
        % Array to hold filtered data
        GF_data = zeros(length(data),1);

```

```

        % Start at j=2 position, avoid calling -j index
        for j=2:length(data)
            GF_data(j,1) = (1-alpha)*GF_data(j-1,1) + alpha*data(j,1);
        end
    case 'Low Pass'
        [b, a] = butter(1, 2*fc/fs);
        GF_data = filter(b,a, data);
    otherwise
        GF_data=ones(length(data));
    end
end

figure(1)
cla
plot(data, 'b');
hold on;
plot(GF_data, 'r')
    title('Filtered data')
    xlabel('Samples')
    ylabel('Acceleration (g)')
    legend('Unfiltered',sprintf('%s Filter', type),'location','NW')

end

function myfft( data, Fs, handles )
%-----
% Description: Compute the single sided Fast Fourier Transform
%
% Inputs:   data    = signal
%           Fs      = sampling frequency
%           handles structure
%
% Output:   None
%
% Author:      Dean Starkey
% Student ID:  0061038897
% Created:     August 2016
% Assoc m files: 'Arduino_real_time.m'
% Version:     1
%-----
% Detailed explanation goes here
x = data;
T = 1/Fs;           % sampling period
L = length(x);      % length of signal
t = (0:L-1)*T;      % time vector
n = 2^nextpow2(L);  % pad with zeros for efficiency
dim = 2;            % operates along rows of x

Y = fft(x,n);       % compute Fourier Transform of the signal

P2 = abs(Y/L);       % compute the two sided spectrum P2

P1 = P2(1:n/2+1);   % compute single sided spectrum based on P2

P1(2:end-1) = 2*P1(2:end-1);

% Define the Frequency Domain and plot the single sided FFT
f = Fs*(0:(n/2))/n;
axes(handles.fft_plot);
plot(f,P1)

```

```

        title('Single-Sided Amplitude Spectrum of X(t)')
        xlabel('f (Hz)')
        ylabel('|P1(f)|')

    end

function s = Open_ports(b, f, p, d, st, t, handles)
%-----
% Description: Open serial ports using input parameters from gui
%
% Inputs:   b = buffer
%           f = flowcontrol
%           p = parity
%           d = databits
%           st = stopbits
%           t = timeout
%           handles structure
%
% Output:   s = serial_object
%
% Author:      Dean Starkey
% Student ID:  0061038897
% Created:     August 2016
% Assoc m files: 'Arduino_real_time.m'
% Version:     1
%-----

com = get(handles.com_popup, 'UserData'); % Get com port from GUI
com = get(handles.Comport, 'String'); % Get com port from GUI
s = serial(com); % Create a serial port object

% Get baud rate from gui & convert to number
bauds = get(handles.setbaudrate, 'SelectedObject');
baudrate = str2num(get(bauds, 'String'));

% Set serial communication parameters
set(s, 'InputBufferSize', b);
set(s, 'FlowControl', f);
set(s, 'BaudRate', baudrate);
set(s, 'Parity', p);
set(s, 'DataBits', d);
set(s, 'StopBit', st);
set(s, 'Timeout', t);

% Open serial object
fopen(s);

end

function statistical( data, binwidth, handles )
%-----
% Description: Plot distribution and probability density function
%
% Inputs:   data = data to be analysed
%           binwidth = range of grouped data
%           handles structure
%
% Output: None
%
% Author:      Dean Starkey

```

```

% Student ID:    0061038897
% Created:      August 2016
% Assoc m files: 'Arduino_real_time.m'
% Version:      1
%-----
%data1 = data;
data(data>2) = 2;
data(data<-2) = -2;

mu_x = mean(data);
s_x = std(data);

% Create the first bin by rounding down the minimum
first_bin = floor(min(data)/binwidth)*binwidth + binwidth/2;
% Create the last bin by rounding up the maximum
last_bin = ceil(max(data)/binwidth)*binwidth - binwidth/2;
% Find bin center
binCent = first_bin : binwidth : last_bin;
[y_abs, bins] = hist(data, binCent);
% Scaled frequency
y_scaled = y_abs/sum(y_abs)/binwidth;

%Plot distribution
axes(handles.pdf);
cla
%First plot the scaled histogram
bar(bins, y_scaled,...
    'FaceColor','b','EdgeColor',[0 .9 .9],'LineWidth',1.5)
    title('Scaled Frequency')
    xlabel('Acceleration (g)'), ylabel('Probability')
    axis([-2,2,0,inf])
%Calculate the probability density function
Y = pdf('Normal',first_bin: last_bin, mu_x, s_x);
%On top of first plot, plot the pdf
hold on
plot(first_bin : last_bin, Y, '-r','LineWidth',4)
axes(handles.alldata);
plot(data)
    title('Acceleration All Data')
    xlabel('Samples')
    ylabel('Acceleration (g)')
    axis([0,length(data),-2,2])

% data1=data;
% data1(data1>2) = 2;
% data1(data1<-2) = -2;
% axes.figure(2))
% figure(2)
% plot(data1)
end

function varargout = Live_plotter(varargin)
%-----
% Description: GRAPHICAL USER INTERFACE CODE
%
%
% Author:      Dean Starkey
% Student ID:  0061038897
% Created:    August 2016
% Assoc m files: 'Arduino_real_time.m'

```

```

% Version:      1
%-----
% Begin initialization code - DO NOT EDIT
gui_Singleton = 1;
gui_State = struct('gui_Name',       mfilename, ...
                  'gui_Singleton',   gui_Singleton, ...
                  'gui_OpeningFcn', @Live_plotter_OpeningFcn, ...
                  'gui_OutputFcn',  @Live_plotter_OutputFcn, ...
                  'gui_LayoutFcn',  [] , ...
                  'gui_Callback',    []);
if nargin && ischar(varargin{1})
    gui_State.gui_Callback = str2func(varargin{1});
end

if nargout
    [varargout{1:nargout}] = gui_mainfcn(gui_State, varargin{:});
else
    gui_mainfcn(gui_State, varargin{:});
end
% End initialization code - DO NOT EDIT


% --- Executes just before Live_plotter is made visible.
function Live_plotter_OpeningFcn(hObject, eventdata, handles, varargin)
handles.output = hObject;

% Update handles structure
guidata(hObject, handles);


function varargout = Live_plotter_OutputFcn(hObject, eventdata, handles)
varargout{1} = handles.output;


% --- Executes on button press in Startbutton.
function Startbutton_Callback(hObject, eventdata, handles)
clc; %clear the screen

%clear the plot, in case anything remains from prev. run
cla(handles.liveplot,'reset');

% Initialise stop button
Stopbutton_data.stop = false; % Stop = false
set(handles.Stopbutton,'UserData',Stopbutton_data) % Store the Stop data
set(handles.text_output,'String','Processing') % Clear txt string

% As the button has been pushed, make it red and display the words "running"
% Copy the initial color value
Startbutton_data.color = get(handles.Startbutton,'BackgroundColor');
% Store the colour value
set(handles.Startbutton,'UserData',Startbutton_data);
% Make start button light red
set(handles.Startbutton,'BackgroundColor',[1 .5 .5]);
% Display Running and disable
set(handles.Startbutton,'String','Running','Enable','off');
% Enable the stop button
set(handles.Stopbutton,'Enable','on');
set(handles.serial_info,'String','Connecting to the Arduino...');
drawnow; % update button visually

```

```

%Call the main code script (m-file)
Arduino_real_time

% --- Executes on button press in Stopbutton.
function Stopbutton_Callback(hObject, eventdata, handles)
Stopbutton_data.stop = true; % Set stop = true
set(handles.Stopbutton, 'UserData', Stopbutton_data) % Store the Stop data

% Turn start button back to normal
Startbutton_data = get(handles.Startbutton, 'UserData');
set(handles.Startbutton, 'BackgroundColor', Startbutton_data.color);
set(handles.Startbutton, 'String', 'Start', 'Enable', 'on');
set(handles.Stopbutton, 'Enable', 'off');
drawnow; %force button redraw

guidata(hObject, handles);

% --- Executes on button press in data_out.
function data_out_Callback(hObject, eventdata, handles)
% Export data by calling the function
Gdata = get(handles.Live_plotter, 'UserData');
Export_data(Gdata)

% --- Executes on button press in fft_button.
function fft_button_Callback(hObject, eventdata, handles)
% FFT data plot
ds = get(handles.datasources, 'SelectedObject'); % Selected data source
data_source = get(ds, 'String'); % Get 'Log file' or 'Live data'
x = strcmp(data_source, 'Log file'); % Compare, if log then 1
if x == 1
    log_data = get(handles.datasources, 'UserData');
    data = log_data(:,4);
    tdata = log_data(:,5);
else
    live_data = get(handles.Live_plotter, 'UserData');
    data = live_data(:,4);
    tdata = log_data(:,5);
end
samp_f = mean(diff(tdata(1:100))*1e-3)^-1;
myfft(data, samp_f, handles)

function fft_button_ButtonDownFcn(hObject, eventdata, handles)

% --- Executes on button press in psd.
function psd_Callback(hObject, eventdata, handles)
% Perform Welches Power Spectral Density
ds = get(handles.datasources, 'SelectedObject'); % Selected data source
data_source = get(ds, 'String'); % Get 'Log file' or 'Live data'
x = strcmp(data_source, 'Log file'); % Compare, if log then 1
if x == 1
    log_data = get(handles.datasources, 'UserData');
    data = log_data(:,4);
else

```

```

        live_data = get(handles.Live_plotter, 'UserData');
        data = live_data(:,4);
    end

    t = (0:length(x)-1)*1/1000;
    % Some harmonics added for testing only
    x1 = 0.75*sin(2 .* pi .* 100 .* t);
    x2 = 0.25*sin(2 .* pi .* 200 .* t);
    x3 = 0.5*sin(2 .* pi .* 300 .* t);
    x = x'+x1+x2+x3;
    axes(handles.fft_plot);
    hold(handles.liveplot, 'on');
    pwelch(data)

function mins_Callback(hObject, eventdata, handles)

% --- Executes during object creation, after setting all properties.
function mins_CreateFcn(hObject, eventdata, handles)

if ispc && isequal(get(hObject, 'BackgroundColor'), get(
(0, 'defaultUiControlBackgroundColor'))
    set(hObject, 'BackgroundColor', 'white');
end

% --- Executes on button press in statistics.
function statistics_Callback(hObject, eventdata, handles)
%Perform Statistical Analysis
ds = get(handles.datasources, 'SelectedObject'); % Selected data source
data_source = get(ds, 'String'); % Get 'Log file' or 'Live data'
x = strcmp(data_source, 'Log file'); % Compare, if log then 1
if x == 1
    log_data = get(handles.datasources, 'UserData');
    data = log_data(:,4);
else
    live_data = get(handles.Live_plotter, 'UserData');
    data = live_data(:,4);
end

% Run statistical function, set bin width
statistical(data,0.1,handles)

% --- Executes on button press in loadfile.
function loadfile_Callback(hObject, eventdata, handles)
% Open file explorer and select file
[filename1,filepath1]=uigetfile({'*.*','All Files'},...
    'Select Data File 1');
cd(filepath1);
log_data = importdata([filepath1 filename1], '\t', 4);
set(handles.datasources, 'UserData', log_data.data);
guidata(hObject, handles);

% --- Executes on button press in live_button.
function live_button_Callback(hObject, eventdata, handles)
% Use live data stored in User Data
handles = guidata(hObject)
livedata = get(handles.Live_plotter, 'UserData');

```



```

guidata(hObject, handles);

% --- Executes on button press in log_button.
function log_button_Callback(hObject, eventdata, handles)
% Use logged data
% Retrieve GUI data (the handles structure)
handles = guidata(hObject)

% Update handles structure
guidata(hObject, handles);

% --- Executes on button press in Apply_filter.
function Apply_filter_Callback(hObject, eventdata, handles)
% hObject      handle to Apply_filter (see GCBO)
% eventdata    reserved - to be defined in a future version of MATLAB
% handles      structure with handles and user data (see GUIDATA)
ds = get(handles.datasources, 'SelectedObject'); % Selected data source
data_source = get(ds, 'String');                  % Get 'Log file' or 'Live data'
x = strcmp(data_source, 'Log file');               % Compare, if log then 1
if x == 1
    log_data = get(handles.datasources, 'UserData');
    data = log_data(:,4);
    tdata = log_data(:,5);
else
    live_data = get(handles.Live_plotter, 'UserData');
    data = live_data(:,4);
    tdata = log_data(:,5);
end

samp_f = mean(diff(tdata(1:100))*1e-3)^-1;

ft = get(handles.filtersselect, 'SelectedObject'); % Selected filter type
filter_type = get(ft, 'String');                  % Get 'EMA' or 'Low pass'

% Filter Data
G_filter(data, filter_type, samp_f, handles)

% -----
%                               END OF CODE

```

## APPENDIX C. ARDUINO CODE

```
//Add the SPI library so we can communicate with the ADXL345 sensor
#include <SPI.h>

//Assign the Chip Select signal to pin 10.
int CS=10;

//ADXL345 Register Addresses
#define DEVID 0x00 //Device ID Register
#define THRESH_TAP 0x1D //Tap Threshold
#define OFSX 0x1E //X-axis offset
#define OFSY 0x1F //Y-axis offset
#define OFSZ 0x20 //Z-axis offset
#define DURATION 0x21 //Tap Duration
#define LATENT 0x22 //Tap latency
#define WINDOW 0x23 //Tap window
#define THRESH_ACT 0x24 //Activity Threshold
#define THRESH_INACT 0x25 //Inactivity Threshold
#define TIME_INACT 0x26 //Inactivity Time
#define ACT_INACT_CTL 0x27 //Axis enable control for activity and inactivity detection
#define THRESH_FF 0x28 //free-fall threshold
#define TIME_FF 0x29 //Free-Fall Time
#define TAP_AXES 0x2A //Axis control for tap/double tap
#define ACT_TAP_STATUS 0x2B //Source of tap/double tap
#define BW_RATE 0x2C //Data rate and power mode control
#define POWER_CTL 0x2D //Power Control Register
#define INT_ENABLE 0x2E //Interrupt Enable Control
#define INT_MAP 0x2F //Interrupt Mapping Control
#define INT_SOURCE 0x30 //Source of interrupts
#define DATA_FORMAT 0x31 //Data format control
#define DATA0 0x32 //X-Axis Data 0
#define DATA1 0x33 //X-Axis Data 1
#define DATA0 0x34 //Y-Axis Data 0
#define DATA1 0x35 //Y-Axis Data 1
#define DATA0 0x36 //Z-Axis Data 0
#define DATA1 0x37 //Z-Axis Data 1
#define FIFO_CTL 0x38 //FIFO control
#define FIFO_STATUS 0x39 //FIFO status

// Set constant for

//This buffer will hold values read from the ADXL345 registers.
char values[10];
char output[20];
//These variables will be used to hold the x,y and z axis accelerometer values.
int x,y,z;

void setup(){
  //Initiate an SPI communication instance.
  SPI.begin();
  //Configure the SPI connection for the ADXL345.
  SPI.setDataMode(SPI_MODE3);
  //Create a serial connection to display the data on the terminal.
  // 115200 works, 57600 works good, 9600 for testing
  Serial.begin(9600);

  // Check serial communication acknowledgement routine
  char a = 'b';
  while (a != 'a')
  {
    // Wait for a specific character from the PC
    a=Serial.read();
  }
  Serial.println('a'); // sending a character to the PC

  //Set up the Chip Select pin to be an output from the Arduino.
  pinMode(CS, OUTPUT);
  //Before communication starts, the Chip Select pin needs to be set high.
```

```

digitalWrite(CS, HIGH);

//Create an interrupt that will trigger when a tap is detected.
//attachInterrupt(0, tap, RISING);

//Put the ADXL345 into +/- G range by writing the value to the DATA_FORMAT register.
char Two_G = 0x00; // +/- 2G
char Four_G = 0x01; // +/- 4G
writeRegister(DATA_FORMAT, Two_G);

// Set data rate to highest 3200Hz 0x0F - 100Hz 0x0A
writeRegister(BW_RATE, 0x0F);

// Put the ADXL345 into Measurement Mode by writing 0x08 to the POWER_CTL register.
writeRegister(POWER_CTL, 0x08); //Measurement mode
readRegister(INT_SOURCE, 1, values); //Clear the interrupts from the INT_SOURCE register.
// Delay a little
delay(1);
}

void loop(){
  //Reading 6 bytes of data starting at register DATA0 will retrieve the x,y and z
  acceleration values from the ADXL345.
  //The results of the read operation will get stored to the values[] buffer.
  //Serial.println(millis());
  //Loop readings to pop FIFO buffer
  //for(int i = 0; i < 100; ++i){
  readRegister(DATA0, 6, values);

  //The ADXL345 gives 10-bit acceleration values, but they are stored as bytes (8-bits). To
  get the full value, two bytes must be combined for each axis.
  //The X value is stored in values[0] and values[1].
  x = ((int)values[1]<<8)|(int)values[0];
  //The Y value is stored in values[2] and values[3].
  y = ((int)values[3]<<8)|(int)values[2];
  //The Z value is stored in values[4] and values[5].
  z = ((int)values[5]<<8)|(int)values[4];

  Serial.print(x, DEC);
  Serial.print(',');
  Serial.print(y, DEC);
  Serial.print(',');
  Serial.print(z, DEC);
  Serial.print(',');
  Serial.println(millis());
  //}
}

//This function will write a value to a register on the ADXL345.
//Parameters:
// char registerAddress - The register to write a value to
// char value - The value to be written to the specified register.
void writeRegister(char registerAddress, char value){
  //Set Chip Select pin low to signal the beginning of an SPI packet.
  digitalWrite(CS, LOW);
  //Transfer the register address over SPI.
  SPI.transfer(registerAddress);
  //Transfer the desired register value over SPI.
  SPI.transfer(value);
  //Set the Chip Select pin high to signal the end of an SPI packet.
  digitalWrite(CS, HIGH);
}

//This function will read a certain number of registers starting from a specified address
and store their values in a buffer.
//Parameters:

```

```

// char registerAddress - The register address to start the read sequence from.
// int numBytes - The number of registers that should be read.
// char * values - A pointer to a buffer where the results of the operation should be stored
void readRegister(char registerAddress, int numBytes, char * values){
    //Since we're performing a read operation, the most significant bit of the register
    address should be set.
    char address = 0x80 | registerAddress;
    //If we're doing a multi-byte read, bit 6 needs to be set as well.
    if(numBytes > 1)address = address | 0x40;

    //Set the Chip select pin low to start an SPI packet.
    digitalWrite(CS, LOW);
    //Transfer the starting register address that needs to be read.
    SPI.transfer(address);
    //Continue to read registers until we've read the number specified, storing the results to
    the input buffer.
    for(int i=0; i<numBytes; i++){
        values[i] = SPI.transfer(0x00);
    }
    //Set the Chips Select pin high to end the SPI packet.
    digitalWrite(CS, HIGH);
}

```

# APPENDIX D. DGA REPORTS

Insulation Assessment Laboratory  
14 Nelson St, Chatswood NSW 2067



**Report Number: 160315020**

Customer: Ausgrid, Technical Operations Southern-East (Zetland)  
Steven Panman

## Sample Details:

Substation name:	Site 1	Substation number:	1	Equipment:	Transformer
Position:	2	Inventory No.:		Sampling Pt (DGA):	Bottom of main tank
SAP identifier:		Serial No.:		Sampling Pt (o.s.):	Bottom of main tank
Manufacturer:	Tyree	Voltage ratio (kV):	132/33	Sampled on:	15/03/2016
Fluid type:	Mineral Oil	Tap changer:	1-17	Received on:	15/03/2016
Temp.: Oil (°C)	58	Winding (°C):	68	Ambient (°C):	35

(Sample analysed as received)

Test	Component	Results	Units	Method
DGA				CH 01; CH 02; IEC 60567
	Hydrogen (H <sub>2</sub> )	213	µl/l	
	Oxygen (O <sub>2</sub> )	1,160	µl/l	
	Nitrogen (N <sub>2</sub> )	45,600	µl/l	
	Methane (CH <sub>4</sub> )	92	µl/l	
	Carbon Monoxide (CO)	809	µl/l	
	Carbon Dioxide (CO <sub>2</sub> )	3,340	µl/l	
	Ethylene (C <sub>2</sub> H <sub>4</sub> )	207	µl/l	
	Ethane (C <sub>2</sub> H <sub>6</sub> )	38	µl/l	
	Acetylene (C <sub>2</sub> H <sub>2</sub> )	23	µl/l	
	Propane (C <sub>3</sub> H <sub>8</sub> )	56	µl/l	
	Total gas	52.0	ml/l	
	TDCG	1,438	µl/l	
Water				CH 05; IEC 60814
	Water	73	ppm	
Acidity				AS 1767.1
	Acidity	0.64	mg KOH/g oil	
IFT				CH 06
	IFT	14.4	mN/m	
Dielectric BV				IEC 60156; AS 1767.2.1
	Dielectric Breakdown Voltage	42.9	kV	
DDF				CH 08; IEC 60247
	DDF @ 90°C	380.6	*0.001	
	Resistivity @ 90°C	0.5	Gohm.m	
AOX				In-house
	Oxidation inhibitor Concentration	None [ND]	ppm	
Furans				CH 03; IEC 61198
	5-HMF-(5-hydroxymethyl-2fural)	<0.05	ppm	
	2-FOL-(2-furfural)	<0.05	ppm	
	2-FAL-(2-furaldehyde)	0.15	ppm	
	2-ACF-(2-acetyl-furan)	<0.05	ppm	
	5-MEF-(5-methyl-2-furaldehyde)	<0.05	ppm	
Passivator				In-house
	Passivator Concentration	None [ND]	ppm	

## Other information: Follow-up

Comments: DGA: DGA results indicate that the discharge(s) of high energy are probably present as well as excessive consumption of oxygen.

Oil screen: Hazy appearance; appears to contain sludge; failed water content, acidity, IFT; lower breakdown voltage; higher DDF.

Significantly oxidized oil

## Report Number: 160418017

Customer: Ausgrid, Technical Operations Southern-East (Zetland)  
Steven Panman

### Sample Details:

Substation name:	Site 2	Substation number:	2	Equipment:	Transformer
Position:	4	Inventory No.:		Sampling Pt (DGA):	Bottom of main tank
SAP identifier:		Serial No.:		Sampling Pt (o.s.):	Bottom of main tank
Manufacturer:	Tyree	Voltage ratio (kV):	132/33	Sampled on:	18/04/2016
Fluid type:	Mineral Oil	Tap changer:	1-8	Received on:	18/04/2016
Temp.: Oil (°C)	48	Winding (°C):	47	Ambient (°C):	

(Sample analysed as received)

Test	Component	Results	Units	Method
DGA	Hydrogen (H <sub>2</sub> )	81	µl/l	CH 01; CH 02; IEC 60567
	Oxygen (O <sub>2</sub> )	969	µl/l	
	Nitrogen (N <sub>2</sub> )	78,500	µl/l	
	Methane (CH <sub>4</sub> )	147	µl/l	
	Carbon Monoxide (CO)	1,400	µl/l	
	Carbon Dioxide (CO <sub>2</sub> )	4,770	µl/l	
	Ethylene (C <sub>2</sub> H <sub>4</sub> )	49	µl/l	
	Ethane (C <sub>2</sub> H <sub>6</sub> )	117	µl/l	
	Acetylene (C <sub>2</sub> H <sub>2</sub> )	11	µl/l	
	Propane (C <sub>3</sub> H <sub>8</sub> )	132	µl/l	
	Total gas	88.0	ml/l	
	TDCG	1,937	µl/l	
Water	Water	65	ppm	CH 05; IEC 60814
Acidity	Acidity	0.57	mg KOH/g oil	AS 1767.1
IFT	IFT	15.8	mN/m	CH 06
Dielectric BV	Dielectric Breakdown Voltage	71.8	kV	IEC 60156; AS 1767.2.1
DDF	DDF @ 90°C	625.0	*0.001	CH 08; IEC 60247
	Resistivity @ 90°C	0.4	Gohm.m	
AOX	Oxidation inhibitor	[NT]		In-house
	Concentration	[NT]	ppm	
Furans	5-HMF-(5-hydroxymethyl-2fural)	[NT]	ppm	CH 03; IEC 61198
	2-FOL-(2-furfural)	[NT]	ppm	
	2-FAL-(2-furaldehyde)	[NT]	ppm	
	2-ACF-(2-acetyl-furan)	[NT]	ppm	
	5-MEF-(5-methyl-2-furaldehyde)	[NT]	ppm	
Passivator	Passivator	[NT]		In-house
	Concentration	[NT]	ppm	

### Other information: Follow-up sample

Comments: DGA results indicate that the mixtures of electrical and thermal faults are probably present, as well as an excessive consumption of oxygen.

Failed acidity, water content, IFT and DDF. Furans test to follow.

Significantly oxidized oil.

## Report Number: 160301013

Customer: Ausgrid, Tech Operations Southern-South (Oatley)  
Richard Rowinski

### Sample Details:

Substation name:	Site 3	Substation number:	3	Equipment:	Transformer
Position:	1	Inventory No.:		Sampling Pt (DGA):	Bottom of main tank
SAP identifier:		Serial No.:		Sampling Pt (o.s.):	Bottom of main tank
Manufacturer:	ABB	Voltage ratio (kV):	132/11	Sampled on:	22/02/2016
Fluid type:	Mineral Oil	Tap changer:	14-2	Received on:	1/03/2016
Temp.: Oil (°C)	70	Winding (°C):	85	Ambient (°C):	25

(Sample analysed as received)

Test	Component	Results	Units	Method
DGA				CH 01; CH 02; IEC 60567
	Hydrogen (H <sub>2</sub> )	196	µl/l	
	Oxygen (O <sub>2</sub> )	21,000	µl/l	
	Nitrogen (N <sub>2</sub> )	72,500	µl/l	
	Methane (CH <sub>4</sub> )	27	µl/l	
	Carbon Monoxide (CO)	622	µl/l	
	Carbon Dioxide (CO <sub>2</sub> )	4,260	µl/l	
	Ethylene (C <sub>2</sub> H <sub>4</sub> )	38	µl/l	
	Ethane (C <sub>2</sub> H <sub>6</sub> )	2	µl/l	
	Acetylene (C <sub>2</sub> H <sub>2</sub> )	239	µl/l	
	Propane (C <sub>3</sub> H <sub>8</sub> )	8	µl/l	
	Total gas	100	ml/l	
	TDCG	1,131	µl/l	
Water				CH 05; IEC 60814
	Water	28	ppm	
Acidity				AS 1767.1
	Acidity	0.06	mg KOH/g oil	
IFT				CH 06
	IFT	21.9	mN/m	
Dielectric BV				IEC 60156; AS 1767.2.1
	Dielectric Breakdown Voltage	35.5	kV	
DDF				CH 08; IEC 60247
	DDF @ 90°C	28.1	*0.001	
	Resistivity @ 90°C	7.0	Gohm.m	
AOX				In-house
	Oxidation inhibitor Concentration	PBN		
		567	ppm	
Furans				CH 03; IEC 61198
	5-HMF-(5-hydroxymethyl-2-fural)	<0.05	ppm	
	2-FOL-(2-furfural)	<0.05	ppm	
	2-FAL-(2-furaldehyde)	0.41	ppm	
	2-ACF-(2-acetylfuran)	<0.05	ppm	
	5-MEF-(5-methyl-2-furaldehyde)	<0.05	ppm	
Passivator				In-house
	Passivator Concentration	None		
		[ND]	ppm	

#### Comments:

Oil Screen: Failed breakdown voltage, higher water content;

DGA: The DGA results are similar to 150514001 except the level of CO and CO<sub>2</sub> have significantly increased, refer to the comments on 150514001-Electrical discharge of low energy might have occurred.

Recommendation: Continue to monitor the fault gas production, and water content.

## Report Number: 151116013

Customer: Ausgrid, Technical Operations Northern, Chatswood  
Alex Worrall

### Sample Details:

Substation name:	Site 4	Substation number:	4	Equipment:	Transformer
Position:	2	Inventory No.:		Sampling Pt (DGA):	Radiator
SAP identifier:		Serial No.:		Sampling Pt (o.s.):	Main tank
Manufacturer:	Asea Brown Boveri	Voltage ratio (kV):	132/11	Sampled on:	9/11/2015
Fluid type:	Mineral Oil	Tap changer:	6-12	Received on:	16/11/2015
Temp.: Oil (°C)	60/30	Winding (°C):	65/30	Ambient (°C):	20

(Sample analysed as received)

Test	Component	Results	Units	Method
DGA				CH 01; CH 02; IEC 60567
	Hydrogen(H <sub>2</sub> )	28	ppm	
	Oxygen (O <sub>2</sub> )	9,310	ppm	
	Nitrogen (N <sub>2</sub> )	55,500	ppm	
	Methane (CH <sub>4</sub> )	4	ppm	
	Carbon Monoxide (CO)	746	ppm	
	Carbon Dioxide (CO <sub>2</sub> )	1,010	ppm	
	Ethylene (C <sub>2</sub> H <sub>4</sub> )	<1	ppm	
	Ethane (C <sub>2</sub> H <sub>6</sub> )	<1	ppm	
	Acetylene (C <sub>2</sub> H <sub>2</sub> )	<1	ppm	
	Propane (C <sub>3</sub> H <sub>8</sub> )	<1	ppm	
	Total gas	68.0	ml/L	
	TDCG	778	ppm	
Water				CH 05; IEC 60814
	Water	4	ppm	
Acidity				AS 1767.1
	Acidity	0.06	mg KOH/g oil	
IFT				CH 06
	IFT	42.1	mN/m	
Dielectric BV				IEC 60156; AS 1767.2.1
	Dielectric Breakdown Voltage	76.4	kV	
DDF				CH 08; IEC 60247
	DDF @ 90°C	1.4	*0.001	
	Resistivity @ 90°C	388.3	Gohm.m	
AOX				In-house
	Oxidation inhibitor	None		
	Concentration	[ND]	ppm	
Furans				CH 03; IEC 61198
	5-HMF(5-hydroxymethyl-2-furaldehyde)	<0.01	ppm	
	2-FOL (2-furfural)	<0.02	ppm	
	2-FAL (2-furaldehyde)	<0.02	ppm	
	2-ACF (2-acetyl-furan)	<0.10	ppm	
	5-MEF (5-methyl-2-furaldehyde)	<0.02	ppm	
Passivator				In-house
	Passivator	None		
	Concentration	[ND]	ppm	

#### Comments:

Oil Screen: Fluid condition is within acceptable in- service parameters.

DGA: DGA test results indicate that there is an excessive oxygen consumption, and abnormal ratio of CO<sub>2</sub>/CO. But each gas level is stable and similar to previous results-131210026.

S/No. 140412 on the tag.



Insulation Assessment Laboratory  
14 Nelson St, Chatswood NSW 2067  
Telephone:-  
Tim Yang (02) 9410 5117 [tyyang@ausgrid.com.au]  
Facsimile: (02) 9410 5181



## Test Report No - 131213019

For: Ausgrid  
Mr Peter Gleeson

PTVR Chatswood

### Sample Details:

Origin: **Site 5**  
Equipment: **Transformer**  
Asset No:  
Sampling Pt: **Radiators**  
T/C: **4-9**  
Temp: **Oil 56°C; winding 58°C; ambient 32°C.**

Sub No: **5**  
Position: **1**  
Serial No:  
Voltage:  
Phase:  
Sampled on: **10.12.2013**  
Received on: **13.12.2013**

### Test Results:

(Sample analysed as received)

Test	Component	Results	Units	Method
DGA	Hydrogen	2.8	ppm	CH/01; CH/02; mod. IEC 60567
	Oxygen	31900	ppm	
	Nitrogen	66300	ppm	
	Methane	0.8	ppm	
	Carbon Monoxide	40	ppm	
	Carbon Dioxide	424	ppm	
	Ethylene	0.5	ppm	
	Ethane	0.08	ppm	
	Acetylene	ND	ppm	
	Propane	0.1	ppm	
	Total gas	100	mL/L	

*The test results are satisfactory.*

## Test Report No - 131213021

For: Ausgrid  
Mr Peter Gleeson

PTVR Chatswood

### Sample Details:

Origin: **Site 6**  
Equipment: **Transformer**  
Asset No:  
Sampling Pt: **Radiators**  
T/C: **4-7**  
Temp: **Oil 50°C; winding 56°C; ambient 32°C.**

Sub No: **3**  
Position: **2**  
Serial No:  
Voltage:  
Phase:  
Sampled on: **10.12.2013**  
Received on: **13.12.2013**

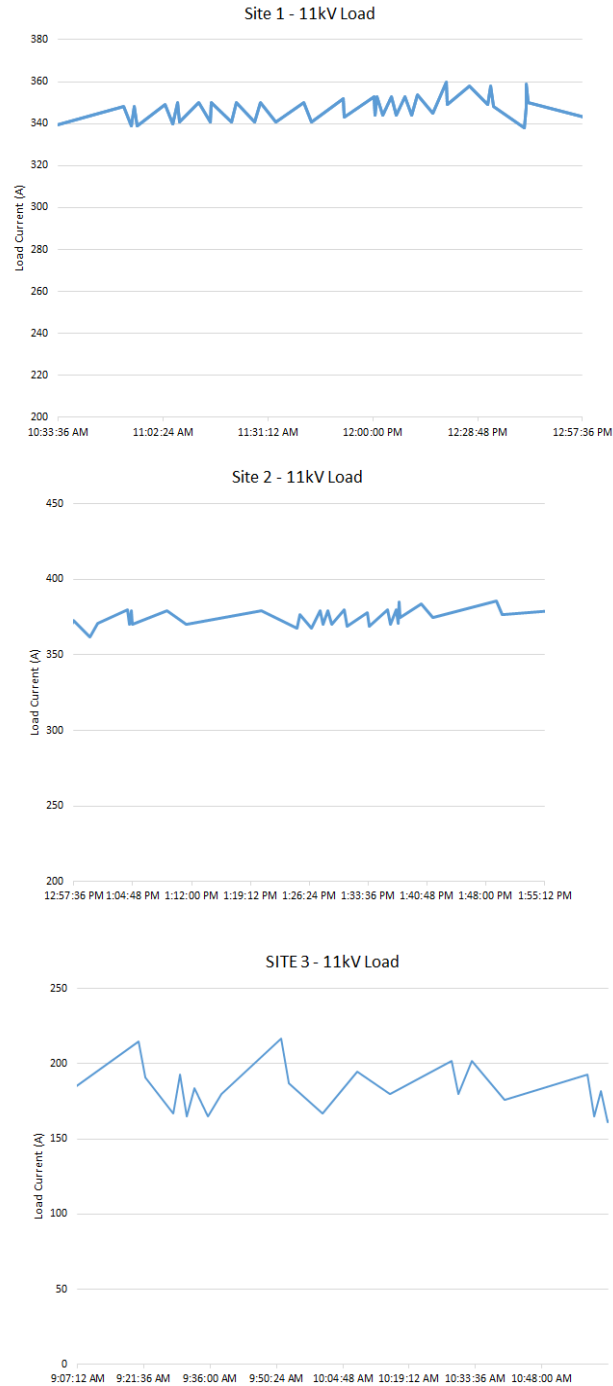
### Test Results:

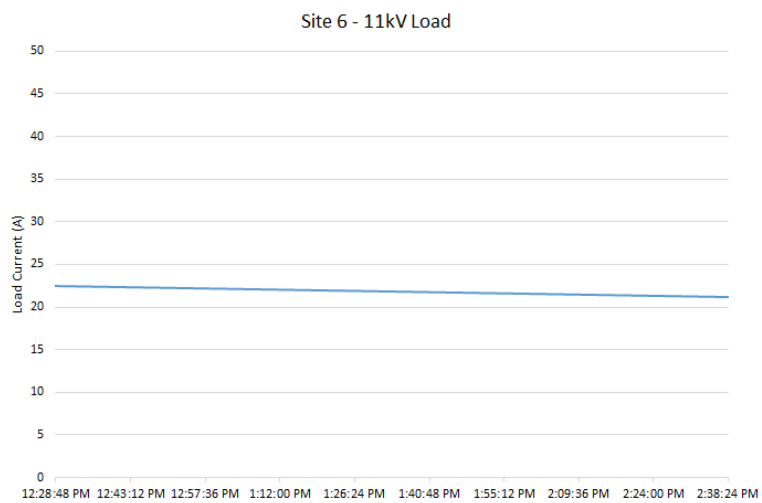
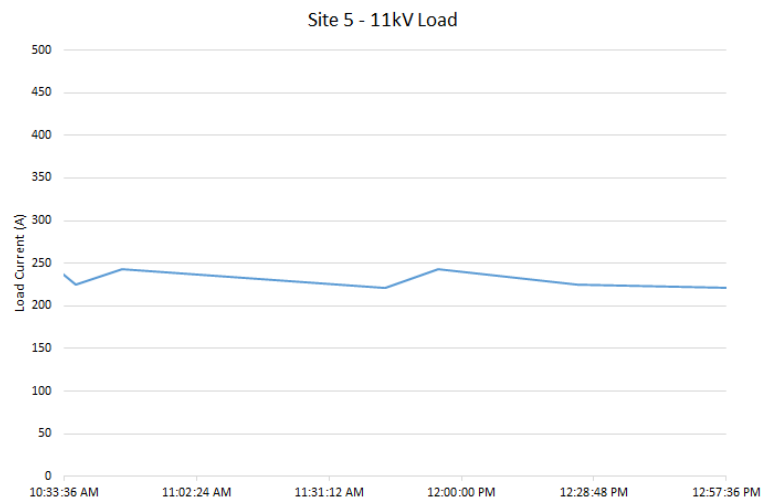
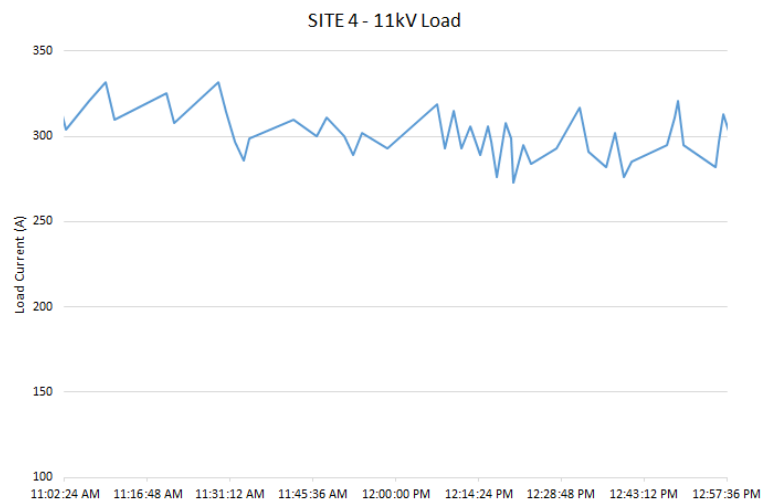
(Sample analysed as received)

Test	Component	Results	Units	Method
DGA	Hydrogen	6.3	ppm	CH/01; CH/02; mod. IEC 60567
	Oxygen	31400	ppm	
	Nitrogen	66800	ppm	
	Methane	0.9	ppm	
	Carbon Monoxide	83	ppm	
	Carbon Dioxide	534	ppm	
	Ethylene	0.6	ppm	
	Ethane	0.1	ppm	
	Acetylene	ND	ppm	
	Propane	0.5	ppm	
	Total gas	100	mL/L	

*The test results are satisfactory.*

## APPENDIX E. LOAD PROFILES





## APPENDIX F. RISK ANALYSIS

Risks associated with physical safety are assessed and categorised in line with workplace procedures and safe work method statements (SWMS). As part of workplace safety policy before commencing work a hazard assessment check (HAC) form will be required to document worksite specific hazards. This document is to be completed in association with reading the relevant SWMS for the task.

A strategy employed to mitigate risk is applying a hierarchy of controls with the most effective control being elimination and least effective control is the use of personal protective equipment (PPE). Working through the list of controls is a method of reducing the level of risk to the lowest possible, these are:

- |                  |  |
|------------------|--|
| • Eliminate      | Removal of the hazard completely                     |
| • Substitute     | Change process or item to reduce risk                |
| • Isolate        | Use preventative measures                            |
| • Engineer       | Use mechanical aids, barriers etc.                   |
| • Administrative | Develop safe work procedures                         |
| • PPE            | Use protective equipment, e.g. gloves, hard hat etc. |

The installation of an acoustic measuring device requires substation access to mount the device on the transformer walls. Gaining access to substations is part of current employment duties and whilst considered a common task in the work place various hazards are introduced and need to be assessed. Risks are standardised using the risk matrix in Table 7-1 and common risks associated with working in substations are identified in Table 7-2.

Table 7-1 Risk Matrix

		CONSEQUENCE				
		Insignificant	Minor	Moderate	Major	Severe
LIKELIHOOD	Almost Certain	11	16	20	23	25
	Likely	7	12	17	21	24
	Possible	4	8	13	18	22
	Unlikely	2	5	9	14	19
	Rare	1	3	6	10	15

Table 7-2 Hazards and Controls

Hazards	Assess Risk	Control	Residual Risk
Uncontrolled discharged or contact with electricity	22	PPE where proximity <500mm to exposed low voltage mains.  PPE includes:  Safety boots, safety goggles, arc rated uniform, insulated gloves, outer leather gloves	15
Exposure to hazardous materials	14	Awareness via a visual inspection prior to installation to ensure no transformer oil leaks or chemicals present.	10
Motor Vehicle Accident	14	Care taken whilst driving to locations	10
Struck by falling/moving object	9	PPE to be worn in switchyards and awareness of possible falling hazards.	6

Hazards	Assess Risk	Control	Residual Risk
Incident whilst undertaking lifting operations	5	Use suitable lifting methods and tools if pits require lifting.	3
Breach of controlled worksite	18	Lock gates to substations once entered to ensure no public access.	10

# APPENDIX G. ADXL345 DATA SHEET

Data Sheet has been summarised into the following core information.



## 3-Axis, $\pm 2\text{ g}/\pm 4\text{ g}/\pm 8\text{ g}/\pm 16\text{ g}$ Digital Accelerometer

### ADXL345

#### FEATURES

- Ultralow power:** as low as 40  $\mu\text{A}$  in measurement mode and 0.1  $\mu\text{A}$  in standby mode at  $V_S = 2.5\text{ V}$  (typical)
- Power consumption scales automatically with bandwidth**
- User-selectable resolution**
  - Fixed 10-bit resolution
  - Full resolution, where resolution increases with  $g$  range, up to 13-bit resolution at  $\pm 16\text{ g}$  (maintaining 4 mg/LSB scale factor in all  $g$  ranges)
- Embedded, patent pending FIFO technology minimizes host processor load**
- Tap/double tap detection**
- Activity/inactivity monitoring**
- Free-fall detection**
- Supply voltage range:** 2.0 V to 3.6 V
- I/O voltage range:** 1.7 V to  $V_S$
- SPI (3- and 4-wire) and I<sup>2</sup>C digital interfaces**
- Flexible interrupt modes mappable to either interrupt pin**
- Measurement ranges selectable via serial command**
- Bandwidth selectable via serial command**
- Wide temperature range** ( $-40^\circ\text{C}$  to  $+85^\circ\text{C}$ )
- 10,000  $g$  shock survival**
- Pb free/RoHS compliant**
- Small and thin:** 3 mm  $\times$  5 mm  $\times$  1 mm LGA package

#### APPLICATIONS

- Handsets
- Medical instrumentation
- Gaming and pointing devices
- Industrial instrumentation
- Personal navigation devices
- Hard disk drive (HDD) protection
- Fitness equipment

#### GENERAL DESCRIPTION

The ADXL345 is a small, thin, low power, 3-axis accelerometer with high resolution (13-bit) measurement at up to  $\pm 16\text{ g}$ . Digital output data is formatted as 16-bit twos complement and is accessible through either a SPI (3- or 4-wire) or I<sup>2</sup>C digital interface.

The ADXL345 is well suited for mobile device applications. It measures the static acceleration of gravity in tilt-sensing applications, as well as dynamic acceleration resulting from motion or shock. Its high resolution (4 mg/LSB) enables measurement of inclination changes less than  $1.0^\circ$ .

Several special sensing functions are provided. Activity and inactivity sensing detect the presence or lack of motion and if the acceleration on any axis exceeds a user-set level. Tap sensing detects single and double taps. Free-fall sensing detects if the device is falling. These functions can be mapped to one of two interrupt output pins. An integrated, patent pending 32-level first in, first out (FIFO) buffer can be used to store data to minimize host processor intervention.

Low power modes enable intelligent motion-based power management with threshold sensing and active acceleration measurement at extremely low power dissipation.

The ADXL345 is supplied in a small, thin, 3 mm  $\times$  5 mm  $\times$  1 mm, 14-lead, plastic package.

#### FUNCTIONAL BLOCK DIAGRAM

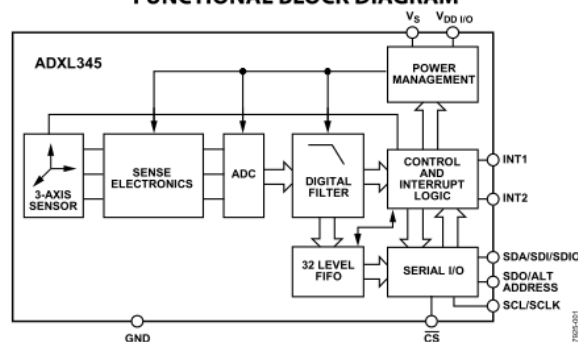


Figure 1.



## SPECIFICATIONS

$T_A = 25^\circ\text{C}$ ,  $V_S = 2.5\text{ V}$ ,  $V_{DD I/O} = 1.8\text{ V}$ , acceleration = 0 g,  $C_S = 1\text{ }\mu\text{F}$  tantalum,  $C_{IO} = 0.1\text{ }\mu\text{F}$ , unless otherwise noted.

**Table 1. Specifications<sup>1</sup>**

Parameter	Test Conditions	Min	Typ	Max	Unit
SENSOR INPUT	Each axis				
Measurement Range	User selectable		$\pm 2, \pm 4, \pm 8, \pm 16$		g
Nonlinearity	Percentage of full scale		$\pm 0.5$		%
Inter-Axis Alignment Error			$\pm 0.1$		Degrees
Cross-Axis Sensitivity <sup>2</sup>			$\pm 1$		%
OUTPUT RESOLUTION	Each axis				
All g Ranges	10-bit resolution		10		Bits
$\pm 2\text{ g}$ Range	Full resolution		10		Bits
$\pm 4\text{ g}$ Range	Full resolution		11		Bits
$\pm 8\text{ g}$ Range	Full resolution		12		Bits
$\pm 16\text{ g}$ Range	Full resolution		13		Bits
SENSITIVITY	Each axis				
Sensitivity at $X_{OUT}, Y_{OUT}, Z_{OUT}$	$\pm 2\text{ g}$ , 10-bit or full resolution	232	256	286	LSB/g
Scale Factor at $X_{OUT}, Y_{OUT}, Z_{OUT}$	$\pm 2\text{ g}$ , 10-bit or full resolution	3.5	3.9	4.3	mg/LSB
Sensitivity at $X_{OUT}, Y_{OUT}, Z_{OUT}$	$\pm 4\text{ g}$ , 10-bit resolution	116	128	143	LSB/g
Scale Factor at $X_{OUT}, Y_{OUT}, Z_{OUT}$	$\pm 4\text{ g}$ , 10-bit resolution	7.0	7.8	8.6	mg/LSB
Sensitivity at $X_{OUT}, Y_{OUT}, Z_{OUT}$	$\pm 8\text{ g}$ , 10-bit resolution	58	64	71	LSB/g
Scale Factor at $X_{OUT}, Y_{OUT}, Z_{OUT}$	$\pm 8\text{ g}$ , 10-bit resolution	14.0	15.6	17.2	mg/LSB
Sensitivity at $X_{OUT}, Y_{OUT}, Z_{OUT}$	$\pm 16\text{ g}$ , 10-bit resolution	29	32	36	LSB/g
Scale Factor at $X_{OUT}, Y_{OUT}, Z_{OUT}$	$\pm 16\text{ g}$ , 10-bit resolution	28.1	31.2	34.3	mg/LSB
Sensitivity Change Due to Temperature			$\pm 0.01$		%/ $^\circ\text{C}$
0 g BIAS LEVEL	Each axis				
0 g Output for $X_{OUT}, Y_{OUT}$		-150	$\pm 40$	+150	mg
0 g Output for $Z_{OUT}$		-250	$\pm 80$	+250	mg
0 g Offset vs. Temperature for x-, y-Axes			$\pm 0.8$		mg/ $^\circ\text{C}$
0 g Offset vs. Temperature for z-Axis			$\pm 4.5$		mg/ $^\circ\text{C}$
NOISE PERFORMANCE					
Noise (x-, y-Axes)	Data rate = 100 Hz for $\pm 2\text{ g}$ , 10-bit or full resolution		<1.0		LSB rms
Noise (z-Axis)	Data rate = 100 Hz for $\pm 2\text{ g}$ , 10-bit or full resolution		<1.5		LSB rms
OUTPUT DATA RATE AND BANDWIDTH	User selectable				
Measurement Rate <sup>3</sup>		6.25		3200	Hz
SELF-TEST <sup>4</sup>	Data rate $\geq 100\text{ Hz}$ , $2.0\text{ V} \leq V_S \leq 3.6\text{ V}$				
Output Change in x-Axis		0.20		2.10	g
Output Change in y-Axis		-2.10		-0.20	g
Output Change in z-Axis		0.30		3.40	g
POWER SUPPLY					
Operating Voltage Range ( $V_S$ )		2.0	2.5	3.6	V
Interface Voltage Range ( $V_{DD I/O}$ )	$V_S \leq 2.5\text{ V}$	1.7	1.8	$V_S$	V
	$V_S \geq 2.5\text{ V}$	2.0	2.5	$V_S$	V
Supply Current	Data rate $> 100\text{ Hz}$		145		$\mu\text{A}$
	Data rate $< 10\text{ Hz}$		40		$\mu\text{A}$
Standby Mode Leakage Current			0.1	2	$\mu\text{A}$
Turn-On Time <sup>5</sup>	Data rate = 3200 Hz		1.4		ms
TEMPERATURE					
Operating Temperature Range		-40		+85	$^\circ\text{C}$
WEIGHT					
Device Weight			20		mg